Twenty-Seventh Annual

GASEOUS ELECTRONICS CONFERENCE

Houston, Texas, 1974

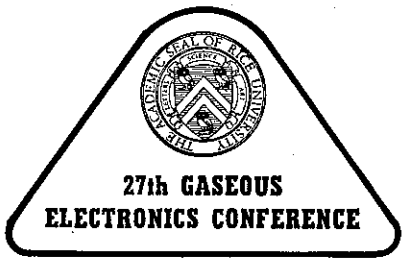

PROGRAM AND ABSTRACTS

October 22-25, 1974

Houston, Texas

A topical conference of The American Physical Society

Sponsored by

Rice University
The American Physical Society, Division of Electron and Atomic Physics

GASEOUS ELECTRONICS CONFERENCE EXECUTIVE COMMITTEE

Chairman

G. I. Weissler
University of Southern California

Honorary Chairman

W. P. Allis
Massachusetts Institute of Technology

Chairman Elect

R. H. Bullis
United Aircraft Research Laboratories

Secretary

R. D. Rundel
Rice University

Treasurer

D. M. Benenson
SUNY of Buffalo

A. Garscadden
Wright-Patterson AFB

C. C. Lin
University of Wisconsin

A. V. Phelps
JILA

L. D. Schearer
University of Missouri Rolla

J. F. Waymouth
GTE Sylvania

LOCAL ARRANGEMENTS COMMITTEE

F. B. Dunning

C. J. Latimer

J. W. Keto

R. F. Stebbings

N. F. Lane

G. K. Walters

PROGRAM

TWENTY-SEVENTH ANNUAL

GASEOUS ELECTRONICS CONFERENCE

RECEPTION-MIXER AND REGISTRATION

8:00 PM - 10:00 PM
Monday, October 21
TEJAS ROOM (18th FLOOR) RICE HOTEL

SESSION AA. CO_2 ELECTRIC DISCHARGE AND UV PREIONIZATION LASERS

8:30 AM - 10:15 AM, Tuesday, October 22
Crystal Ballroom
Chairman: M.J.W. Boness, Avco Everett

AA-1 THEORETICAL PERFORMANCE CHARACTERISTICS OF CW CO_2 ELECTRIC LASERS (7 min.)
H. H. Legner and J. H. Jacob

AA-2 EXPERIMENTAL CHARACTERISTICS OF A SUBSONIC CW CO_2 ELECTRIC LASER (7 min.)
M. J. Yoder and D. R. Ahouse

AA-3 A SIX-TEMPERATURE CO_2 LASER KINETICS MODEL (20 min.)
L. H. Taylor, L. A. Weaver, and R. W. Liebermann

AA-4 THEORETICAL AND EXPERIMENTAL GAIN AND OUTPUT IN ELECTRON-BEAM SUSTAINER LASERS (7 min.)
D. H. Douglas-Hamilton, R. S. Lowder, and R. M. Feinberg

AA-5 ELECTRON ATTACHMENT AND RECOMBINATION RATE MEASUREMENTS RELEVANT TO CO_2 AND CO LASER OPERATION (7 min.)
Alan E. Hill

AA-6 CHARGED PARTICLES LOSS PROCESSES IN ELECTRON BEAM CONTROLLED DISCHARGE (7 min.)
D. Pigache, G. Fournier, and P. Gotchiguian

AA-7 TIME DEPENDENCE OF ROTATIONAL TEMPERATURE IN A HIGH PRESSURE PULSED CO_2 LASER (7 min.)
W. T. Leland, M. J. Kircher, M. J. Nutter, and G. T. Schappert

AA-8 VOLUMETRIC UV PHOTO-IONIZATION IN CO_2 LASER MEDIA (7 min.)
R. V. Babcock

AA-9 GLOW DISCHARGE FORMATION WITH UV VOLUME PREIONIZATION (7 min.)
L. E. Kline and L. J. Denes

SESSION AB. NEGATIVE IONS

9:00 AM - 10:10 AM, Tuesday, October 22
Brazos Room
Chairman: J. L. Franklin, Rice University

AB-1 ELECTRON DETACHMENT IN COLLISIONS OF Cl^- WITH THE RARE GASES (7 min.)
R. L. Champion and L. D. Doverspike

AB-2 ENDOERGIC ION-MOLECULE-COLLISION PROCESSES OF NEGATIVE IONS (7 min.)
Kamel M. A. Refaey

AB-3 CHARGE TRANSFER OF H^- AND D^- WITH O_2 (7 min.)
P. E. Chaplin and W. R. Snow

AB-4† NEGATIVE IONS FROM CHARGE EXCHANGE
G. P. Reck, S. Y. Tang, and E. W. Rothe

AB-5† ADIABATIC ELECTRON AFFINITIES FROM COLLISIONAL IONIZATION (10 min.)
C. B. Leffert, S. Y. Tang, and E. W. Rothe

AB-6 ANGULAR DISTRIBUTION OF O^- FROM DISSOCIATIVE ELECTRON ATTACHMENT TO NO (7 min.)
R. J. Van Brunt and L. J. Kieffer

†Combined presentation, total time allotted for both papers 10 minutes.

AB-7 NEGATIVE ION FORMATION IN CERIUM TRIIODIDE (7 min.)
P. J. Chantry

SESSION B. MOLECULAR DISCHARGE INSTABILITIES

10:45 AM - 12:05 PM, Tuesday, October 22
Crystal Ballroom
Chairman: L. Denes, Westinghouse

B-1 THERMAL INSTABILITY IN HIGH POWER LASER DISCHARGES (7 min.)
J. H. Jaçob and Siva A. Mani

B-2 CAUSES OF ARCING IN CO_2 LASER DISCHARGES (20 min.)
W. L. Nighan and W. J. Wiegand

B-3 INITIAL DEVELOPMENT OF GLOW-TO-ARC TRANSITION DUE TO ELECTRIC FIELD DISTORTION (20 min.)
Gerald L. Rogoff

B-4 THE DISPERSION OF IONIZATION WAVES IN THE PRESENCE OF NEGATIVE IONS (7 min.)
W. H. Long, Jr., W. F. Bailey, and A. Garscadden

B-5 STABILIZATION OF A MEDIUM PRESSURE DISCHARGE BY TURBULENT FLOWS (7 min.)
O. Biblarz and L. J. Aunchmam

SESSION CA. CO AND N_2 LASERS

1:30 PM - 2:50 PM, Tuesday, October 22
Crystal Ballroom
Chairman: S. Rockwood, Los Alamos

CA-1 OBSERVATIONS OF SMALL SIGNAL GAIN IN A HIGH PRESSURE PULSED CO ELECTRIC DISCHARGE LASER (7 min.)
M.J.W. Boness and R. E. Center

CA-2 V-V PUMPING IN HIGH POWER CO LASERS (7 min.)
W. L. Thweatt, G. W. Sullivan, and R. F. Weber

CA-3 HIGH POWER E-BEAM PLASMA DIODE CO LASER (7 min.)
B. B. O'Brien

CA-4 ACOUSTIC VELOCITY MEASUREMENTS TO DETERMINE LASER GAS HEATING RATE (7 min.)
R. G. Eguchi, G. L. McAllister, and V. G. Draggoo

CA-5 MONTE-CARLO CALCULATION OF IONIZATION PROFILE DUE TO ELECTRON BEAM IN CO-He SYSTEM (7 min.)
Frank T. Wu and Eric A. Lundstrom

CA-6 A STUDY OF CHARGED PARTICLE DENSITIES AND ELECTRIC FIELD IN E-BEAM SUSTAINED GAS DISCHARGES (7 min.)
C. Baugh, J. Bradley, E. Malarkey, and H. Trenchard

CA-7 EXPERIMENTAL INVESTIGATION OF HIGH POWER N_2 LASERS (7 min.)
W. A. Fitzsimmons, L. W. Anderson, and J. M. Vrtilek

CA-8 A THEORETICAL TREATMENT OF THE NITROGEN LASER (7 min.)
C. E. Riedhauser, L. W. Anderson, and W. A. Fitzsimmons

SESSION CB. CHARGE TRANSFER

1:45 PM - 2:55 PM, Tuesday, October 22
Brazos Room
Chairman: R. F. Stebbings, Rice University

CB-1 ELECTRON-TRANSFER IN COLLISIONS BETWEEN ATOMIC IONS AND RARE-GAS ATOMS (7 min.)
William B. Maier II

CB-2 ELASTIC SCATTERING AND CHARGE TRANSFER OF LOW-ENERGY He^{++} IONS WITH Ne, Ar, and Kr (7 min.)
T. M. Austin, J. M. Mullen, C. L. Bottoms, and T. L. Bailey

CB-3 CHARGE TRANSFER FROM O^+ AND N^+ TO NEUTRAL URANIUM AND THORIUM (7 min.)
J. A. Rutherford and D. A. Vroom

CB-4 MEASUREMENT OF THE CHARGE TRANSFER CROSS SECTIONS FOR GROUND AND EXCITED STATE O^+ IN COLLISION WITH O_2 AND NO (7 min.)
J. A. Rutherford and D. A. Vroom

CB-5 ENERGIES OF PRODUCTS FOR CHARGE-TRANSFER OF N_2^+ IN O_2 (7 min.)
G. D. Magnuson and R. H. Neynaber

CB-6 NONRESONANT BEHAVIOR OF THE SYMMETRIC CHARGE-TRANSFER CROSS SECTION FOR DEUTERIUM MOLECULES (7 min.)
H. L. Rothwell, Bert Van Zyl, and R. C. Amme

CB-7 VIBRATIONAL TRANSITIONS IN $H_2^+ - H_2$ AND $D_2^+ - D_2$ CHARGE-TRANSFERRING COLLISIONS (7 min.)
Robert N. Stocker and Herschel Neumann

SESSION DA. DIMER AND OTHER LASERS

3:30 PM - 5:25 PM, Tuesday, October 22
Crystal Ballroom
Chairman: P. W. Hoff, Lawrence Livermore

DA-1† A NITROGEN ION LASER PUMPED BY CHARGE TRANSFER IN THE HIGH PRESSURE AFTERGLOW OF AN e-BEAM DISCHARGE
C. B. Collins, A. J. Cunningham, and M. Stockton

DA-2† ELECTRON-BEAM EXCITED Ar and Ar-H_2 AFTERGLOWS
L. C. Pitchford and C. B. Collins

DA-3† ION-ELECTRON RECOMBINATION AS A PUMPING MECHANISM FOR e-BEAM LASERS (20 min.)
A. J. Cunningham, G. D. Myers, R. A. Waller, M. Stockton, and C. B. Collins

DA-4‡ SPECTRA AND KINETICS OF NaXe EXCIMERS IN HIGH PRESSURE HIGH POWER NaXe DISCHARGES
R. W. Harwell, L. A. Schlie, D. L. Drummond, and B. D. Guenther

DA-5‡ HIGH POWER RESONANT OPTICAL PUMPING OF ALKALI-XENON MIXTURES (7 min.)
D. L. Drummond, L. A. Schlie, and B. D. Guenther

DA-6 ULTRA-VIOLET (2000-3250 Å) PHOTOIONIZATION FOR POTENTIAL ALKALI VAPOR - INERT GAS EXCIMER AND ALKALI DIMER LASER PLASMAS (7 min.)
L. A. Schlie, D. L. Drummond, and B. D. Guenther

†Combined presentation, total time allotted for all papers 20 min.
‡Combined presentation, total time allotted for both papers 7 min.

SESSION DB. CHARGE TRANSFER AND ION-MOLECULE REACTIONS

3:45 PM - 4:55 PM, Tuesday, October 22
Brazos Room
Chairman: F. B. Dunning, Rice University

DB-3 MERGING BEAMS STUDY OF THE $D^+(H_2,H)HD^+$ AND $H_2^+(D,H)HD^+$ REACTION MECHANISMS (7 min.)
A. B. Lees and P. K. Rol

DB-4 DRIFT TUBE MEASUREMENT OF THE ENERGY DEPENDENCE OF THE REACTION RATE FOR $NO^+ + H_2O + N_2$ (7 min.)
H. L. Brown, Rainer Johnsen, and Manfred A. Biondi

DB-5 RATE COEFFICIENTS FOR OXIDATION OF Ti^+ AND Th^+ BY O_2 AND NO AT LOW ENERGIES (7 min.)
Rainer Johnsen, F. R. Castell, and Manfred A. Biondi

DB-6 RATE CONSTANTS FOR THE REACTION OF METASTABLE O_2^+ ($a\ ^4\pi_u$) WITH H_2, N_2, AND Ar AT RELATIVE KINETIC ENERGIES 0.05 TO 2 eV (7 min.)
M. McFarland, W. Lindinger, and D. L. Albritton

DB-7 THE ION CHEMISTRY OF HNO_3 AND NO_2 (7 min.)
F. C. Fehsenfeld and Carleton J. Howard

SESSION WA. WORKSHOP ON DISCHARGE INSTABILITIES

7:30 PM, Tuesday, October 22
Brazos Room
Chairman: Alan Garscadden, Wright-Patterson Air Force Base

WA-1 INTRODUCTION AND OVERVIEW
Alan Garscadden

WA-2 BREAKDOWN INSTABILITIES
F. Jaeger

WA-3 PULSED DISCHARGE INSTABILITIES
G. Rogoff

WA-4 PULSED DISCHARGE WITH EXTERNAL IONIZATION
D. Douglas-Hamilton

WA-5 INFLUENCE OF GAS TURBULENCE ON DISCHARGE STABILITY

Oscar Biblarz

WA-6 THE VIBRATIONAL-THERMAL INSTABILITY
W. Wiegand

SESSION E. ELECTRON EXCITATION OF MOLECULES I

9:00 AM - 10:15 AM, Wednesday, October 23
Crystal Ballroom
Chairman: M.F.A. Harrison, Culham

E-1 VIBRATIONAL EXCITATION OF N_2, CO, AND N_2O BY LOW ENERGY ELECTRONS (20 min.)
S. F. Wong and G. J. Schulz

E-2 VIBRATIONAL AND ROTATIONAL EXCITATION OF CO_2 BY LOW-ENERGY ELECTRONS (7 min.)
M. Morrison and N. F. Lane

E-3 VIBRATIONAL STRUCTURE IN KINETIC ENERGY SPECTRA OF O^+ IONS FROM ELECTRON IMPACT DISSOCIATIVE IONIZATION OF O_2: PRE-DISSOCIATION OF THE $B^2\Sigma_g^-$ STATE OF O_2^+ (7 min.)
J.A.D. Stockdale and Liliana Deleanu

E-4 VIBRATIONAL EXCITATION AND TRANSMISSION SPECTROSCOPY IN HYDROGEN HALIDES (7 min.)
J. P. Ziesel, I. Nenner, and G. J. Schulz

E-5 EXCITATION OF H_2 BY LOW-ENERGY ELECTRON IMPACT (7 min.)
J. Watson, Jr., J. N. Adams, and R. J. Anderson

E-6 EXCITATION OF THE $B^3\pi_g$ AND $C^3\pi_u$ STATES OF N_2 BY ELECTRON IMPACT (7 min.)
S. T. Chen, R. J. Anderson, and R. H. Hughes

SESSION FA. EQUILIBRIUM PHENOMENA IN ARCS I

10:30 AM - 12:25 PM, Wednesday, October 23
Brazos Room
Chairman: J. H. Ingold, General Electric

FA-1 DERIVATION OF THE MICROFIELD DISTRIBUTION FROM THE LINEARIZED KLIMONTOVICH-EQUATIONS (20 min.)
G. Ecker and A. Schumacher

FA-2 MEASUREMENTS AND CALCULATIONS ON A CsI-Hg-Ar DISCHARGE (20 min.)
J. H. Waszink and L.G.M. De Greef

FA-3 CONSTRUCTION OF ARCS IN MIXTURES OF MERCURY AND IODINE (20 min.)
R. J. Zollweg, J. J. Lowke, and R. W. Liebermann

FA-4 MULTIPLE-LINE BARTELS' METHOD OF DETERMINATION OF AXIS TEMPERATURES OF LTE ARCS (7 min.)
John F. Waymouth

FA-5 ELECTRONIC RAMAN SCATTERING FROM Ga, In AND Tl ATOMS IN METAL HALIDE ARCS (7 min.)
L. Vriens and M. Adriaansz

FA-6 TIME-DEPENDENT PLASMA TEMPERATURE MEASUREMENTS OF THE HIGH PRESSURE SODIUM ARC (7 min.)
P. D. Johnson and T. H. Rautenberg, Jr.

FA-7 TIME-DEPENDENT MODELING OF THE HIGH PRESSURE SODIUM ARC COLUMN (7 min.)
R. E. Kinsinger

SESSION FB. ELECTRON EXCITATION OF MOLECULES II

10:45 AM - 12:00 NOON, Wednesday, October 23
Crystal Ballroom
Chairman: R. J. Anderson, Arkansas

FB-1 ELECTRON EXCITATION FUNCTIONS OF THE $B^1\Sigma^+$, $d^3\Delta$, $b^3\Sigma^+$, and $a'^3\Sigma^+$ STATES OF THE CO MOLECULE (7 min.)
A. R. Filippelli, Sunggi Chung, and Chun C. Lin

FB-2 EXCITATION OF THE GAMMA BANDS OF NITRIC OXIDE BY ELECTRON IMPACT (7 min.)
Mahmood Imami and Walter L. Borst

FB-3 DISSOCIATIVE EXCITATION OF H_2--LOW RYDBERG AND HIGH RYDBERG FRAGMENTS (7 min.)
Robert S. Freund, James A. Schiavone, Donna F. Brader, and Kermit C. Smyth

FB-4 ELECTRON IMPACT EXCITATION OF FLUORESCENCE IN ORGANIC MOLECULES (7 min.)
Kermit C. Smyth, James A. Schiavone, and Robert S. Freund

FB-5 DISSOCIATION OF THE HYDROGEN MOLECULE BY ELECTRON COLLISION (7 min.)
Sunggi Chung and Edward T. P. Lee

FB-6 DETERMINATION OF ABSOLUTE CROSS SECTIONS FOR ELECTRON-MOLECULE COLLISION PROCESSES AT INTERMEDIATE ENERGIES (20 min.)
S. Trajmar

SESSION GA. GAS DYNAMIC AND MAGNETIC PHENOMENA I

1:30 PM - 2:55 PM, Wednesday, October 23
Crystal Ballroom
Chairman: W. C. Roman, United Aircraft

GA-1 THEORETICAL ASPECTS OF MASS SEPARATION AND PRESSURE DISTRIBUTION IN ROTATING ARCS (20 min.)
J. J. McClure and N. Nathrath

GA-2 CATHODE AND ANODE CURRENT DISTRIBUTION IN A SHORT MOVING ARC (7 min.)
R. Beaudet and M. G. Drouet

GA-3 ACCELERATING RAIL ARCS (7 min.)
T. N. Meyer

GA-4 CORRELATION OF MPD ARC DISCHARGE HIGH SPEED PHOTOGRAPHY AND ARC PARAMETERS DURING TRANSITION FROM THE CONSTRICTED TO THE DIFFUSE MODE (7 min.)
D. L. Murphree, J. K. Owens, and C. S. McMillan

GA-5 ALTERNATING CURRENT CROSS-FLOW ARCS (7 min.)
J-L Wu and D. M. Benenson

GA-6 INVESTIGATION OF AN RF ARGON PLASMA VORTEX WITH UF_6 INJECTION (7 min.)
Ward C. Roman

GA-7 CHARACTERISTICS OF XENON FLASH LAMPS IN HIGH MAGNETIC FIELDS (7 min.)
Paul Schreiber

SESSION GB. ELECTRON COLLISIONS

1:45 PM - 3:00 PM, Wednesday, October 23
Brazos Room
Chairman: R.J.W. Henry, Louisiana State

GB-1 THE MULTICHANNEL EIKONAL TREATMENT OF ELECTRON-ATOM COLLISIONS (20 min.)
M. R. Flannery and K. J. McCann

GB-2 ABSOLUTE EXPERIMENTAL CROSS SECTIONS FOR THE IONIZATION OF Tl^+ IONS BY ELECTRON IMPACT (7 min.)
T. F. Divine, R. K. Feeney, J. W. Hooper, and W. E. Sayle II

GB-3 ELECTRON IMPACT AUTOIONIZATION IN POTASSIUM, RUBIDIUM, AND CESIUM (7 min.)
K. J. Nygaard

GB-4 THE FREDHOLM METHOD IN e-H_2 SCATTERING (7 min.)
T. G. Winter and N. F. Lane

GB-5 ABSOLUTE e-H_2 ELASTIC COLLISION CROSS SECTIONS (7 min.)
Santosh K. Srivastava

GB-6 MICROWAVE TRANSIENT RESPONSE MEASUREMENTS OF ELASTIC MOMENTUM TRANSFER COLLISION FREQUENCY (7 min.)
D. A. McPherson, R. K. Feeney, and J. W. Hooper

SESSION H. GAS DYNAMIC AND MAGNETIC PHENOMENA II

3:30 PM - 5:00 PM, Wednesday, October 23
Crystal Ballroom
Chairman: T. Fohl, GTE Sylvania

H-1† DECAYING ARCS IN STRONG AXIAL GAS FLOWS
W. Hermann, U. Kogelschatz, L. Niemeyer, K. Ragaller, and E. Schade

H-2† INVESTIGATION OF DECAYING ARCS WITH A DIFFERENTIAL INTERFEROMETER OF HIGH FRAMING RATE (25 min.)
U. Kogelschatz

†Combined presentation, total time allotted for both papers 25 min.

IA-5 RADIATIVE LIFETIMES AND PRODUCTION MECHANISMS FOR THE V.U.V. TRANSITIONS OF Ar_2^* AND Xe_2^* (7 min.)
J. W. Keto, R. E. Gleason, and G. K. Walters

IA-6 PHOTODESTRUCTION AND ION-MOLECULE REACTIONS OF NEGATIVE IONS IN CO_2/H_2O MIXTURES (7 min.)
J. T. Moseley, P. C. Cosby, R. A. Bennett, and J. R. Peterson

IA-7 DISSOCIATION YIELDS AS A FUNCTION OF ENERGY (7 min.)
G. M. Lawrence

SESSION IB. AFTERGLOWS

9:00 AM - 10:10 AM, Thursday, October 24
Brazos Room
Chairman: J. W. Keto, Rice University

IB-1 QUENCHING RATES FOR RARE-GAS EXCIMER MOLECULES AND EXCITED ATOMIC OXYGEN (7 min.)
Felton W. Bingham, A. W. Johnson, and James K. Rice

IB-2 FORMATION AND DESTRUCTION OF $XeO(^1S)$ IN HIGH PRESSURE Xe AND N_2O AND CO_2 MIXTURES (7 min.)
G. C. Tisone and J. M. Hoffman

IB-3 KINETIC AND SPECTRAL BEHAVIOR OF HIGH PRESSURE, HIGH POWER Hg VAPOR DISCHARGES (7 min.)
L. A. Schlie, B. D. Guenther, and D. L. Drummond

IB-4 EXCIMER FORMATION RATE IN NaAr (7 min.)
J. G. Eden, J. T. Verdeyen, and B. E. Cherrington

IB-5 VACUUM-ULTRAVIOLET EMISSIONS FROM NEON (7 min.)
P. K. Leichner and J. D. Cook

IB-6 TIME DEPENDENCE IN THE EARLY AFTERGLOW OF ARGON SPECTRAL LINE INTENSITY IN HIGH PRESSURE NEON/ARGON PENNING MIXTURES (7 min.)
W. E. Ahearn and O. Sahni

IB-7 ELECTRON TEMPERATURE DEPENDENCE OF RECOMBINATION OF NO^+ IONS WITH ELECTRONS (7 min.)
C-M Huang, M. A. Biondi, and R. Johnsen

SESSION J. BUSINESS MEETING AND INVITED PAPER

10:45 AM - 12:15 PM, Thursday, October 24, 1974
Crystal Ballroom

Chairman: G. L. Weissler, USC

THE GASEOUS ELECTRONICS OF IDEAL LIGHT SOURCES
R. Bleekrode
Philips Research Laboratory

SESSION KA. EQUILIBRIUM PHENOMENA IN ARCS II, AND NON-EQUILIBRIUM AND VACUUM ARC PHENOMENA

1:30 PM - 3:00 PM, Thursday, October 24
Crystal Ballroom
Chairman: P. W. Schreiber, Wright-Patterson AFB

KA-1 AN IMPROVED METHOD FOR VUV RADIOMETRIC CALIBRATIONS USING HYDROGEN ARCS (7 min.)
W. R. Ott and G. Gieres

KA-2 METHANE/CARBON DIOXIDE DECOMPOSITION IN AN ARGON PLASMA (7 min.)
C. H. Leigh and E. A. Dancy

KA-3 WALL-STABILIZED ARC IN AIR (7 min.)
R. S. Devoto, U. H. Bauder, J. Cailleteau, and E. Shires

KA-4† ON THE RANGE OF VALIDITY OF MTE PLASMA DIAGNOSTICS
T. L. Eddy

KA-5† THE CONTINUUM EMISSION COEFFICIENT RELATION FOR THE MULTITHERMAL EQUILIBRIUM MODEL FOR NON-LTE PLASMAS (10 min.)
T. L. Eddy

†Combined presentation, total time allotted for both papers 10 minutes.

KA-6 NON-LTE EXCITATION OF MOLECULES IN TIN-IODIDE ARCS (7 min.)
E. Fischer and L. Rehder

KA-7 OBSERVATION OF STIMULATED RAMAN EMISSION AT UHF FROM LABORATORY PLASMAS (7 min.)
C. C. Leiby, Jr. and B. Prasad

KA-8 COPPER VAPOR PLASMA PRODUCED FROM A VACUUM ARC SOURCE (7 min.)
Dennis P. Malone

KA-9 NEUTRAL VAPOR TEMPERATURES DERIVED FROM PULSED VACUUM ARCS (7 min.)
C. L. Chen and P. J. Chantry, and T. Utsumi

KA-10 PROJECTION TUBE STUDIES OF VACUUM ARCS FROM TUNGSTEN AND NIOBIUM WIRES (7 min.)
G. H. Miley

SESSION KB. HOLLOW CATHODES AND ELECTRON TRANSPORT

1:30 PM - 2:40 PM, Thursday, October 24
Republic of Texas Room (3rd Floor)
Chairman: L. Frommhold, University of Texas

KB-1 REACTIONS OF IONS IN N_2 + H_2O IN A HOLLOW CATHODE DISCHARGE (7 min.)
F. Howorka, W. Lindinger, and R. N. Varney

KB-2 MASS SPECTROMETRIC ANALYSIS OF N_2, SF_6, AND NH_3 GASES IN CYLINDRICAL HOLLOW CATHODE DISCHARGE (7 min.)
M. Saporoschenko

KB-3 EXPERIMENTAL ELECTRON-ENERGY DISTRIBUTIONS IN TRANSVERSE HOLLOW-CATHODE DISCHARGES (7 min.)
R. A. Olson, D. R. Nordlund, and B. Sarka, Jr.

KB-4 ELECTRICAL PROBE DIAGNOSTICS OF ANISOTROPIC PLASMAS IN LASERS (7 min.)
I. P. Shkarofsky and A. Bonnier

KB-5 RELAXATION PHENOMENA OF ELECTRONS EMITTED FROM A WALL (7 min.)
G. Ecker and A. Scholz

KB-6 ELECTRON DENSITY MEASUREMENTS IN COLLISION DOMINATED PLASMAS (7 min.)
T. V. George and L. J. Denes

KB-7 NEGATIVE DIFFERENTIAL CONDUCTIVITY IN MOLECULAR GAS-RARE GAS MIXTURES: NITROGEN-ARGON (7 min.)
W. H. Long, Jr., W. F. Bailey, and A. Garscadden

SESSION LA. ION MOBILITY AND HELIUM AFTERGLOWS

3:30 PM - 4:45 PM, Thursday, October 24
Crystal Ballroom
Chairman: C. Collins, U. of Texas at Dallas

LA-1 MOBILITY OF INTERMEDIATE SIZED AQUEOUS IONS IN AN ARGON GAS (7 min.)
D. E. Hagen, P. C. Yue, and J. L. Kassner, Jr.

LA-2 SEMI-EMPIRICAL CONSTRUCTION OF JOINT ION-NEUTRAL SPEED DISTRIBUTIONS (7 min.)
S. B. Woo, J. H. Whealton, and S. P. Hong

LA-3† CONVERGENT ION TRANSPORT THEORY FOR LARGE ION DENSITY GRADIENTS
J. H. Whealton

LA-4† ASYMPTOTIC ION TRANSPORT THEORY FOR SMALL ION DENSITY GRADIENTS (10 min.)
J. H. Whealton

LA-5 MONTE-CARLO SIMULATION OF THE DRIFT OF H^- IONS IN He (7 min.)
S. L. Lin and J. N. Bardsley

LA-6 AN EXPERIMENTAL STUDY OF ELECTRON TEMPERATURE AND METASTABLE ATOMS IN A RECOMBINING HELIUM PLASMA (7 min.)
C. C. Poon and F. Robben

†Combined presentation, total time allotted for both papers 10 min.

LA-7 IONIZATION AND ELECTRON HEATING BY METASTABLE ATOMS IN HELIUM AFTERGLOWS (7 min.)
F. R. Castell and M. A. Biondi

LA-8 THE HELIUM AFTERGLOW (7 min.)
J. B. Gerardo, J. R. Freeman, F. O. Lane, and A. W. Johnson

SESSION LB. RESONANT SCATTERING

3:30 PM - 4:35 PM, Thursday, October 24
Republic of Texas Room (3rd Floor)
Chairman: F. Read, JILA

LB-1 H^- SHAPE RESONANCE STUDIES WITH AN ARC PLASMA (20 min.)
J. Slater, G. Gieres, and W. R. Ott

LB-2 RESONANCES AND THEIR EFFECTS ABOVE AND BELOW THE ELECTRON IMPACT IONIZATION THRESHOLD (7 min.)
A. Weingartshofer, M. Eyb, E. M. Clarke, and J. W. McGowan

LB-3 ELECTRON SCATTERING ON Na and K (7 min.)
M. Eyb

LB-4 RESONANCES IN MERCURY VAPOR (7 min.)
P. D. Burrow and J. A. Michejda

LB-5 RESONANT ELECTRON-MOLECULE SCATTERING: THE IMPULSE APPROXIMATION IN N_2O (7 min.)
L. Dube and A. Herzenberg

RECEPTION AND BANQUET

6:30 PM, Thursday, October 24
Social Hour, Cohen House, Rice University

8:00 PM, Thursday, October 24
Banquet, Rice Memorial Center

Chairman: G. L. Weissler, USC

Speaker: Dr. Robert Parker, NASA
"A Quick Look at Some Skylab Scientific Results"

SESSION MA. PENNING IONIZATION

9:00 AM - 10:25 AM, Friday, October 25
Crystal Ballroom
Chairman: G. K. Walters, Rice University

MA-1 TEMPERATURE DEPENDENCE OF DE-EXCITATION RATE CONSTANTS OF He(2^3S) BY VARIOUS NEUTRALS (20 min.)
W. Lindinger, A. L. Schmeltekopf, and F. C. Fehsenfeld

MA-2 CHEMI-IONIZATION IN COLLISIONS OF METASTABLE Ne WITH Ar (7 min.)
R. H. Neynaber and G. D. Magnuson

MA-3 ASSOCIATIVE IONIZATION AND EXCITATION TRANSFER IN HELIUM (7 min.)
J. S. Cohen

MA-4 ASSOCIATIVE IONIZATION INVOLVING RARE GAS METASTABLE ATOMS (7 min.)
W. P. West, T. B. Cook, F. B. Dunning, R. D. Rundel, and R. F. Stebbings

MA-5 COLLISIONAL TRANSFER OF EXCITATION AND NON-METASTABLE PENNING IONIZATION OF NITROGEN BY NEON $2p_1$ (7 min.)
P. E. Thiess, G. H. Miley, J. L. Gorecki, and L. Zinkiewicz

MA-6 ABSOLUTE RATES OF COLLISIONAL DEACTIVATION OF Hg($6p\ ^3P_2$) BY NITROGEN AND CARBON MONOXIDE (7 min.)
R. Burnham and N. Djeu

MA-7 MEASUREMENTS INVOLVING RARE GAS ATOMS IN HIGH RYDBERG STATES (7 min.)
T. B. Cook, W. P. West, F. B. Dunning, and R. F. Stebbings

SESSION MB. POSITIVE COLUMN AND IONIZATION

9:00 AM - 10:10 AM, Friday, October 25
Brazos Room
Chairman: A. V. Phelps, JILA

MB-1 POSITIVE COLUMN OF A.C. OPERATED Na-Ne-Ar LOW-PRESSURE DISCHARGES (7 min.)
H. v. Tongeren and J. de Ruyter

MB-2 CALCULATIONS ON LOW PRESSURE SODIUM-MERCURY-NEON DISCHARGES (7 min.)
T. G. Verbeek

MB-3 RADIATION MEASUREMENTS OF LOW PRESSURE CADMIUM-NEON DISCHARGES (7 min.)
H.J.F.G. Smets and T. G. Verbeek

MB-4 MAINTENANCE ELECTRIC FIELDS IN A H_2-He D.C. GLOW DISCHARGE (7 min.)
C. H. Muller and A. V. Phelps

MB-5 INVESTIGATION OF THE TWO FORMS OF THE OXYGEN DISCHARGE (7 min.)
J. W. Dettmer and A. Garscadden

MB-6 DETERMINATION OF TOWNSEND'S FIRST IONIZATION COEFFICIENT FOR 0_2 USING H_2 TO SUPPRESS THE REACTIONS OF 0^- (7 min.)
R. J. Corbin and L. Frommhold

MB-7 SPECTROSCOPIC MEASUREMENTS OF THE ELECTRON DENSITY EVOLUTION WITHIN A CORONA DISCHARGE IN OXYGEN (7 min.)
F. Bastien, B. Fertil, and E. Marode

SESSION NA. LASER BREAKDOWN AND DISCHARGE MODELING

10:45 AM - 11:55 AM, Friday, October 25
Crystal Ballroom
Chairman: B. E. Cherrington, U. of Illinois

NA-1 TWO-DIMENSIONAL MODEL FOR SUBSONIC LASER SPARKS (7 min.)
J. H. Batteh and D. R. Keefer

NA-2 SPECTROSCOPIC STUDY OF A STATIONARY LASER PRODUCED AIR PLASMA (7 min.)
Dennis R. Keefer, Bruce B. Henriksen, and William F. Braerman

NA-3 LOSS MECHANISMS IN ARGON GAS BREAKDOWN USING 10.6μ RADIATION (7 min.)
Carlton D. Moody

NA-4 EXPERIMENTAL EVIDENCE FOR TWO-STEP EXCITATION/IONIZATION IN HIGH PRESSURE RARE GAS DC TOWNSEND DISCHARGES (7 min.)
P. E. Thiess and G. H. Miley

NA-5 NON-MAXWELLIAN ELECTRON EXCITATION IN HELIUM (7 min.)
E. L. Maceda and G. H. Miley

NA-6 NUMERICAL SIMULATION OF AC GAS DISPLAY DISCHARGES (7 min.)
C. Lanza, W. E. Howard, and O. Sahni

NA-7 ELECTRON BEAM CONTROLLED LOW IMPEDANCE DISCHARGES (7 min.)
R. O. Hunter

SESSION NB. HEAVY PARTICLES

10:45 AM - 11:45 AM, Friday, October 25
Brazos Room
Chairman: C. Latimer, Rice University

NB-1 RADIATIVE LIFETIMES OF THE (0,0) BAND OF THE $B^2\Sigma^-$ STATE OF CH (7 min.)
D. M. Wilcox and R. A. Anderson

NB-2 MEASUREMENT OF THE DISSOCIATIVE LIFETIMES OF DOUBLY-IONIZED METASTABLE DIATOMIC MOLECULES-CO^{++} (7 min.)
R. G. Hirsch, R. J. Van Brunt, and W. D. Whitehead

NB-3 RATE PROCESSES RELATED TO THE JESSE EFFECT IN He (7 min.)
M. G. Payne, G. S. Hurst, and C. E. Klots

SESSION AA

8:30 AM - 10:15 AM, Tuesday, October 22

Crystal Ballroom

CO_2 ELECTRIC DISCHARGE AND UV PREIONIZATION LASERS

Chairman: M.J.W. Boness, Avco Everett

AA-1 Theoretical Performance Characteristics of CW CO_2 Electric Lasers.* H. H. LEGNER and J. H. JACOB
Avco Everett Res. Lab., Inc., Everett, Massachusetts.
Predictions of small signal gain, optical quality (medium refractive index), and output power are presented for CW CO_2 electric laser configurations. The fluid mechanics, plasma dynamics, and kinetic rate processes have been solved simultaneously for two cavity configurations: flow parallel and flow transverse to the electric field. We consider both recombination and attachment dominated discharges. The coupling is a result of the density dependent electrical conductivity and temperature (both gas and electron) dependence of the kinetic rates. Most of the electrical power goesinto excitation of the upper CO_2 laser level. Because of collisional deactivation some of this energy ends up as gas temperature. However collisional deactivation depopulates the upper level more slowly than laser flux. As a result there can be a marked difference between the lase/no lase characteristics. Comparison with experiment has been made. [1]

[1] M. J. Yoder and D. R. Ahouse, 27th Gaseous Electronics Conf. (1974) (following paper)

*Supported by DARPA/ONR under Contract No. N00014-73-C-0363

AA-2 Experimental Characteristics of a Subsonic CW CO_2 Electric Laser.* M. J. YODER and D. R. AHOUSE,
Avco Everett Res. Lab., Inc., Everett, Massachusetts.
Experiments have been carried out with an electron-beam-sustained electric-discharge flowing carbon dioxide subsonic CW laser in which the gas flow is parallel to the electric field. Input power, electron density, electric field per particle, and other experimental parameters have been obtained for several different gas mixtures. Small signal gains and interferometric gas density measurements show a significant fraction of the input energy to be "hung-up" in the vibrational excited states in agreement with theory. [1] As a result, meaningful medium homogeneity (optical quality) measurements must be obtained under lasing conditions and cannot be extrapolated from zero flux results.

[1] H. H. Legner and J. H. Jacob, 27th Gaseous Electronics Conf. (1974) (preceding paper).

*Supported by DARPA/ONR under Contract No. N00014-73-C-0363.

AA-3 A Six-Temperature CO_2 Laser Kinetics Model. L. H. TAYLOR, L. A. WEAVER, and R. W. LIEBERMANN. Westinghouse Research Labs.--A six-temperature Boltzmann equilibrium model has been developed for pulsed CO_2 lasers composed of CO_2, N_2, He and H_2O. The N_2 vibrational mode, the H_2O bending mode and the CO_2 asymmetric, symmetric, and bending modes are considered to be perfect harmonic oscillators characterized by individual Boltzmann temperatures. The gas temperature is described by an energy balance equation, and the effects of external mirrors are treated through a laser photon flux equation. Electrical excitation, uniform gas flow cooling, and 24 temperature-dependent collisional relaxation rates are included. Computer solutions have been compared with temporally-resolved measurements of 10.59 μm gain and gas temperature for self-sustained discharges in 600 Torr, 1:2:3 laser mixtures. Excellent agreement was obtained when the portion of electronic excitation contributing to direct gas heating was adjusted to 24%. Neglecting this single fitting parameter yielded substantial deviations from measured values, particularly the gas temperature. Thus previously undocumented sources of gas heating significantly affect relaxation processes in self-sustained CO_2 laser discharges, and are likely important in CO lasers as well.

AA-4 Theoretical and Experimental Gain and Output in Electron-beam Sustainer Lasers. D.H. DOUGLAS-HAMILTON, R.S. LOWDER, R.M. FEINBERG,* Avco Everett Res. Lab. -- Theoretical predictions of gain and laser output from a six temperature model of the CO_2 laser system are compared with experiments performed on electron-beam sustainer lasers at both atmospheric and 1/10 atmospheric pressure. Gain and laser output measurements have been made at temperatures near 200°K and 300°K. Various gas mixtures have been investigated theoretically and experimentally. Specific output $J > 100$ joule/liter atm was obtained both in $He: N_2: CO_2: H_2$ 3: 2: 1: 0 and 0: 3: 1: .08, with efficiencies near 30%. In all cases there appears to be good agreement between theoretical prediction and experiment.

* This work was supported in part by Air Force Special Weapons Center, Kirtland AFB, New Mexico, under Contract No. F29601-73-C-0116.

AA5 Electron Attachment and Recombination Rate Measurements Relevent to CO_2 and CO Laser Operation. Alan E. Hill, Air Force Weapons Laboratory---Attachment and recombination rates for gases used in molecular laser are derived from current conductivity time dependence measurements. The initial ionization source is a 50 nanosecond photo-preionized avalanche discharge. E/P and temperature conditions during the measurements simulate laser conditions for which little experimental data currently exists--for example at 77°K and when E/P is below townsend breakdown values in CO. Preliminary results indicate recombination coefficients are lower than previously thought for CO_2 laser mixtures and that attachment plays a non-negligible role.

AA-6 Charged Particles Loss Processes in Electron Beam Controlled Discharge*° D. PIGACHE, G. FOURNIER and P. GOTCHIGUIAN, Office National d'Etudes et de Recherches Aérospatiales (ONERA)- A pulsed electron beam controlled discharge has been studied for a pressure between 100 and 600 Torr, and electron density between 10^{10} and 10^{12} cm^{-3} and a reduced electric field E/N between 10^{-18} and 2×10^{-16} Vcm^3. Difficulties due to electron attachment on impurities diffusing from the electrodes had to be overcome; good measurements of the recombination coefficient have then been obtained in pure nitrogen. A $\varepsilon^{-3/2}$ law is observed for the recombination coefficient (where ε is the average electron energy). This method is being used to measure the recombination coefficient in gas mixture of practical interest in electron beam CO_2 laser.

* Submitted by J. Taillet

° Work supported by the DRME (Research Department of the French Ministry of Defense).

AA-7 Time Dependence of Rotational Temperature In A High Pressure Pulsed CO_2 Laser. W. T. LELAND, M.J.KIRCHER M.J.NUTTER & G.T.SCHAPPERT, Los Alamos Scientific Laboratory.--The time variation of CO_2 rotational temperature has been deduced from small signal gain measurements on an e-beam stabilized 600 torr discharge in a $3/\frac{1}{4}/1$: $He/N_2/CO_2$ mixture. As has been noted by other investigators, knowledge of the small signal gain over a span of P and R branch lines can be used to gain information about rotational temperature and level densities provided one knows the functional dependence of gain on line number, rotational temperature, level density, etc.

Our data yields a better fit to theoretical predictions if we include a rotation vibration interaction factor similar to that noted by Arie. Specifically we use:

$$g = g_o J_G \frac{(1+.0012J_G\Delta J)}{\lambda_J} \left\{ \exp\left[\frac{-.55647J_U(J_U+1)}{T_{Rot}}\right] - 1.0007 \frac{n_{100}}{n_{001}} \exp\left[\frac{-.56064J_L(J_L+1)}{T_{Rot}}\right]\right\}$$

where g_o is a constant; J_G is the larger of the J values involved; and ΔJ is 1 or -1 for P or R branch lines respectively.

AA-8 Volumetric UV Photo-Ionization in CO_2 Laser Media.* R. V. BABCOCK, Westinghouse Research Labs.--Self-sustained discharges initiated by UV volume photo-ionization are an excellent means of pumping pulsed, high-power lasers. To aid in scaling uniform discharges to large volume, photoelectron generation from a bare spark source was measured versus source distance (d = 2-22 cm), gas composition and pressure (P = 0.2-1 atm), peak spark current (j = 10-1200 amp), spark supply energy (J = 0.0125-2.5 Joules), and spark duration (T = 0.02-40 μs). The controlling physical mechanisms are now sufficiently understood to specify the initial electron distribution produced by an array of spark sources in an arbitrary CO_2, N_2, He discharge volume. Electron production results entirely from direct one-photon ionization of $\approx 10^{-6}$ atm of impurities, by 10.0-10.6 eV photons. Spatial distribution is determined entirely by non-ionizing attenuation of these photons by the CO_2 fraction, and geometry. Electron production from a bare spark is adequately described by $n_e = K \times 10^4\ j\ J^{1/2}\ d^{-2}\ P^m \exp(-1.45\ P_c d)$ electrons/cm^3, where P_c = atm. CO_2, K = 25.5, 15.2, or 7.4 for CO_2:N_2:He = 1:7:0, 1:2:3, or 1:1:8, and m = 3/2 or 1/2, depending on the source of the ionizing impurity.

*Work supported by AFWL.

AA-9 Glow Discharge Formation with UV Volume Preionization* L. E. KLINE and L. J. DENES, Westinghouse Research Laboratories --Discharge formation has been studied experimentally and theoretically for CO_2 planar TEA laser discharges. The theory predicts preionization densities, the spatiotemporal development of the discharge plasma, and voltage and current waveforms which are in very good agreement with experimental results. The theoretical model accounts for cathode photoemission and anode collection of electrons, discharge circuit interactions, and gaseous ionization processes. The results of calculations, which assume strong preionization and moderate overvoltages, show that 1) the formative time is independent of discharge volume, 2) the glow formation threshold is a few percent below the Townsend breakdown voltage, and 3) cathode photoemission and anode collection of electrons can be neglected. Formation calculations for a large volume discharge show that a uniform glow discharge develops even when the preionization is nonuniform along the electric field.

*Work supported in part by the U.S. Air Force Weapons Laboratory under Contract No. F29601-73-C-0121

SESSION AB

9:00 AM - 10:10 AM, Tuesday, October 22

Brazos Room

NEGATIVE IONS

Chairman: J. L. Franklin, Rice University

AB-1 Electron Detachment in Collisions of Cl^- with the Rare Gases.* R. L. CHAMPION and L. D. DOVERSPIKE, Col. of William and Mary.--Relative elastic differential scattering cross sections have been measured for the systems $Cl^- + X \rightarrow Cl^- + X$ (Where X = Ne, Ar, Kr, Xe) in the energy range 5 - 50 eV. All the differential cross sections exhibit dramatic thresholds at values of $E\theta \sim 1100$ eV. deg. which correspond to the onset of electron detachment. These results have been analyzed in terms of the complex potential theory. Using existing expressions for the real parts of the potentials, we are able to determine the regions in which the discrete states cross the neutral curves (i.e. the states corresponding to $Cl + X + e^-$) as well as the imaginary parts of the potentials. Further implications of the complex potential model for the systems will be discussed.

AB-2 Endoergic Ion-Molecule-Collision Processes of Negative Ions. KAMEL M.A. REFAEY*, Physics Department, Cairo University, Cairo, Arab Republic of Egypt, and J. L. FRANKLIN, Chemistry Department, Rice University, Houston, Texas 77001 - A new method[1] for the investigation of endoergic ion-molecule-collision processes of negative ions has been developed. This method is, in effect, an extension of an earlier one developed by Refaey and Chupka[2] used in connection with positive ions. The method will be described in detail. Results of measurements of collision of I^- on O_2 will be presented.

* Present Address - Chemistry Department, Rice University, Houston, Texas 77001

1. Refaey, Kamel M.A., Franklin, J. L. J. Chem. Phys., 61, 733 (1974)

2. Refaey, Kamel M.A., Chupka, W. A. J. Chem. Phys., 43, 2544 (1965)

AB-3 Charge Transfer of H^- and D^- with O_2*. P.E. CHAPLIN and W.R. SNOW, University of Missouri-Rolla--A relative measurement of the charge transfer cross section for H^- and D^- with O_2 has been made using a crossed beam technique over an energy range of 20 eV to 10 keV. The magnitude of the cross sections was determined by normalization to the O^-+O_2 charge transfer data of Rutherford and Turner[1]. The cross sections appear identical within experimental error and have a single maximum of 14 $Å^2$ at a relative velocity of 1.3×10^7 cm/sec. Agreement with the data of Bailey and Mahadevan[2] is good except at energies below 40 eV. Extrapolation of the D^- data to 9 eV fits well with the measurement of Tiernan, et al.,[3] from 0.3 to 9 eV. At high energies the present experiment fits well with data of Pilipenko[4] and Fogel[5] whose measurements extended from 10 to 50 keV.

*Supported in part by the National Science Foundation.
[1]J.A. Rutherford, B.R. Turner, J.G.R., 72, 3795 (1967).
[2]T.L. Bailey and P. Mahadevan, J. Chem. Phys., 52, 179 (1970).
[3]T.O. Tiernan, et al., J. Chem. Phys. 55, 5692 (1971).
[4]D.V. Pilipenko, et al., Sov.Phys.-JETP 22, 965 (1966).
[5]Y.M. Fogel, et al., Sov. Phys.-JETP 13, 8 (1961).

AB-4 Negative Ions from Charge Exchange*

G.P. RECK, S.Y. TANG, and E.W. ROTHE, Wayne State Univ.--A 5-350 eV neutral cesium beam is crossed with a beam of target molecules forming Cs^+ and negative ions as previously described.[1] The negative ions are focused into a quadrupole mass filter and are counted. The observed mass spectra are qualitatively different from those produced by electron impact. Parent ions are observed from a variety of molecules such as PBr_3, $SnCl_4$, $TiCl_4$, CF_3COCF_3, CF_3I, while only fragments were counted with PF_3, $SiCl_4$, CH_3COCH_3, CH_3I. The implications of these results will be discussed.

*Supported by the Air Force Office of Scientific Research and Army Research Office - Durham.
[1]S.Y. Tang, E.W. Rothe and G.P. Reck, Int. J. Mass Spectrom. Ion Physics 14, 79 (1974).

AB-5 Adiabatic Electron Affinities from Collisional Ionization* C.B. LEFFERT, S.Y. TANG, and E.W. ROTHE, Wayne State Univ.--A previously described time-of-flight apparatus[1] is used to obtain the energy dependence of the collisional ionization cross section for the formation of Cs^+ in the near-threshold range. This experiment has low center-of-mass energy spread. The data is deconvoluted and the c.m. threshold is determined. This value is subtracted from the ionization potential of Cs to obtain the adiabatic electron affinity. For Cl_2, Br_2, and I_2, the electron affinity is 2.50, in good agreement with previous results. For SF_6 and CF_3I, the electron affinities are 0.75 and 1.29eV, respectively.

*Supported by the Air Force Office of Scientific Research and by the Army Research Office-Durham.

[1]C.B. Leffert, W.M. Jackson and E.W. Rothe, J. Chem. Phys. 58, 5801 (1973).

AB-6 Angular Distribution of O^- from Dissociative Electron Attachment to NO.†R.J. VanBrunt, Univ. of Va., L.J. Kieffer,* Joint Institute for Laboratory Astrophysics.* — The electron energy dependence of the angular distribution of O^- from NO has been measured in the energy range 8.0 to 11.0 eV. The distributions are found to be anisotropic and of a form that is nearly $\sin^2\theta$ at all energies. Deviations from a $\sin^2\theta$ dependence are discussed in terms of the relative contributions of the different partial waves of the incident electron to the differential cross section. The results indicate that the final repulsive negative ion resonances involved must be either Σ or Δ states, and can be most simply explained by assuming that dissociative attachment proceeds via a single $^3\Sigma^-$ state analogous to the $B^3\Sigma_u^-$ state of isoelectronic O_2.

†Supported by the National Science Foundation.
*Of the National Bureau of Standards and the University of Colorado.

AB-7 Negative Ion Formation in Cerium Triiodide.
P.J. CHANTRY, Westinghouse Research Labs.--The formation of negative ions in CeI_3 has been studied by heating solid samples to $\sim 1000°K$ and confinement of the resulting vapor in a collision chamber held at a suitably higher temperature. The collision chamber is traversed by an electron beam and the resulting ions are mass-analyzed. Fragment ions I^-, I_2^-, CeI^- and CeI_2^- are observed, and their appearance potentials are interpreted in the light of available knowledge of bond strengths (D) and affinities (A). Resulting derived quantities include $D(CeI_2 - I) \leq 3.0$ eV; $A(CeI_2) \geq 0.3$ eV; $D(CeI - I_2) \leq 5.7$ eV; $D(Ce-I) \geq 3.8$ eV, and $D(Ce - 2I) \geq 8.0$ eV. CeI_3^- is also observed, formed by direct attachment of very low energy electrons, and additionally by charge transfer from CeI_2^-. Background ions, not formed by the electron beam, include I^- and CeI_4^-. Their relative intensities are consistent with the reaction $CeI_4^- \rightleftharpoons CeI_3 + I^-$ being in equilibrium at the collision chamber temperature. Based on the above we can conclude that the negative ions produced by the addition of Ce to a mercury arc already containing iodine[1] will be insignificant compared with the existing I^- ions.

1. See for example R. J. Zollweg, J. J. Lowke, and R. W. Liebermann, this conference.

SESSION B

10:45 AM - 12:05 PM, Tuesday, October 22

Crystal Ballroom

MOLECULAR DISCHARGE INSTABILITIES

Chairman: L. Denes, Westinghouse

B-1 Thermal Instability in High Power Laser Discharges. J. H. JACOB and SIVA A. MANI, Avco Everett Research Laboratory, Inc., Everett, MA. -- We have obtained a dispersion relation for unstable acoustic and thermal waves in a high pressure discharge. The thermal wave is a low frequency wave whose growth rate can be larger than the frequency of oscillation. The coupling between electrical power into the gas and the acoustic and density disturbances occurs because of a density dependent conductivity. We find the growth rate of the instability to be proportional to the power density. Effects of fluid viscosity and thermal conductivity have been neglected. One of the modes has a large growth rate under certain conditions and this may lead to the constriction of the discharge[1] and eventual arcing.

[1]E. F. Jaeger and A. V. Phelps, Bull. Am. Phys. Soc. 19, 147 (1974).

B-2 Causes of Arcing in CO_2 Laser Discharges*. W. L. NIGHAN and W. J. WIEGAND, United Aircraft Research Laboratories.-- Analysis of collision processes in volume dominated CO_2 lasers has identified the fundamental factors causing glow-to-arc transition. It is shown that arcing can be initiated by the growth of disturbances in either translational or vibrational energy density. Calculations for pressures up to atmospheric and cw electrical power densities up to 100 Wcm^{-3} indicate that thermal and/or vibrational instabilities will occur for most laser conditions of interest. However, since the growth time for these instabilities is on the order of a millisecond, locally unstable fluid elements can be convectively removed in a time less than the arc formation time resulting in an apparently stable discharge. Factors influencing the growth rate of these instabilities will be discussed in detail. Measured arc formation times are consistent with computed values. *Work performed in part through the sponsorship of the Office of Naval Research, the AF Aerospace Research Laboratories and the AF Weapons Laboratory under Contract No. F33615-73-C-4107.

B-3 Initial Development of Glow-to-Arc Transition Due to Electric Field Distortion. GERALD L. ROGOFF, Westinghouse Res. Labs.--Calculations indicate that distortion of the axial field distribution by nonuniformities in the electrical conductivity is important in the constriction of a diffuse glow discharge. For current continuity, a local increase in conductivity σ causes an enhanced field intensity E in regions adjacent axially and a reduced E in regions adjacent radially. If σ is a function of E and local positive feedback occurs, the field nonuniformity can lead to axial growth of the perturbation in σ and current constriction. A two-dimensional, time-dependent model has been developed and applied numerically to the case of a simple diatomic gas which can thermally dissociate, with the electron temperature V_e increasing with dissociation due to the removal of molecular excitation as an electron energy loss mechanism. Since σ is a sensitive function of V_e through the ionization rate, the increases in V_e due to the field-distortion-enhanced gas heating and dissociation lead to a propagating ionization instability. Calculations have been made for conditions similar to those of nitrogen spark discharges (150-300 Torr) for which published experimental data exist. Propagation velocities compare well. Results include contours of filamentary channels of enhanced conductivity.

B-4 The Dispersion of Ionization Waves in the Presence of Negative Ions. W. H. LONG, JR., W. F. BAILEY, and A. GARSCADDEN, Aerospace Research Laboratories, WPAFB, O.--The moment equations for a plasma consisting of positive ions, negative ions and electrons, and Maxwell's equations for the electric field were solved numerically using boundary conditions appropriate to the positive column of an electric discharge. Oscillatory solutions were found which appear to correspond to experimentally observed standing and moving striations. The processes driving the oscillations are production by ionization and detachment and losses through attachment and diffusion. These rates were then varied to determine the effects of each on the frequency and amplification of the striations. Also, the dispersion relation was derived for small-amplitude waves as a function of the propagation direction. The frequency, wavelength, phase relationships and onset conditions determined from this analysis are compared with the numerical calculations and experimental observations.

B-5 Stabilization of a Medium Pressure Discharge by Turbulent Flows.* O. BIBLARZ and L.J. AUNCHMAM, Naval Postgraduate School.--Grid-generated turbulence has been studied as a stabilizing agent in atmospheric air and nitrogen discharges. Spectral turbulence data, obtained with a hot wire anemometer, are compared with the discharge characteristics for various grids and several velocities. It is found that certain turbulent flows have a profound effect on the stability of the discharge and that this effect appears to go beyond the creation of a more homogeneous velocity distribution. Also, the mere lengthening of ion paths falls short of explaining the observations. Turbulent mixing seems to play a fundamental role on the cumulative processes that lead to streamer formation.

*Submitted by A.E. FUHS.

SESSION CA

1:30 PM - 2:50 PM, Tuesday, October 22

Crystal Ballroom

CO AND N_2 LASERS

Chairman: S. Rockwood, Los Alamos

CA-1 Observations of Small Signal Gain in a High Pressure Pulsed CO Electric Discharge Laser.*
M. J. W. BONESS and R. E. CENTER, Avco Everett Research Laboratory, Inc. -- Measurements of small signal gain and spectral distribution in a high pressure, low temperature, pulsed, carbon monoxide electric-discharge laser are reported. These are the first reported measurements performed in a high pressure, large volume, uniformly excited CO laser. Theoretical calculations based upon a model which predicts partial inversions on several vibrational bands as a consequence of anharmonic pumping show qualitative agreement with the measured quantities. A detailed comparison between the theory and experiment will be presented.

*Work supported by the Advanced Research Products Agency.

CA-2 V-V Pumping In High Power CO Lasers. W. L. Thweatt, G. W. Sullivan and R. F. Weber, Air Force Weapons Laboratory---Time resolved spectral measurements of high power CO laser pulses at 300°K are presented for CO and mixtures containing N_2, Ar and He. These results confirm that V-V pumping of high CO vibrational levels does occur at room temperature with high input power densities. The data illustrates the time dependence of single line laser emission for the various gas mixtures; relative intensity as a function of the upper vibrational level of the transition; laser onset time vs. upper vibrational level for various gas mixtures; and a comparison of experimental results with predicted single line intensities. Energy transfer from N_2 is observed to result in laser output on relatively high lines (v = 10 to 15) indicating strong V-V pumping of these vibrational levels. The high energy loading (1 KJ/L-atm) was accomplished with a 2 μsec discharge sustained by a previously described[1] cold-cathode electron beam.

[1] R. D. Hunter, G. W. Sullivan, W. Beggs, presented at 1973 CLEA, Washington D. C. May 1973

CA-3 High Power E-Beam Plasma Diode CO Laser. B. B. O'BRIEN, Northrop Research and Technology Center, Laser Technology Laboratories - A small simple electron beam stabilized electric discharge CO pulse laser was designed as a source of high power, medium energy CO radiation. The laser produces short pulse (~20μs) multiline radiation in excess of 0.5 MW (pulse energy up to 13J). The discharge is stabilized by a plasma electron gun[1] and has an extractable excited volume 13 cm long x 4.35 cm diameter. With a CO/N_2 mixture at 0.58 amagat, the maximum electrical pump power is 45 kW/cm^3 (0.6 J/cm^3 energy disposition). Laser performance with argon and nitrogen diluents at 150 and 170°K and various pump rates will be reported. The output spectrum contained radiation between 5.023 and and 5.430μm.

1. B. B. O'Brien, "Characteristics of a Cold Cathode Plasma Electron Gun," Appl. Phys. Letters 22, 10, 1973.

CA-4 Acoustic Velocity Measurements to Determine Laser Gas Heating Rate.* R. G. EGUCHI, G. L. McALLISTER, and V. G. DRAGGOO, Northrop Research and Technology Center. --The bulk gas heating in a pulsed electric discharge laser gives rise to acoustic waves which propagate with a temperature dependent velocity. The change in acoustic velocity with the change in electric excitation rate has been used as a simple technique for approximate measurement of the heating rate for a 500 Joule/pulse CO electric discharge laser. Interferometric measurements of the acoustic waves and the coincidence of perturbations in the laser intensity as the acoustic waves pass through the optical axis of an unstable resonator have been used to demonstrate this technique.

This research was supported in part by the ARPA of the Department of Defense and was monitored by the Office of Naval Research under Contract N00014-72-C-0043.

*Submitted by M. L. BHAUMIK.

CA-5 Monte-carlo Calculation of ionization profile due to electron beam in CO-He System. Frank T. Wu, Comarco Engineering Div., Ridgecrest, Calif. and Eric A. Lundstrom Naval Weapons Center, China Lake, Calif.

A Monte-carlo method has been performed to simulate the behavior of electron-beam with tens of kilo-electron volts of energy entering a CO-He mixture. The fast electrons lose energy and suffer scattering during the encounter with the molecules in the system. As a result, the energy deposition of fast electron in the system presents a nonuniformity in both incident and transverse directions. Accordingly, it is found that the secondary electrons are distributed in patterns that are non-uniform in both incident and transverse directions.

CA-6 A Study of Charged Particle Densities and Electric Field in E-Beam Sustained Gas Discharges. C. BAUGH, J. BRADLEY, E. MALARKEY and H. TRENCHARD, Westinghouse Electric Corp., Baltimore. -- Equations are derived to determine the space-time development of electron and ion densities and the electric field inside an E-beam sustained gas discharge. The cavity may have cylindrical or planar symmetry. A code was written to determine the requisite quantities; it employs an explicit difference scheme to first order and contains a diffusion-like term in the continuity equations to insure convergence. Applications were made to pure N_2 in both geometries. Primary E-beam ionization was estimated using Spencer's dose curves; all transport coefficients express field dependence where appropriate. Calculations were carried out up to 160 nsecs; the results for cylindrical and planar symmetries are similar in this time interval. The development of a "cathode-fall" is apparent from t=0, and for an initial field of 3.5 KV/cm and after Townsend ionization becomes effective, the field at the cathode drops at a fairly constant rate of 1 KV/cm per nsec. The space-time variation of the E-field in the "positive column" has been determined, and after 50 nsecs a slight excess of elections is evident in this region.

CA-7 Experimental Investigation of High Power N_2 Lasers*
W.A.Fitzsimmons, L.W.Anderson, and J.M.Vrtilek, University of Wisconsin, Madison, Wisc. Measurements of the peak power and pulse duration of various megawatt N_2 lasers have been carried out as a function of E/P in the laser, repetition rate, impedance of the energy delivery transmission line, switch and laser tube inductance, speed and uniformity of gas flow, gas mixture composition, and laser tube length. The laser output is a maximum when E/P $\sim$ 100 V/cm torr, and when the gas flow leaves a uniform ion distribution to seed the next discharge. The output power at high repetition rates appears to be limited by the residual ionization in the gas and not by long lived metastable states. The addition of He up to partial pressures of 1 atmosphere does not affect the N_2 laser performance; but even 5 torr of Ar added to the N_2 quenches the 337.1 nm laser light. These experimental results will be interpreted in terms of a simple model for the N_2 laser in the next paper. We have not achieved a traveling wave discharge and the criterion for such a discharge will be discussed.

*Work supported by the U.S. Atomic Energy Commission and the National Science Foundation.

CA-8 A Theoretical Treatment of the Nitrogen Laser*
C.E.Riedhauser, L.W.Anderson, W.A.Fitzsimmons, University of Wisconsin, Madison, Wisc. A model of the N_2 laser is presented and compared with the experimental results of the previous paper. The time dependent loading of the transient high voltage source is determined by using Townsend ionization and drift velocity data to establish the temporal behavior of E/P in the discharge. The Townsend coefficient is used also to determine the electron temperature in order to calculate the instantaneous electron excitation rates of the $C^3\Pi$ and $B^3\Pi$ upper and lower laser levels. The photon rate equation is solved to give laser peak power and pulse width. The numerical solutions to the coupled non-linear rate equations give very close agreement with the broad range of experimental data. The effects of added He and Ar are explained in terms of the effect of these atoms on the electron temperature. The application of this model to other lasers and the possibility of more powerful N_2 lasers will be discussed.

*Work supported in part by U.S. Atomic Energy Commission and the National Science Foundation.

SESSION CB

1:45 PM - 2:55 PM, Tuesday, October 22

Brazos Room

CHARGE TRANSFER

Chairman: R. F. Stebbings, Rice University

CB-1 Electron-Transfer in Collisions Between Atomic Ions and Rare-Gas Atoms. WILLIAM B. MAIER II, Los Alamos Scientific Laboratory.--Cross sections, σ, have been measured for electron transfer between rare gas atoms and H^+, He^+, Ne^+, Ar^+, and Kr^+, for center-of-mass energies $E_o \leq 60$ eV. The cross sections all decrease rapidly as E_o is lowered below some value, and many appear to have thresholds. These apparent threshold energies, $-Q_a$, do not correspond to energy absorbed in the production of ground-state products. For given primary ion, $-Q_a$ is larger for heavier target atoms. For given primary ion and E_o, heavier target atoms correspond to larger σ. Considerable forward momentum is transferred from the primary ions to the product ions in these electron-transfer reactions, and the laboratory-energy distribution of secondary ions may have more than one peak. Structure is found in the cross section for $Kr^+ + Ar \rightarrow Ar^+ + \ldots$ and may also occur for $Ne^+ + Ar \rightarrow Ar^+ + \ldots$

CB-2 Elastic Scattering and Charge Transfer of Low-Energy He^{++} Ions with Ne, Ar, and Kr.* T. M. AUSTIN, J. M. MULLEN, C. L. BOTTOMS, and T. L. BAILEY, U. of Florida.--Relative differential cross-sections for elastic scattering, and for the formation of He^+ by charge transfer, have been measured in ion-beam gas-target experiments for the collision pairs He^{++}-Ne,Ar, and Kr, over the laboratory KE range $8 \leq E_1 \leq 60$ eV. An analysis of the data, based on an approximate form of the optical model, indicates that the pronounced shoulders observed in the $\sigma_{el}(\theta)$ vs. θ curves arise from elastic scattering by an attractive potential well, in the presence of concurrent inelastic scattering. This analysis (in conjunction with the data) gives estimated well-depths for the ground electronic states of $(HeNe)^{++}$, $(HeAr)^{++}$, and $(HeKr)^{++}$ of (respectively): 1.0, 2.1, and 2.6 eV. Information concerning the internal states of the charge transfer products was also obtained, from measurements of the KE distributions of the product He^+ ions. It was found that for He^{++}-Ar and He^{++}-Kr, transfer proceeds via a number of channels, whereas for He^{++}-Ne, transfer proceeds via the single channel: $He^{++} + Ne = Ne^+(2s2p^6\ ^2S) + He^+(^2S)$. In a separate apparatus, measurements of absolute total cross-sections for He^+ formation in all three collision systems are in progress.

* Supported by the U. S. Office of Naval Research

CB-3 Charge Transfer From O^+ and N^+ to Neutral Uranium and Thorium.* J. A. RUTHERFORD and D. A. VROOM, Intelcom Rad Tech. --Cross sections for charge transfer from O^+ and N^+ to neutral uranium and thorium have been measured in the energy range from 1 to 500 eV ion energy. In the course of the work, data were also obtained for charge transfer from N_2^+ and CO_2^+ to the metal atoms. The measurements were carried out using crossed ion modulated neutral beam techniques. The metal atom beams were formed by heating the pure metals to approximately 2500°K in resistively heated tantalum tubes. These tubes had a double wall structure such that the bulk of the molten metal (U or Th) did not come in contact with the outer wall of the furnace. The cross sections for all reactions measured exhibits similar behavior in that they increase in magnitude as the energy of ions decreases. The cross sections for the molecular ions are larger than those for the atomic ions.

*Work supported by the Defense Nuclear Agency under Contract No. DNA001-74-C-0036.

CB-4 Measurement of the Charge Transfer Cross Sections for Ground and Excited State O^+ in Collision with O_2 and NO.* J. A. RUTHERFORD and D. A. VROOM, Intelcom Rad Tech. --Cross sections for the reactions $O^+(^4S) + O_2 \rightarrow O + O_2^+$, $O^+(^2D) + O_2 \rightarrow O + O_2^+$, $O^+(^4S) + NO \rightarrow O + NO^+$, and $O^+(^2D) + NO \rightarrow O + NO^+$ have been measured in the energy range from 1 to 500 eV ion energy. In the ion source of our crossed beam apparatus, control of the electron energy allows formation of ion beams containing only ground state O^+ or composite beams containing both ground and metastable state O^+. Excited state cross sections are determined from knowledge of the ground state cross section, the composite beam cross section and the fraction of metastable present in the mixed beam. This latter information is obtained from attenuation experiments performed independently in our laboratory.

*Work supported by the Defense Nuclear Agency under Contract No. DNA001-74-C-0036.

CB-5 Energies of Products for Charge-Transfer of N_2^+ in O_2.* G. D. MAGNUSON and R. H. NEYNABER, Intelcom Rad Tech.--Information on W', the total relative kinetic energy of the products in the center-of-mass system, was obtained for the charge-transfer reaction $N_2^+ + O_2 \rightarrow N_2 + O_2^+$ (3.5 eV exothermic for ground-state reactants and products). This information was extracted from laboratory-energy distributions of O_2^+, which were measured by a merging-beams technique over a range of interaction energy W from 0.1 to 5 eV. The conclusions are that for ground-state reactants virtually all of the O_2^+ is confined to scattering spheres in the center-of-mass system for which $W' \approx W$, almost all of this scattering is in the direction of the reactant O_2, and the products are in excited states.

*Supported by the Office of Naval Research, Contract No. N00014-74-C-0011.

CB-6 Nonresonant Behavior of the Symmetric Charge-Transfer Cross Section for Deuterium Molecules. HAROLD L. ROTHWELL, BERT VAN ZYL, AND ROBERT C. AMME, U. of Denver.--Measurements have been performed of the symmetric charge transfer cross section for D_2^+ ions on a gaseous D_2 target. The energy range covered is from 50 eV to 2000 eV, sufficient to connect the results of other investigators[1,2]. Ions were formed in an electron impact source with energy spread of 0.7 eV FWHM, operating at 18 eV electron energy. The measured cross section was found to be nearly independent of electron energy above this value. The cross section was found to exhibit a relative minimum at an energy of about 600 eV, a conclusion reported earlier[3] for the $H_2^+ + H_2$ case. The results for the two isotopic species are nearly identical from 50 to 500 eV. Above 600 eV, both symmetric charge transfer cross sections increase with increasing energy.

[1]W. H. Cramer and A. B. Marcus, J. Chem. Phys. 32,1(1960)
[2]O. Hollricher, Z. Phys. 187, 41 (1965).
[3]H. C. Hayden and R. C. Amme, Phys. Rev. 172,1 (1968).

CB-7 Vibrational Transitions in $H_2^+ - H_2$ and $D_2^+ - D_2$ Charge-Transferring Collisions. ROBERT N. STOCKER and HERSCHEL NEUMANN, U. of Denver.--Cross sections in the center of mass energy range 25 eV to 5 keV for charge transfer involving the lowest 6 ion-molecule vibrational state products, for initial ion and neutral vibrational quantum numbers $v' = 0-3$ and $v = 0$, respectively, have been calculated by a semiclassical impact parameter method. Upper vibrational states, which become significantly populated at higher impact energies and affect some of the calculated cross sections even at lower energies, were accounted for by 6 linear combinations of ion-molecule upper-state products chosen to have maximum coupling to the 6 low-lying state products. Near 25 eV, resonant-transition cross sections are generally the largest, followed by those for nearest-to-resonant transitions. Above about 1 keV cross sections are ordered according to Franck-Condon factors for the transitions. Total cross sections depend slightly on v', are similar for the two collision systems, and in reasonable agreement with experimental data.

SESSION DA

3:30 PM - 5:25 PM, Tuesday, October 22

Crystal Ballroom

DIMER AND OTHER LASERS

Chairman: P. W. Hoff, Lawrence Livermore

DA-1 A Nitrogen Ion Laser Pumped by Charge Transfer in the High Pressure Afterglow of an e-Beam Discharge.*
C. B. COLLINS, A. J. CUNNINGHAM, and M. STOCKTON, U. of Texas at Dallas--As recently suggested by Collins, et. al.,[1] resonant charge transfer reactions provide nearly ideal laser pumping mechanisms utilizing the ionization stored in the afterglows of e-beam discharges into high pressure gases. This report discusses the first nitrogen ion laser[2] pumped by charge transfer from He_2^+. Intense laser emission in the violet at 427 nm. has been observed and found to have a linewidth less than 0.3 nm. Excitation current densities producing the 7 atmosphere afterglow were 1.4 KA/cm^2 at 1MV over a 1x10 cm transverse geometry. Under these conditions the radiative efficiency was found to be 1.9%.

*This research was supported by the U.S. Advanced Research Projects Agency of the Department of Defense and monitored by ONR under Contract No.N00014-67-A-0310-0007.

1. C. B. Collins, A. J. Cunningham, S. M. Curry, B. W. Johnson and M. Stockton, Appl. Phys. Lett. 24,477(1974).
2. C. B. Collins, A. J. Cunningham, and M. Stockton, Appl. Phys. Lett. (pending).

DA-2 Electron-beam Excited Ar and Ar-H_2 Afterglows.*
L.C. PITCHFORD and C.B. COLLINS, U. of Texas at Dallas--High pressure argon and argon-hydrogen afterglows excited by an electron-beam have been investigated in the context of high pressure gas lasers. The spontaneous emission spectra of the afterglow of mixtures of 1-50 Torr hydrogen in 3 atm. argon show two main features. A broad continuum extends to 4500 Å and is identified as the $a^3\Sigma_g^+ \rightarrow b^3\Sigma_u^+$ transition in hydrogen, the lower state being the repulsive first excited triplet state. Richardson[1] reports the peak of this continuum to be around 2500 Å. Preliminary measurements indicate lifetimes on the order of 10-20 ns at 3 atmos. total gas pressure. The second spectral feature is a line at 6965 Å identified as the $4p_{01}' \rightarrow 4s_{12}$ transition in atomic argon. Lifetimes in this case are 60-70 ns at 3 atmos. total gas pressure. The intensity of the 6965 Å line increases with decreasing concentration of H_2. A general kinetic model and evaluation of the potential of the Ar-H_2 mixture as a lasing medium will be presented.

*Supported by the U.S. Advance Research Projects Agency of the Department of Defense and monitored by ONR under Contract No. N00014-67-A-0310-0007.

1. O.W. Richardson, Molecular Hydrogen and Its Spectrum (Yale U. Press, 1934).

DA-3 Ion-Electron Recombination as a Pumping Mechanism for e-Beam Lasers.* A.J.CUNNINGHAM, G.D.MYERS, R.A. WALLER, M.STOCKTON, and C. B.COLLINS, U. of Texas at Dallas--Ion-electron recombination has been shown to hold considerable promise as a pumping mechanism for e-Beam lasers in high pressure gases.[1] Amplifiers pumped by the collisionally stabilized recombination of He_2^+ have been constructed for operation at 6400, 5170 and 4450 Å. Dissociative recombination of $C_2O_2^+$ in a similar system excited by 3 nsec pulses of 2KA/cm^2 at 0.5 MeV has been found to selectively pump the $A^3\Pi_g$ level of C_2. Excited state chemistry and performance typical of both types of recombination pumping will be discussed.

*Supported by the U.S. Advanced Research Projects Agency of the Department of Defense and monitored by ONR under Contract No. N00014-67-A-0310-0007.

1. C. B. Collins, A. J. Cunningham, S. M. Curry, B. W. Johnson, and M.Stockton, Appl. Phys. Lett. 24, 245 (1974).

DA-4 Spectra And Kinetics Of NaXe Excimers In High Pressure High Power NaXe Discharges. R.W. Harwell, L.A. Schlie, D.L. Drummond, and B.D. Guenther+, Air Force Weapons Lab, Kirtland AFB, N.M. 87117---A Febetron 701 retrofitted electron gun (400 KeV, 1.5 amp, 3 ns) was used to examine the kinetics and the spectral content of high pressure (10^{15} - 10^{17}/cm^3 of Na and 100-7600 Torr Xe), high power (~600 MW) NaXe electric discharges. Both the spectral and kinetic behavior of the discharges were examined. Spectrographs of the emitted radiation are given for various mixtures of Na vapor and Xe gas densities. The NaXe excimer radiation ($A^2\pi_{1/2} \rightarrow X^2\Sigma_{1/2}$) appears to be centered at 6750 Å. Also, from the analysis of the transient behavior of these bands the formation and decay rates are determined. Preliminary laser experiments using a large electron gun (1.5 MeV, 20 ns, 600 joules, 15 cm wide beam) will also be reported.

+ Permanent Address: Physical Sciences Directorate, Army Missile Command, Redstone Aresenal, Alabama 35809

DA-5 High Power Resonant Optical Pumping Of Alkali-Xenon Mixtures. D.L. Drummond, L.A. Schlie, and B.D. Guenther Air Force Weapons Lab, Kirtland AFB, N.M. 87117--Pulsed alkali vapor lamps have been made for resonant optical pumping studies of potential alkali-xenon excimer lasers Efficient coupling may be achieved between a lamp containing up to 20 Torr of alkali vapor and a mixture containing 10^{-2} Torr of alkali vapor and over 10^{+4} Torr of xenon. In this way, it is possible to have both an efficient high power discharge in the lamp and an extremely low concentration of unwanted alkali dimers in the laser mixture. In addition, because of the selective nature of resonance lamp pumping, the resulting spectra are easier to interpret that would be that from direct electrical pumping. The absorption line of the laser mixture is from 5 to 15 Å wide, due to the extremely high xenon pressure. The lamp emission profile is matched to this absorption width by varying the self reversal of the resonance line. This is done by means of an external heater which controls the alkali density. Lamp peak power densities of over 10 KW/cm^3 have been achieved in the alkali resonance lines.

+ Permanent Address: Physical Sciences Directorate Army Missile Command, Redstone Arsenal, Alabama 35809

DA6 Ultra-Violet (2000-3250 Å) Photoionization For Potential Alkali Vapor - Inert Gas Excimer and Alkali Dimer Laser Plasmas. L.A. Schlie, D.L. Drummond and B.D. Guenther+. Air Force Weapons Lab, Kirtland AFB, N.M. 87117. External selective ionization of alkali vapor-inert gas discharge by 2000-3250 Å ultra-violet radiation are analyzed in detail for potential alkali vapor-inert gas excimer and alkali dimer laser systems. This external ionization scheme is unique since the alkali vapor is simultaneously used as both the ionizing and the lasing specie unlike the "seeded" photoionized CO_2 lasers. While discussing the laser kinetics, particulary the stimulated emission cross section and required population inversions, of these bound-free electronic systems, it will be shown that optimum alkali vapor density is 10^{16} to 10^{17}/cm^3 with approximately 10 atm of Xe. The alkali metals have photoionizing cross section in the range from 10^{-18} to 10^{-20} cm^2 over the 2000-3250 Å radiation region which results in mean free paths from 10-100 cm. It will be shown that for 2500 Å radiation intensities of 100 watts/cm2, electron-ion densities of 10^{12}-10^{13}/cm^3 or larger can be produced, comparable to densities produced via e-beams. Also preliminary experimental work will be presented for NaXe and RbXe with various radiation sources.

DA-7 Ar-N_2 Transfer Laser at 3577Å and 3805Å.*
EARL R. AULT and N. THOMAS OLSON, Northrop Research and Technology Center.--
Laser emission has been observed at the 3577Å (0-1) and 3805Å (0-2) transitions of the nitrogen second positive band. The laser is of the transfer type in which argon excimers, produced by electron energy deposition in high pressure (100 to 200 psia) mixtures of argon and nitrogen, transfer energy to molecular nitrogen excited electronic states. Results have been obtained for two conditions of electron beam parameters: 1 MeV, 500A/cm^2 at 15 ns; and 3 MeV, 1000A/cm^2 at 50 ns. For the 15 ns e-beam only the 3577Å line was observed while both the 3577Å and 3805Å lines were observed from the 50 ns e-beam.

* This work was supported in part by ARPA and monitored by ONR under Contract N00014-72-C-0456.

DA-8 Kinetic Model of N_2 Second Positive Band Emission In Electron Beam Pumped Ar-N_2 Energy Transfer Lasers.*
G.A. HART† and S.K. SEARLES, Naval Research Laboratory -
A kinetic model was developed which explains both the absolute magnitude and temporal dependence of the $N_2C(^3\pi_u)$ population observed as 3371, 3577 and 3805 Å side fluorescence in a series of Ar-N_2 mixtures excited with a pulsed 500 keV electron beam (e-beam). In the model only Ar is directly pumped by the e-beam yielding ions and excited neutrals. The ions subsequently dimerize followed by dissociative recombination producing additional excited neutrals. The excited neutrals are assumed to be rapidly converted to the Ar $^3P_0$ and $^3P_2$ metastables from which energy transfer to $N_2(X)$ subsequently forms $N_2(C)$ and $N_2(B)$. Over a pressure range of 200-5000 torr at Ar:N_2 ratios of 100, 20 and 10 a comparison of absolute experimental $N_2(C)$ fluorescence intensity with the model showed close agreement. These results suggest that neither Ar$_2^*$ nor $N_2(A)$ are involved in important energy pathways although recent chemical dosimetry measurements of the energy absorbed from the e-beam indicate that $N_2(A)$ energy pooling cannot as yet be totally excluded from consideration.

* Work sponsored in part by DARPA

† NRC-NRL Postdoctoral Research Associate 1973-Present

DA-9 Scaling and Efficient Operation of the 1720 Å Xenon Laser, R. O. HUNTER, and J. SHANNON, Maxwell Laboratories, W. M. HUGHES, Los Alamos Scientific Laboratory -- An output energy of 8 joules, a peak power in excess of 4×10^8 watts, and an efficiency greater than .02 relative to energy input to the active volume were simultaneously obtained from a pure Xenon working medium. By operating with low Xenon atom (2×10^{20} cm^{-3}) and excited state (3×10^{16} cm^{-3}) densities, energy was extracted from an electron beam excited Xenon laser without optical damage or optical pulse cutoff driving the pump pulse. An 850 kV, 80 KA electron beam of 40 ns duration and with an area of 5 x 50 cm delivered 500 joules to a 1.8 liter volume cavity. Correlation of the time resolved fluorescence with lasing action resulted in an upper limit for the reduced photoabsorption cross section (2.5×10^{-37} cm^5) and indicated that about .25 of the deposited energy was converted to excited state energy and an optical extraction efficiency of .10. The efficiency may be further improved by utilizing larger optical fluxes for energy extraction as well as lowering the pressure and excited state density. The results are discussed in terms of collisional and radiative processes.

DA-10 Theory of Laser Emission from the Resonance Transitions of C IV and Other Multiply Ionized Atoms. C.B. ZAROWIN IBM T.J. Watson Research Center-A model of the C IV laser emission at 1550 A will be given which is in substantial agreement with experiment[1]. The population inversion in C IV results from the recombination of C V. This model predicts higher threshold exitation rates at still shorter wavelengths (to 700 A) from isoelectronic species of higher ionicity. The electrical discharges used for the C IV laser are unable to produce the excitation rates required for the proposed shorter wavelength lasers. It will be shown that 10 ps pulsed Nd laser excited plasmas are capable of achieving these rates, and would produce a travelling wave of inversion in synchronism with the exciting laser pulse in a manner proposed by Knyazev and Letokhov[2].

(1)R.W. Waynant,Appl.Phys.Letters 22,419 (1973)
(2)I.N. Knyazev and V.S. Letokhov,Opt.&Spectr.33,59(1972)

DA-11 High Current Density Pulsed Metal Vapor Laser. R. S. ANDERSON, L. W. SPRINGER, B. G. BRICKS, and T. W. KARRAS, General Electric Co., Space Sciences Lab. - A series of experiments have been performed with a self-heated laser, similar to that reported by Isaev*, that clarify the dependence of specific laser pulse energy on discharge current density. Using a copper vapor lasant and a longitudinal discharge, specific laser pulse energies of up to 17 $\mu j/cm^3$ resulted from peak current densities of up to 4.8×10^3 amp/cm^2. Average power densities were .93 W/cm^2 (.26 W in 6 mm bore). Variations in copper vapor density had only a second order effect upon the specific energy. Specific laser pulse energies with lead vapor of 2 $\mu j/cm^3$ were reached with 6.7×10^3 amp/cm^2. The significance of these results with regard to plasma kinetics and lasant inversion will be discussed.

*A. A. Isaev, M. A. Kazaryan, and G. G. Petrash ZhETF Psi Red 16, 40 (1972), JETP Lett 16, 27 (1972).

DA-12 Calculations for a Sodium Vapor VUV Laser (372Å) Pumped by Radiation from an Exploding Wire. Walter W. Jones and A. W. Ali, Naval Research Laboratory.--We have solved (numerically) a set of rate equations which govern the time histories of the upper level, the lower level, the electron density and the laser power density of sodium vapor coupled to the black-body like radiation from an exploding wire.[1] The laser transition is $2p^6$ - $2p^5(P_{\frac{1}{2}})3s$ which arises as a result of photon pumping which preferentially ionizes the (2p) shell, leading to inversion. We obtain, for a cylindrical cell 10cm×1cm containing an initial neutral density of $10^{16} cm^{-3}$, a maximum gain of 0.5 and the corresponding power density of 5k watts cm^{-3}. This results from using a flux reduced by 10^{-2} from the black-body level to account for an experimental arrangement. Further details and results will be given.

[1]D. Mosher, S. J. Stephanakis, I. M. Vitkovitsky, D. M. Dozier, L. S. Levine, and D. J. Nagel, Appl. Phys. Letters 23, 429 (1973).

DA-13 Lasing in a Ternary Mixture of He-Ne-O_2 at Pressures Up To 200 Torr. R. DeYOUNG, S. BECKMAN, W. E. WELLS and G. H. MILEY, Univ. of Illinois--The problems of rapid deterioration which usually beset lasing in mixtures with oxygen have been avoided in a ternary mixture of He-Ne-O_2. Stable lasing has been obtained on the 8446Å line in atomic oxygen in a pulse mode up to pressures of 200 Torr. The upper pressure limit is due mainly to the difficulties in creating discharges above this value. Significant improvements in output power have been obtained with the addition of helium due to the increased production of Ne metastables which collisionally dissociate O_2 to form the upper states for the 8446Å transitions. Concentration studies and crude measurements of the combination of O into O_2 in the presence of He will also be presented. A wavelength shift, due to the selective absorption of the lower level to ground state transition, should be expected.[1] This has been examined theoretically but has not yet been confirmed experimentally. (1) Feld et al., Phys. Rev. A, 7 (1973).

SESSION DB

3:45 PM - 4:55 PM, Tuesday, October 22

Brazos Room

CHARGE TRANSFER AND ION-MOLECULE REACTIONS

Chairman: F. B. Dunning, Rice University

DB-1 Abstract Withdrawn

DB-2 Variational Bounds on Transition Amplitudes. DAVID STORM, The University of Texas at Dallas.-- Within the framework of the semiclassical impact parameter method for ion-atom collisions, it has been possible to derive upper and lower variational bounds which bracket the exact amplitudes for the excitation and charge exchange amplitudes; and thus it is possible, in principle, to obtain exact amplitudes in a variational calculation. The results obtained in a recent calculation of the 1s-charge exchange amplitude in proton-hydrogen-atom scattering will be discussed. In this work it has been possible to judge the quality of a particular trial wave function on an absolute scale, and therefore it will be possible to discuss the importance of various physical effects, such as the polarization of the atom by the incoming ion.

DB-3 Merging Beams Study of the $D^+(H_2,H)HD^+$ and $H_2^+(D,H)HD^+$ Reaction Mechanisms.* A.B. LEES and P.K. Rol, Wayne State University--Lab-energy distributions of HD^+ ions formed in the endoergic $D^+(H_2,H)HD^+$ reaction were measured with high resolution for collisions with relative energy, W, in the range 1.0 eV $\leq$ W $\leq$ 5.0 eV. Because of the high resolution, our results complement another study[1] of this reaction. In addition to observing the transition from long- to short-lived collision complexes and the relative growth of rebound collisions, we also observe directly the participation of charge transfer in the entrance channel. The charge transfer contribution was determined by independent study of the $H_2^+(D,H)HD^+$ reaction. HD^+ ions formed in the $H_2^+(D,H)HD^+$ reaction have recoil energies in the same range as HD^+ ions which appear as a distinct shoulder in the $D^+(H_2,H)HD^+$ product distributions. For W $\geq$ 8 eV, electronically excited products of the $H_2^+(D,H)HD^+$ reaction were observed.

*Acknowledgment is made to the donors of the Petroleum Research Fund, administered by the American Chemical Society, for support of this research.

1. J.R. Krenos, R.K. Preston, R. Wolfgang, J.C. Tully, J.Chem.Phys. 60, 1634 (1974) and references therein.

DB-4 Drift Tube Measurement of the Energy Dependence of the Reaction Rate for $NO^+ + H_2O + N_2$.* H. L. BROWN**, RAINER JOHNSEN and MANFRED A. BIONDI, University of Pittsburgh. -- A modified "additional residence time" technique has been used[1] to determine the rate coefficient for first hydration of the nitric oxide ion. The rate is observed to decrease sharply from $\sim 1.3 \times 10^{-28}$ cm^6/sec at ~ 0.039 eV (300 K) to $\sim 8.6 \times 10^{-30}$ cm^6/sec at ~ 0.70 eV. The dependence can be explained in terms of the energy dependence of the lifetime of the intermediate $NO^+ \cdot H_2O$ complex formed as the initial step in the three-body collision process. Mobilities have been measured for NO^+ in H_2O ($\mu_o = 0.89$ $cm^2/Vsec$) and NO^+ in N_2 ($\mu_o = 2.6$ $cm^2/Vsec$) at 300 K.

*Supported, in part, by the Army Research Office.
**Present address, Stanford Research Institute, Menlo Park, California.
[1]J. Heimerl, R. Johnsen, and M. A. Biondi, J. Chem. Phys. 51, 5041 (1969).

DB-5 Rate Coefficients for Oxidation of Ti^+ and Th^+ By O_2 and NO at Low Energies.* RAINER JOHNSEN, F. R. CASTELL, and MANFRED A. Biondi, University of Pittsburgh. -- Rate coefficients have been determined in a drift tube-mass spectrometer apparatus for the oxidation reactions of Ti^+ and Th^+ ions in O_2 and NO for ion mean energies ranging from thermal (300 K) to 5 eV. Formation of the first oxides of metal ions M^+ in the reactions $M^+ + O_2$ (NO) $\rightarrow$ $MO^+ + O$ (N) is found to occur with rate coefficients close to the theoretical maximum values ($\sim 6 \times 10^{-10}$ cm^3/sec) (i.e. the "Langevin" limit), except for $Ti^+ + NO$, which proceeds more slowly ($\sim 10^{-10}$ cm^3/sec). Further oxidation in the reactions $MO^+ + O_2$ (NO) $\rightarrow$ $MO_2^+ + O$ (N) has been detected only for M=Th and with small rate coefficients ($\sim 10^{-11}$ cm^3/sec). The associative ionization reaction, $Th + O_2 \rightarrow ThO_2^+ + e$, has been observed to occur, although no rate coefficient can be obtained from our measurements. In addition, thermal energy ionic mobilities of thorium and titanium ions in helium are found to be $\mu_o(Ti^+) = (25.5 \pm 1)$ and μ_o $(Th^+) = (15.75 \pm 0.5)$ $cm^2 \cdot V^{-1} \cdot sec^{-1}$ at 300 K.

*Supported in part by the Army Research Office.

DB-6 Rate Constants for the Reaction of Metastable O_2^+ ($a\ ^4\Pi_u$) with H_2, N_2, and Ar at Relative Kinetic Energies 0.05 to 2 eV.* M.McFARLAND, W. LINDINGER**, D. L. ALBRITTON, NOAA/ERL, Aeronomy Laboratory, Boulder, CO 80302--Metastable O_2^+, presumably the $a\ ^4\Pi_u$ state at 16.11 eV above the ground state of O_2, has been created in the flow-drift tube in sufficient numbers to measure the rate constants of the reactions of this metastable with H_2, N_2, and Ar, which cannot react with the $X\ ^2\Pi_g$ ground state of O_2^+. At room temperature, the rate constant of the reaction of $O_2^+(a\ ^4\Pi_u)$ with H_2 is 1.2×10^{-9} cm^3/sec and with N_2 and Ar is 4×10^{-10} cm^3/sec. The rate constants increase only very slightly in the relative kinetic energy range 0.05 to 2 eV.

* This research was supported in part by DNA.

** Max Kade Foundation Fellow on leave from the University of Innsbruck, 1973-1974.

DB-7 The Ion Chemistry of HNO_3 and NO_2.* F. C. FEHSENFELD AND CARLETON J. HOWARD, NOAA/ERL, Aeronomy Laboratory, Boulder CO 80302--The ion chemistry of HNO_3 and NO_2 have been studied in a flowing afterglow system at 296°K. In the negative ion sequence, HNO_3 rapidly attaches electrons by the reaction

$$e + HNO_3 \rightarrow NO_2^- + OH, \qquad (1)$$

$k_1 = 8 \pm 4 \times 10^{-8}$ cm^3/sec. HNO_3 reacts by proton transfer with most negative ions, e.g.,

$$X^- + HNO_3 \rightarrow NO_3^- + HX,\ X = Cl,\ NO_2 \qquad (2)$$

is fast, $k \sim 10^{-9}$ cm^3/sec.

In the positive ion chemistry, the proton transfer reaction

$$H_3O^+ + HNO_3 \rightarrow H_2NO_3^+ + H_2O \qquad (3)$$

is fast indicating P.A.(HNO_3) $\geq$ P.A.(H_2O) = 7.2 eV. In addition, the product of the proton transfer reaction, $H_2NO_2^+$, appears to be identical to the isomer $NO_2^+ \cdot H_2O$ formed by hydrating the nitronium ion, NO_2^+

$$NO_2^+ + H_2O + M \rightarrow NO_2^+ \cdot H_2O + M. \qquad (4)$$

The mechanisms and rate constants for these reactions and other processes involving HNO_3 and NO_2 will be discussed.

* This research was supported in part by DNA.

SESSION E

9:00 AM - 10:15 AM, Wednesday, October 23

Crystal Ballroom

ELECTRON EXCITATION OF MOLECULES I

Chairman: M.F.A. Harrison, Culham

E-1 Vibrational Excitation of N_2, CO, and N_2O by Low Energy Electrons.* S.F. WONG and G.J. SCHULZ, Yale U -- A crossed-beam apparatus with electron beam resolution 22-35 meV is used to study the absolute differential vibrational cross sections to v=1 and v=2 of the ground state of N_2, in the energy range 1-30 eV. Two new broad resonant peaks are observed near 8 eV and 13.7 eV respectively, and they are interpreted as shape resonances. —In CO, which is isoelectronic with N_2, an additional mechanism was found:[1] Sharp structures have been observed in the elastic and vibrational cross sections at energies coincident with the v=0, 1 and 2 levels of the $a^3\Pi$ state of CO. The large electric dipole moment (1.38 D) associated with the $a^3\Pi$ state appears sufficient to bind temporarily the incoming electrons at or near the top of the potential well.—In N_2O, the vibrational excitation via the 2.3 eV $^2\Sigma$ resonance is found to consist of four series of modes (n00,n10,n01 and n02). The present experiment together with the calculation of Dubé and Herzenberg show that the impulse-limit theory is applicable to the $^2\Sigma$ state of N_2O^-.

*Work supported by NSF and by DNA through AROD

[1]S.F. Wong and G.J. Schulz, Phys. Rev. Letters 33, 134 (1974)

E-2 Vibrational and Rotational Excitation of CO_2 by Low-Energy Electrons*--M.Morrison† and N.F.Lane, Physics Department, Rice U. In electron-CO_2 collisions, relatively large $\Delta j = \pm 1$ rotational-excitation and de-excitation cross sections arise from the (transient) dipole moment which accompanies transitions between the ground state (000) and the bending mode (010). A model[1] in which the electron is scattered from a "frozen dipole" is shown to yield a total scattering cross section under restricted circumstances. Cross sections for transitions involving the bending mode 010 will be presented and discussed.

*Supported in part by U.S. Atomic Energy Comm. and Robert A. Welch Foundation.

†Fannie and John Hertz Foundation Fellow.

[1]R. Tice and D. Kivelson, J. Chem. Phys. 46, 4748 (1967).

E-3 Vibrational Structure in Kinetic Energy Spectra of O^+ Ions from Electron Impact Dissociative Ionization of O_2. Pre-dissociation of the $B^2\Sigma_g^-$ State of O_2^+.*

J. A. D. STOCKDALE and LILIANA DELEANU**
Health Physics Division, Oak Ridge National Laboratory, Oak Ridge, Tennessee 37830 --

Electron impact dissociative ionization of O_2 has been studied with an apparatus containing crossed molecular and pulsed electron beams. Structure has been observed in the ~ 0.8 eV kinetic energy O^+ ion peak produced by electron impact dissociative ionization of O_2. The spacing between the features observed is approximately 0.08 eV which is consistent with their originating through predissociation of the $B^2\Sigma_g^-$ state of O_2^+.

*Research sponsored by the U. S. Atomic Energy Commission under contract with the Union Carbide Corporation.

**Graduate student, University of Tennessee, Knoxville, Tennessee 37916.

E-4 Vibrational Excitation and Transmission Spectroscopy in Hydrogen Halides.* J.P. ZIESEL,† I. NENNER and G.J. SCHULZ, Yale U. --Vibrational excitation near threshold has been studied in HCℓ (v = 1,2) and DCℓ (v = 1,2,3) with a trapped-electron apparatus. The vibrational cross sections rise steeply near threshold and levels off about 60 meV above threshold. The magnitude of these cross sections have been measured (about 10^{-15} cm^2 for HCℓ v = 1) and are interpreted in terms of a resonant contribution. These large vibrational cross sections produce structure in the transmission spectra of HCℓ, HBr and their isotopes. Additional features are attributed to Wigner cusps.

*Work supported by ONR
†Present address: Collisions Electroniques, Université Paris-Sud, 91405 Orsay (France)

E-5 Excitation of H_2 by Low-Energy Electron Impact* J. Watson, Jr., J. N. Adams and R. J. Anderson, University of Arkansas.--Optical excitation functions for fourteen spectral lines of the neutral H_2 spectrum were measured for incident electron energies in the range 0-200eV. The lines were observed at a spectral slit width of 8Å and were assigned to corresponding vibrational and electronic transitions using the wavelength tables of Dieke[1]. They include the singlet transitions nA → 2B, mD → 2B and mE →2B, and the triplet transitions mc → 2a and 3d → 2c where n=2,3 and m=3,4. In addition the 2K → 2B, 2W → 2B and 2Z → 2B electronic transitions were observed where 2W, 2K and 2Z are states of the doubly excited H_2 spectrum. In addition absolute optical cross section measurements, at 200eV electron energy and 10 mtorr H_2 gas pressure were determined to be within the range 10^{-19} to $10^{-21}cm^2$.

* Research Supported by the Atmospheric Sciences Section, National Science Foundation.

1. G.H. Dieke, The Hydrogen Molecule Wavelength Tables of Gerhard Heinrich Dieke, edited by H.M. Crosswhite (Wiley-Interscience, New York 1972)

E-6 Excitation of the $B^3\Pi g$ and $C^3\Pi u$ States of N_2 by Electron Impact* S.T. Chen, R.J. Anderson and R. H. Hughes, University of Arkansas.--Time resolved spectroscopy has been used to study the excitation of the $B^3\Pi g$ and $C^3\Pi u$ states of N_2 by electron impact. Thirteen spectral lines of the $B^3\Pi g \rightarrow A^3\Sigma u$ transition were observed using a 50 μsecond excitation pulse width. The lines originate from the v=0 to v=12 vibrational levels of the $B^3\Pi g$ state. Two radiative decay components with lifetimes of approximately 4 and 24 μseconds were observed in each case. The long-lived cascade contributions decrease from 37% of the total radiation for the (0,0) transition to 15% for the (12,8) transition and are consistent with theoretical predictions. The λ=3371-Å spectral line of the $C^3\Pi u \rightarrow B^3\Pi g$ transition was also investigated as a function of incident electron energy, gas pressure and pulse width. The $C^3\Pi u$ lifetime was determined to be 39.6 ± 3.3 nanoseconds and the pressure dependence of an observed long-lived cascade component was investigated.

* Supported in part by the NSF and the Research Corporation

SESSION FA

10:30 AM - 12:25 PM, Wednesday, October 23

Brazos Room

EQUILIBRIUM PHENOMENA IN ARCS I

Chairman: J. H. Ingold, General Electric

FA-1 Derivation of the Microfield Distribution from the Linearized Klimontovich-Equations. G. ECKER and A. SCHUMACHER, Ruhr-Universität, Bochum. -- In the past the problem of the plasma microfield distribution has been widely investigated on the basis of ad hoc models. Starting from the linearized Klimontovich-Equations we derive without assumptions a formulation of the microfield distribution which separates into a high frequency and a low frequency part, each of which may be interpreted as the microfield distribution in a system of uncorrelated dressed particles with dynamically screened fields. The low frequency component, which is of prominent interest, has been evaluated and compared with the results of the earlier treatments.

FA-2 Measurements and Calculations on a CsI-Hg-Ar Discharge.* J.H. WASZINK, and L.G.M. DE GREEF, Philips Research Labs., Eindhoven, Netherlands.--Time-resolved measurements have been made in a 50Hz ac discharge at current maximum (5A, p_{Hg}=6 at, tube Ø 16mm). The electron density (n_e) was determined from the Stark broadening of the Cs 8016 Å line (5D-5F). Side-on measurements were made, from which the line shape was obtained as a function of the radial coordinate (r). Comparison with published data on Stark broadening yields $n_e(r)$; $n_e(0)=(0.6\pm0.1)\times10^{22}m^{-3}$. The axis temperature ($5200\pm200$ K) was obtained from self-reversed Hg lines, and the integral of the Cs atom density along a diameter from optical absorption. The results compare favourably with a calculation in which chemical equilibrium is assumed.

*Submitted by R. Bleekrode

FA-3 Constriction of Arcs in Mixtures of Mercury and Iodine. R. J. ZOLLWEG, J. J. LOWKE, and R. W. LIEBERMANN, Westinghouse Research Labs.--The mechanism by which iodine causes constriction of LTE arcs in mercury vapor at ~3 atm was studied quantitatively by measuring temperature profiles and radiation characteristics as functions of the amount of iodine in the Hg-I mixtures. Emission coefficients were obtained by adding contributions from mercury and iodine atoms, electron-ion and electron-neutral bremsstrahlung, electron-Hg^+ recombination radiation, I^- attachment radiation and molecular radiation from HgI and I_2. Self absorption was taken into account by subtracting a component proportional to the Hg resonance radiation and to the density of Hg atoms. Transport properties were calculated from the equilibrium vapor compositions as functions of temperature. Temperature profiles calculated from the energy balance equation using these emission coefficients and transport properties are in good agreement with the experimental results. The theoretical calculations show that the dominant cause of arc constriction is the emission of molecular radiation from HgI. The presence of negative iodine ions and of a maximum in the thermal conductivity due to molecular dissociation have only a small effect on arc constriction in this system.

FA-4 Multiple-line Bartels' Method for Determination of Axis Temperatures of LTE Arcs. JOHN F. WAYMOUTH GTE-Sylvania Lighting Products, Danvers, Mass. Line profiles of self-reversed non-resonant lines in LTE arcs in mercury vapor do not exhibit maximum radiances at wavelengths many Lorentz widths removed from the line centers; consequently, the line profile is not separable into a product of a frequency-dependent term and a position-dependent term. Thus the ratio of maximum radiance to blackbody radiance at the axis temperature differs slightly from that calculated by Bartels[1] and the deviation depends somewhat on the details of the radial temperature profile. Calculations will be presented which show that the two-line-ratio Bartels' method for axis temperature determination recently described by Wesselink et al[2] exhibits no such dependence, since substantially the same deviation occurs for both lines, and cancels out in taking the ratio of maximum radiances. Axis temperatures of AC-operated 1000-watt mercury lamps measured by this method are found to be 6020±55K and 5120±160K at current maximum and zero respectively.

1. H. Bartels, Z. Phys. 127, 243 and 128, 546 (1950)
2. G. Wesselink et al, J. Phys.D (Appl. Phys.) 6 L27 (1973)

FA-5 Electronic Raman scattering from Ga, In and Tl atoms in metal halide arcs. L. Vriens and M. Adriaansz, Philips Research Labs., Eindhoven, The Netherlands.--An argon ion laser and metal halide arcs are used to measure depolarization ratios ρ for anti--Stokes electronic Raman scattering from Ga, In and Tl atoms[1]. In a theoretical analysis, the relative phase factors of the relevant dipole matrix elements are determined using these values of ρ, which lie between 0.86 and 1.08 and are accurate within about 2%. Use is made also of known oscillator strengths, and Stokes and anti-Stokes Raman cross sections are calculated. The cross sections per steradian are in the range of 10^{-26} up to 2×10^{-24} cm^2 for the atoms and wavelengths used in the experiment. The Raman cross sections are of interest for diagnostic purposes, e.g. for temperature determinations in metal halide arcs.

[1] L. Vriens and M. Adriaansz, Optics Comm. in press.

FA-6 Time-Dependent Plasma Temperature Measurements of the High Pressure Sodium Arc. P.D. JOHNSON and T.H. RAUTENBERG,JR., R&D Center, General Electric Co., Schenectady, N.Y.---The plasma temperature of an arc in a mixture of 55 torr Na, 250 torr Hg and 20 torr Xe in sapphire arc tubes has been measured as a function of time with 60 Hz sinewave and 20 Hz squarewave excitation. The maximum plasma temperature is 4100° ±200°K and is substantially independent of power input above an instantaneous input of about 100 W/cm^3 of arc tube volume. At this temperature, about 5% of the Na is ionized, corresponding to an electron density of 6×10^{15} cm^{-3}. On 60 Hz operation the temperature falls to 3200°K and the electron density to about 8×10^{14} cm^{-3} at current zero. Squarewave operation with controlled power-off time indicates that temperature decay to this value occurs in 0.3 msec. The arc reignition voltage increases by a factor of about 4 during this time.

FA-7 Time-Dependent Modeling of the High Pressure Sodium Arc Column. R.E. KINSINGER R&D Center, General Electric Co., Schenectady, N.Y. -- A time-dependent model for a wall-stabalized, cylindrically symmetric arc has been developed. Energy transfer processes included are: Ohmic heating, radial conduction, radial convection, adiabatic heating, and radiation - both optically thick and optically thin components. The model has been used to calculate the behavior of a 7.5 mm diameter, 50 W/cm column in a mixture of 70 torr Na, 340 torr Hg, and 190 torr Xe. LTE is assumed for calculating thermodynamic and transport properties of this mixture in a separate program. The d.c. solution (6.1 A, 8.2 V/cm) decays, when Ohmic heating is turned off, with a conductivity decay time of 0.18 msec. The d.c. results are compared with a.c. results for 60 Hz (low frequency), 600 Hz (intermediate frequency) and 6 kHz (high frequency) sinusoidal currents.

SESSION FB

10:45 AM - 12:00 NOON, Wednesday, October 23

Crystal Ballroom

ELECTRON EXCITATION OF MOLECULES II

Chairman: R. J. Anderson, Arkansas

FB-1 Electron Excitation Functions of the $B^1\Sigma^+$, $d^3\Delta$, $b^3\Sigma^+$, and $a'^3\Sigma^+$ States of the CO Molecule.* A. R. FILIPPELLI, SUNGGI CHUNG, and CHUN C. LIN, Univ. of Wisconsin. -- The excitation functions of the Angstrom system ($B^1\Sigma^+ \rightarrow A^1\Pi$), the Triplet system ($d^3\Delta \rightarrow a^3\Pi$), the Third Positive system ($b^3\Sigma^+ \rightarrow a^3\Pi$), and the Asundi system ($a'^3\Sigma^+ \rightarrow a^3\Pi$) of the CO molecule have been measured. The shape of the excitation function of the $B^1\Sigma^+$ state is in good agreement with theory, whereas considerably larger differences are found for the three triplet states. By applying the Franck-Condon-factor approximation to the measured optical cross sections, we have determined the peak excitation cross section of the $d^3\Delta$ state as 1.2×10^{-17} cm^2 which agrees well with the theoretical value. An estimate of the peak cross section of the $B^1\Sigma^+$ state has been obtained from the optical cross section of the Angstrom system as 6×10^{-18} cm^2 which is consistent with the theoretical value of 9.2×10^{-18} cm^2.

*Work supported in part by the Air Force Cambridge Research Laboratories, Office of Aerospace Research and by the U.S. Air Force Office of Scientific Research.

FB-2 Excitation of the Gamma Bands of Nitric Oxide by Electron Impact.* MAHMOOD IMAMI and WALTER L. BORST, Southern Illinois University at Carbondale. -- Excitation of a number of γ-bands of nitric oxide ($A\ ^2\Sigma^+ \rightarrow X\ ^2\Pi_r$) from threshold to 1000 eV was studied with a high efficiency optical system, that made use of an ellipsoidal mirror and which was calibrated by the molecular branching ratio method. Gas pressures in the ellipsoidal collision chamber were kept deliberately low ($\sim 10^{-4}$ torr) in order to avoid second order effects. Absolute excitation cross sections for γ-bands were obtained by comparison with those for the 2PG(0,0) and 1NG(0,0) bands of nitrogen. In general, the peak excitation cross sections of the more prominent γ-bands were found to be on the order of 10^{-19} cm^2. Details of the cross sections of some of these bands [e.g. (0,1), (0,2), (1,0), (1,4), (1,5), (2,7), (2,8)] as functions of electron energy will be presented.
The present work may be of interest in the study of atmospheric and plasma processes.

*Supported by the Office of Research and Projects, Southern Illinois University at Carbondale.

FB-3 Dissociative Excitation of H_2 ---- Low Rydberg and High Rydberg Fragments. ROBERT S. FREUND, JAMES A. SCHIAVONE, DONNA F. BRADER, AND KERMIT C. SMYTH,* Bell Laboratories, Murray Hill, New Jersey 07974 -- Theories of molecular excitation and dissociation should be most accurate when they are applied to the hydrogen molecule. To test such theories, detailed experimental measurements are required. We have therefore studied electron impact dissociation of H_2 by observing the Balmer α, β, γ, and δ lines of atomic hydrogen for $n = 3$-6 and metastable high Rydberg atoms for $n > 15$. Measurements are made of Balmer line shapes, metastable time-of-flight distributions, appearance potentials, and excitation functions. These experiments reveal two groups of atoms, those with translational energies slightly above thermal and those with energies as high as 6 eV. Interpretation of the results cannot be made solely in terms of well-known molecular states. It is likely that two-electron excited states and non-adiabatic processes play an important role.

* Present address: Institute of Applied Technology National Bureau of Standards, Washington, D.C. 20234

FB-4 Electron Impact Excitation of Fluorescence in Organic Molecules. KERMIT C. SMYTH,* JAMES A. SCHIAVONE, AND ROBERT S. FREUND, Bell Laboratories, Murray Hill, New Jersey 07974 -- Electron impact excitation of organic molecules has been largely neglected as a means of probing excited electronic states. This work reports excitation of fluorescence by electron impact from a number of important aromatic compounds, including benzene, naphthalene, and azulene. The data are presented as (a) fluorescence spectra at a series of electron energies, and (b) optical excitation functions. Both the spectra and the excitation functions exhibit rich structure, indicating a wide variety of excitation processes. Particular emphasis will be placed on assigning the many features in the excitation functions at low electron energy (< 20 eV) in terms of resonances (temporary negative ion states) and non-resonant excitation.

*Present address: Institute of Applied Technology National Bureau of Standards, Washington, D.C. 20234

FB-5 Dissociation of the Hydrogen Molecule by Electron Collision.* SUNGGI CHUNG, Univ. of Wisconsin and EDWARD T. P. LEE, Air Force Cambridge Research Laboratories -- The electron-impact dissociation cross sections of the H_2 molecule into two H(1s) atoms via excitation to the repulsive $b^3\Sigma_u^+$ state have been calculated by Rudge's modification of the Born approximation for impact-energy range of threshold to 150 eV. The electronic wave functions are expressed in terms of Gaussian-type orbitals to facilitate the numerical work. The electronic transition amplitude is calculated at seven different values of internuclear separation between 0.5 and 1.0 Å, and 41 continuum "vibrational" functions of the $b^3\Sigma_u^+$ state are computed for the energies between 2 and 10 eV. The dissociation cross sections are obtained by evaluating the Born integrals numerically without using the Franck-Condon-factor approximation. Comparison of theoretical cross sections with experimental data is discussed.

*Work done at University of Wisconsin and supported by Air Force Cambridge Research Laboratories, Office of Aerospace Research.

FB-6 Determination of Absolute Cross Sections for Electron-Molecule Collision Processes at Intermediate Energies. S. TRAJMAR JPL--A brief review of absolute cross section determinations (including a recently developed technique) will be given. Cross sections will be presented from near threshold to 100 eV impact energies for elastic and superelastic scattering, and for various inelastic processes (including excited state-excited state transitions). The examples will include recent results in He, Xe, Cu, H_2, N_2, O_2, CO, CO_2 and H_2O.

SESSION GA

1:30 PM - 2:55 PM, Wednesday, October 23

Crystal Ballroom

GAS DYNAMIC AND MAGNETIC PHENOMENA I

Chairman: W. C. Roman, United Aircraft

GA-1 Theoretical Aspects of Mass Separation and Pressure Distribution in Rotating Arcs⊕. J. J. McCLURE and N. NATHRATH, Messerschmitt-Bölkow-Blohm GmbH. -- The use of rotating arcs for mass and isotope separation is investigated theoretically. The use of simplified momentum conservation equations leads to mass separation formulas which are identical to those derived in neutral gases. The pressure distribution however is quite different due to the nature of the plasma. The inclusion of several processes such as Coriolis forces, mass transport, carrier gases, Hall effect, Nernst effect and the impediment of ambipolar diffusion leads to important deviations from the simple formulas. The mass (isotope) separation and pressure distribution depend critically on the rotational velocity, calculations of which including several of the above mentioned effects are presented. Results are presented for a model of an electrical arc in an axial magnetic field. Comparisons with the few experimental observations are made.

⊕ This work supported in part by URANIT, Uran-Isotopentrennungs-Gesellschaft, Jülich, Germany.

GA-2 Cathode and Anode Current Distribution in a Short Moving Arc. R. Beaudet and M.G. Drouet, IREQ, P.O.B. 1000, Varennes, Québec, Canada. Simultaneous measurements in an arc of the anode and cathode current distribution along the direction of motion will be reported. The short, 1.6 mm, 700 Amp. arc operates in air at atmospheric pressure; the arc is driven by a transverse magnetic field at a velocity of 170 to 190 ms^{-1}. The technique used has been discussed previously*. Two transverse slits, one on each of the two electrodes, are used to sample the current distribution at the electrode surface as the cathode and anode spots are driven across the slits. The width of the current distribution at the cathode decreases with increasing velocity. At 190 ms^{-1} it is comparable to the width of the current distribution at the anode which does not show any variation over the range of conditions studied. Space resolved high speed photographic recordings of the arc luminosity, recorded simultaneously with the current distribution, at the anode and at the cathode, show that the luminous arc spots carry the current.

* R. Beaudet and M.G. Drouet, IEEE P.A.S. T-74 129-3, Winter Power Meeting, New York 1974.

GA-3 Accelerating Rail Arcs. T. N. MEYER, Westinghouse Research Labs.--High current (2 to 14 kA) arcs in atmospheric pressure air were driven along copper rails by the self induced magnetic field. The rails were enclosed by insulated side walls having 1/4", 3/8" and 1/2" separations. The arc was initiated by a copper fuse wire between rails separated 1/2" and 3/4". Arc velocities and static pressures along the travel length were obtained with sensors mounted in the side walls.

Velocity increased with decreasing rail and side wall separation. The arc accelerated ($0\text{-}10^5$ m/sec^2) along the rail for all currents and separations. The pressure change "ΔP" (.3 to 1.9 atm) as the arc passed the sensor agreed within 11% of that calculated to balance the Lorentz force driving the arc. Where velocities (90-470 m/sec) were lower (i.e., lower currents), pressure propagated ahead of the arc and acceleration is proportionately greater. I concluded a) the arc motion and resulting pressure can be predicted from a transient flow analysis of an accelerating piston driven by the Lorentz force and b) studies of arc motion must include the travel length.

GA-4 Correlation of MPD Arc Discharge High Speed Photography and Arc Parameters During Tranisition from the Constricted to the Diffuse Mode.* D. L. Murphree, J. K. Owens, C. S. McMillan, Mississippi State University -- High speed movies of the transition from a retrograde constricted MPD arc discharge to a diffuse mode with increasing current have been obtained. The pressure, arc current, arc voltage, magnetic field strength, and output from a photo-optical system observing a localized region of the cathode and positive column were recorded. By simultaneously producing timing marks on both the high speed film and the data record, the visual arc discharge behavior was correlated with the arc parameters. The behavior of the cathode spots, positive column, and arc voltage during the transition from a constricted to a diffuse MPD arc mode is presented.

*Work supported by National Science Foundation Grant GK-30543.

GA-5 Alternating Current Cross-Flow Arcs.* J-L WU and D.M. Benenson, State Univ. of N.Y. at Buffalo--Local temperature distributions and arc profiles have been obtained (for the first time) at various points within the current cycle on an a-c cross-flow plasma. Experiments were carried out upon a 61A rms atmospheric argon arc operated in a cross-flow of 1.1m/s; electrode spacing was 11.1mm. The cross-sections of the arc were generally found to be non-circular with major axis parallel to the direction of flow. Deflections of the column depended upon current and temperature. At a given vertical location between the electrodes, the maximum deflection tended to occur where the maximum temperature reached a minimum value. The timewise variation of maximum temperature was about zero near current maximum and about $4.5^{\circ}K/\mu s$ near current zero. A thermal lag of about 0.4ms was found at about mid-height between the electrodes; the magnitude of the lag varied with vertical location. Calculated values of lag were in good agreement with measurements.

*Research supported by National Science Foundation Grants GK-24292 and KO-24292-001 and by Air Force Office of Scientific Research Grant 70-1928.

GA-6 Investigation of an RF Argon Plasma Vortex With UF_6 Injection*. WARD C. ROMAN, United Aircraft Research Lab. -- Experiments are discussed in which an rf heated argon plasma at 1 Atm was seeded continuously with pure UF_6. The objective was confinement of uranium vapor within the plasma while minimizing uranium compound wall deposition. The plasma was a fluid mechanically confined vortex type approximately 3 cm. in diameter and 10 cm. long contained within a quartz cylindrical test chamber. RF energy was supplied by an 80-kw, 13.56 MHz induction heater. Different test chamber flow configurations were tested to permit selection of the configuration offering the best containment characteristics. Test variables included the flow geometries, rf power level, and argon buffer gas/UF_6 flow rates. Diagnostics included measurements of the plasma physical and electrical characteristics, calorimetric power losses, and radiation in different wavelength bands with and without UF_6. Preliminary results include absorption measurements (500-600 nm) and determination of best containment test conditions.

*Work sponsored by NASA-Langley Research Center, Contract NAS1-13291

GA-7 Characteristics of Xenon Flash Lamps in High Magnetic Fields. PAUL SCHREIBER, ARL, WPAFB, O.--The radiative and electrical characteristics of Xenon flash lamps were investigated in magnetic fields up to 10 tesla. The magnetic fields were produced by a cryogenic, pulsed, solenoid having a 6-inch diameter and a 16-inch length. The magnet and the 5MW power supply were capable of producing a peak field of 14 tesla for 0.1 second. The lamp holders were designed to minimize circuit inductance and magnetic forces on the plasma. No failures due to the interaction of the magnetic field with the lamp current occurred. Current, voltage and radiation were recorded simultaneously. Only small changes in lamp characteristics were observed when the lamps were aligned with the magnetic field. The observed changes are attributed to reduced thermal losses to the lamp wall. Good agreement with measurements was obtained when reliable thermodynamic and transport properties were used as input data with an improved computer model.

SESSION GB

1:45 PM - 3:00 PM, Wednesday, October 23

Brazos Room

ELECTRON COLLISIONS

Chairman: R.J.W. Henry, Louisiana State

GB-1 The Multichannel Eikonal Treatment of Electron-atom Collisions, M. R. FLANNERY, and K. J. McCANN*, School of Physics, Ga. Inst. of Tech.--A new multichannel eikonal description of atomic collisions is presented. Different local momenta in the various channels are acknowledged. The basic formula for the scattering amplitude reduces upon successive approximation to expressions previously derived. Multi-channel treatments of e-H(1s), e-He($1\ ^1S$) and e-He($2\ ^{1,3}S$) inelastic scattering are carried out. In an effort to acknowledge full polarization effects, pseudostates are also included for e-H(1s) collisions. The calculated cross sections compare very favorably with other refined theoretical methods (when available) and with experiment.

* Research sponsored by the Air Force Aerospace Research Laboratories, Air Force Systems Command, United States Air Force, Contract F33615-74-C-4003.

GB-2 Absolute Experimental Cross Sections for the Ionization of Tl^+ Ions by Electron Impact.* T. F. DIVINE, R. K. FEENEY, J. W. HOOPER, and W. E. SAYLE II, Georgia Institute of Technology.--Absolute cross sections for the single ionization of Tl^+ ions by electron impact have been measured as a function of incident electron energy from below threshold to approximately 2000 eV. It was found that the cross section increased from a nominally zero value at and below threshold to a maximum value of about 1.7×10^{-16} cm^2 at an incident electron energy of 100 eV. Measurements were made in an all-metal crossed beam facility operating at pressures less than 10^{-8} Torr. A thermionic-type ion source was used, while the electron source was a 6L6GC beam power tube modified by the substitution of a directly heated thoriated iridium filament for the original oxide cathode. The experiment was operated in the pulsed-beam mode with the electron source filament also being pulsed in a manner so as to produce an electron beam of minimum energy spread. Numerous consistency checks were performed to evaluate possible sources of experimental error.

*Work supported in part by the U.S.A.E.C.

GB-3 Electron Impact Autoionization in Potassium, Rubidium, and Cesium*. K.J. NYGAARD, University of Missouri-Rolla+ and Laboratoire de Collisions Electroniques, Université Paris-sud, 91405 Orsay.--Electron collisions with heavy alkali elements lead to excitation of the $(n-1)p^5ns^2$ autoionizing levels. These levels have been studied in K, Rb, and Cs in a crossed beam apparatus. New structures have been observed in Rb at 15.3 eV and in K at 18.7 eV. The results are compared with the theoretical calculations of Roi and Rai.

*Supported in part by the Office of Naval Research.

+Permanent address.

GB-4 The Fredholm Method in e-H_2 Scattering* --T.G. Winter and N.F. Lane, Phys. Dept., Rice U. The Fredholm method using an L^2 basis is presented for electron-molecule scattering in the static-exchange approximation. Using a two-center basis of STO's with fixed exponent for e-H_2 with $^2\Sigma_g^+$ symmetry, the Fredholm determinant is calculated for complex momenta following Murtaugh and Reinhardt[1] and analytically continued to the real line. Elastic s-wave phase shifts are extracted from the determinants obtained from several analytic continuations. Average phase shifts agree with the $J = 0$ close-coupling results of Henry and Lane[2] to at least 1% for $E \leq 1$ eV.

*Supported in part by U.S. Atomic Energy Comm. and Robert A. Welch Foundation.

[1]T.S.Murtaugh and W.P.Reinhardt, J. Chem. Phys. 57, 2129 (1972).

[2]R.J.W. Henry and N.F. Lane, Phys. Rev. 183, 221 (1969); and private communication.

GB-5 Absolute e-H_2 Elastic Collision Cross Sections, SANTOSH K. SRIVASTAVA*, Jet Propulsion Laboratory.--A method will be described which utilizes a cross beam scattering arrangement for measuring the absolute values of differential elastic electron scattering cross sections for any non condensible gas. In particular, this method has been employed for obtaining cross sections for hydrogen molecule at energies 3eV, 5eV, 7eV, 10eV, 15eV, 20eV, 30eV, 40eV, and 60eV. For each energy, measurements have been carried out at angles between 20^{o} and 135^{o}. The estimated accuracy of these cross sections is ± 15%. The results will be presented in tabular form and will be compared with previous experimental measurements and theoretical calculations.

*NRC-NASA Resident Research Associate.

GB-6 Microwave Transient Response Measurements of Elastic Momentum Transfer Collision Frequency.* D. A. McPHERSON, R. K. FEENEY, and J. W. HOOPER, Georgia Institute of Technology.--The elastic momentum transfer collision frequency, ν_m, of electrons in argon gas has been measured as a function of electron energy in the range from approximately thermal energy to several eV. The collision frequencies were determined by the microwave transient response (MTR) technique. The MTR is the electromagnetic response of a weakly ionized gas immersed in a highly homogeneous magnetic field to a short burst of a microwave carrier tuned to the electron cyclotron frequency. Under the proper experimental conditions, the temporal decay of the MTR envelope is directly related to ν_m. The energy variation of ν_m was studied by varying the strength of the applied microwave pulse. Monoenergetic data were derived from the experimental results by an unfolding technique which took into account the spread in electron energies due to thermal and waveguide mode effects.

*Work supported in part by the U.S.A.E.C.

SESSION H

3:30 PM - 5:00 PM, Wednesday, October 23

Crystal Ballroom

GAS DYNAMIC AND MAGNETIC PHENOMENA II

Chairman: T. Fohl, GTE Sylvania

H-1 Decaying Arcs in Strong Axial Gas Flows
W. HERMANN, U. KOGELSCHATZ, L. NIEMEYER, K. RAGALLER, and E. SCHADE, Brown Boveri Res. Ctr., CH-5401 Baden, Switzerland.-- A high current arc burning in a flow of nitrogen at a pressure of 24 bar is subjected to linear current slopes of -24 A/μs and -48 A/μs. Radial temperature profiles are obtained at different times of the decay process using emission spectroscopy, streak schlieren methods, double exposure holography and differential interferometry. The theoretical treatment of arc decay in a flow field is presented and compared to the measurements. The relative importance of radiative transfer as compared to convection and conduction during different phases of the decay is discussed.

H-2 Investigation of decaying arcs with a differential interferometer of high framing rate.
U. KOGELSCHATZ, Brown Boveri Research Center, CH-5401 Baden, Switzerland. -- The decay of an axially blown high current arc was studied with a shearing interferometer using a Wollaston prism.* The combination of a repetitively pulsed light source with a spinning mirror permitted making a sequence of 20 interferograms at 10 μs time intervals. An argon laser with a cavity dumper served as a convenient light source delivering pulses of 30 ns duration. Synchronisation was provided to ensure that the interferograms were taken prior to current-zero of an arc decaying from 2000 A at a rate of about 25 A/μs. The field of view covered the high pressure region in a double nozzle configuration with non-turbulent flow conditions. The working medium was nitrogen at 23 bar.

* U. Kogelschatz, Appl. Opt. 13, 1749 (1974)

H-3 Effect of Magnetic Arc Pumping and Nozzle Energy Clogging on Post-Arc Recovery. L.S. FROST and J.F. PERKINS, Westinghouse Research Laboratories.--Nozzle arc experiments with SF_6 gas-blast have revealed that the coupling between magnetic arc pumping and nozzle energy clogging near current-zero critically affects the increase of dielectric strength after the current is interrupted. For a 1.9 cm electrode spacing, 0.38 cm nozzle throat diameter, and 4 atm (0.4 MN/m^2) upstream pressure, the dielectric recovery rate was measured following dc arc currents, I, of 100 A and 350 A ramped to zero with di/dt's between 10 A/μs and 500 A/μs. The data were analyzed using a model which involves: (i) Arc conductance decay; (ii) Magnetic arc pumping, where gas acceleration away from an arc constriction increases as I^2; and (iii) Nozzle energy clogging, an upstream accumulation of arc energy resulting from the inability of the gas-blast to remove energy at a rate greater than arc power input. By integrating these effects over the current ramp period prior to current-zero, the model permits dielectric recovery times and arc conductance decay to be evaluated.

H-4 A Simple Model for High Current Arcs in Forced Convection. J. J. LOWKE, D. T. TUMA and H. C. LUDWIG, Westinghouse Research Labs.--Analytical and numerical predictions using simple conservation equations indicate that arcs in nozzles have the following simple properties, provided the arc current $I > I_{crit} \sim 500A$. (1) The axial temperature and electric field distributions T(z) and E(z) are independent of arc current, z is the distance from the upstream electrode. (2) T(z) is also approximately independent of the upstream tank pressure. (3) Arc diameter $D(z) \sim (2z/\sigma\rho hv)^{1/4} (4I/\pi)^{1/2}$, σ is the electrical conductivity, ρ the plasma density, h the enthalpy and v the axial plasma velocity. The arc model assumes (1) arc temperatures are independent of radius, (2) the effective radiation emission coefficient U(T) appropriate to the arc center is independent of arc radius, (3) the arc radius is everywhere small compared to the nozzle radius so that the cold gas velocity $v_c(z)$ is determined by the gas dynamic equations, (4) v is given by $v_c(z)a(T)/a_c$ where a(T) and a_c are the sonic velocities in the plasma and cold gas respectively. Fair agreement is obtained between theory and experiment for both D(z) and T(z) for both nitrogen and SF_6. No account is taken in our model of turbulence.

H-5 Experimental Measurements on a DC Arc Burning Coaxially in a Supersonic Nozzle.* R.W. ANDERSON, Univ. of Mich.--A cascade nozzle with a throat diameter of 1 cm, a hyperbolic inner contour with a 45° inlet and 5° exit asymptote matched at the throat, and a variable length is used to study arc gas flow interactions. The nozzle axial pressure distribution, mass flow, axial arc voltage distribution, and apparent arc diameter from Fastax photographs of the arc have been measured at nozzle reservoir pressures from 1-10 atm and DC currents to approximately 250 amperes. The working gas was air. Heat addition from the arc lowers the mass flow and raises the level of the axial pressure distribution. Using the cascade disks as electrical probes, the arc voltage drop was found to be greatest in the high pressure region upstream of the nozzle throat. The measurements also show the arc has a negative voltage-current characteristic at low currents. Photographs show the arc is stable upstream of the throat while becoming diffuse and fluctuating downstream.

*Work supported by RANN of NSF.

H-6 Abstract Withdrawn

H-7 Fluid Instabilities in Axial Flow Electric Arcs, D. R. TOPHAM, Dept. of Electrical Engineering, University of Alberta- Photographic observations of electric arcs in axially accelerating nitrogen flows have revealed a number of arc instabilities. These range from regular axisymmetric pulsations in arc diameter at low Reynolds numbers to highly irregular flow patterns at high Reynolds numbers. The results suggest that the instabilities are fluid dynamic in origin, and arise from radial gradients of axial velocity with the accelerated arc plasma. These observations show the mechanism leading to the fully developed turbulent flow arcs recently reported by other investigators.

H-8 Convective Instability of Arcs in Vertical Closed Cylinders. TIMOTHY FOHL GTE Sylvania Lighting Products, Danvers, Mass. Previous work in the area of the onset ofconvective instabilities in high pressure mercury arcs was based on the concepts of the onset of turbulence in pipe flow at a critical value of Reynolds number.(1) More recent work on thermal convection in enclosures has described the phenomenology of the flow in more detail and characterized the flow regimes in terms of the Rayleigh number.(2) In the present work the flow in the arc is shown to qualitatively resemble that observed in rigid annuli with a hot interior wall and a cool exterior wall. As the Rayleigh number increases, the flow evolves from a single cell convection pattern with cylindrical isotherms to a multiple cell convection pattern with isotherms distorted by the flow. The case of arcs differs from the well studied case of rigid annuli in that there is no rigid hot wall and the Rayleigh number is a strong function of temperature, and hence position. Experimentally determined flow patterns and temperature distributions are presented for ranges of pressures and arc temperature distributions which encompass the transition from single cell to multiple cell convection, roughly one to ten atmospheres.

(1) W. Elenbaas, The High Pressure Mercury Vapor Discharge North Holland, Amsterdam (1951)
(2) J. W. Elder, J. Fluid. Mech. 23 77-98 (1965)

H-9 Acoustical Resonances in a High Pressure Arc. HARALD L. WITTING R&D Center, General Electric Co., Schenectady, N.Y. -- An experimental and theoretical investigation was made of acoustical resonances in the positive column of high pressure sodium discharges that operate in cylindrical arc tubes at frequencies between 1 and 60 kHz. A theory was developed that predicts the resonance frequencies in good agreement with the experimental data. The theory assumes that standing pressure waves are driven by the periodic heat input of I^2R heating at the power frequency. Longitudinal as well as radial resonances and their longitudinal harmonics were observed and photographed. The frequencies of acoustical resonances can be used as an independent measurement of average gas temperature. The formulas given in previous work[1] with spherical geometry are found to be in error.

1 G.F. Gallo and J.E. Courtney, Applied Optics 6, 939, 1967.

SESSION IA

9:00 AM - 10:10 AM, Thursday, October 24

Crystal Ballroom

PHOTON INTERACTIONS

Chairman: R. Hudson, NASA-JSC

IA-1 Multiphoton Excitation of Atomic Rubidium with a Tunable Dye Laser.* C. B. COLLINS, S. M. CURRY, B. W. JOHNSON, M. Y. MIRZA, D. POPESCU and IOVITZU POPESCU, U. of Texas at Dallas, Inst. of Phys. of Bucharest, and U. of Bucharest--The two-photon absorption spectrum of atomic rubidium has been investigated over the 5700 - 6300 Å wavelength region with a c.w. tunable dye laser having a 0.25 Å linewidth and a space charge ionization detector to detect the collisional ionization of the absorption products.[1] The dispersion curve obtained for the photoionization of rubidium has been interpreted in terms of the two-photon transitions from the ground 5^2S level to resonant n^2D and n^2S Rydberg levels. Transitions from n=9 through 18 have been observed for the S-D series and from n=11 through 18 for the S-S series.

*Conducted as part of the U.S.-Romanian Co-operative Program in Science and Technology in association between the University of Texas at Dallas and the Institute of Physics of Bucharest. Financial support was provided in part by the U.S. National Science Foundation Grant GF443 and in part by the Romanian CSEN and CNST.

1. D. Popescu, C.B. Collins, B.W. Johnson, and Iovitzu Popescu, Phys. Rev. A9, 1182 (1974).

IA-2 Photoionization of Excited Potassium.* R.J. CORBIN, J. DANIEL JONES, and KAARE J. NYGAARD, Univ. of Missouri-Rolla--The cross section for the process $K^*(4P) + h\nu \rightarrow K^+ + e^-$ has been determined in a triple crossed beam apparatus previously used to measure the analogous cross section for excited cesium[1]. The unresolved 4S-4P transition lines, 7665 Å and 7699 Å were used to excite a collimated beam of potassium atoms. A second beam of light of variable frequency ν subsequently ionized the excited atoms. The ions thus produced were counted with a large aperature particle detector. The excitation radiation was modulated to allow discrimination against background effects. The relative photoionization cross section vs wavelength will be presented and a method for determining the absolute cross section for this process will be discussed.

*Supported in part by the Air Force Office of Scientific Research and Office of Naval Research.

[1]J. Daniel Jones and K.J. Nygaard, Fourth International Conference on Atomic Physics, Heidelberg, 1974, pp. 356-359.

IA-3 Near Threshold Photoionization and Autoionization of Xenon Metastable Atoms* F. B. DUNNING, R. D. RUNDEL, and R. F. STEBBINGS, Rice Univ., Houston, Texas--A molecular beam apparatus is used with a pulsed tunable uv laser to study the photoionization of xenon metastable atoms in the wavelength range 2700-4400 Å. Major contributions to ionization arise from excitation to $p^5(^2P_{1/2})nf'$ and $p^5(^2P_{1/2})np'$ levels which autoionize into the underlying $P_{3/2}$ continuum. The line shapes for nine such transitions have been fitted to Fano profiles, yielding quantum defects for these levels and their lifetimes against autoionization. In addition, measurement of the absolute photoionization cross sections has enabled the discrete and continuum oscillator strengths to be determined.

*Work supported by NASA contract NGR 44-006-156 and by the Welch Foundation.

IA-4 The Single Photon Technique for Monitoring Production and Decay of Excited States in Dense Gases Excited by a Low-Intensity Electron Beam.* R. E. Gleason, J. W. Keto and G. K. Walters, Rice University. A low-intensity pulsed electron beam is used in measuring the time dependence of the visible and vacuum ultraviolet emissions from gases at 1-40 atm. Previously, measurements have been made using high current (>1 kA) accelerators which generate high electron densities. The interpretation of data obtained at the low excitation intensities of this experiment is simplified because recombination is too slow to populate excited states in the times of interest. Possible reaction sequences are presented which can produce the radiating molecules observed. An analytic technique for removing the photomultiplier response from the data is compared to several numerical techniques. Impurities are shown to affect both the spectra and time dependence of the emission of the excited samples. A gas handling system is described which eliminates these effects.

*Work supported by the U. S. Atomic Energy Comm.

IA-5 Radiative Lifetimes and Production Mechanisms for the V.U.V. Transitions of Ar_2^* and Xe_2^*. J. W. Keto, R. E. Gleason, and G. K. Walters, Rice University. The time dependences of the vacuum ultraviolet emissions from dense argon and xenon are measured following excitation by a low intensity electron beam. Our results indicate that the ultraviolet continuum radiation is due to transitions which originate on the lowest 1_u and 0_u^+ states of the diatomic molecule. We have measured the radiative lifetimes of these states to be 4.2 ± 0.13 nsec (0_u^+) and $3.2\pm.3$ μsec (1_u) for argon and 5.5 ± 1 nsec (0_u^+) and 96 ± 5 nsec (1_u) for xenon. We have fit the time dependence of the argon 0_u^+ emission with a model which consists of a three body production mechanism and a pressure independent decay, which we interpret to be the radiative lifetime. The measured rate coefficient for the three body reaction is $2.6\pm0.3 \times 10^{-33}$ cm^6/sec. Models are discussed suggesting either the $Ar(^2P_{3/2})4s[3/2]_1$ or $Ar(^2P_{1/2})4s[1/2]_1$ states excited by electron impact are the origin for the production of 0_u^+ molecules.

*Work supported by the U.S. Atomic Energy Comm.

IA-6 Photodestruction and Ion-Molecule Reactions of Negative Ions in CO_2/H_2O Mixtures.* J. T. MOSELEY, P. C. COSBY, R. A. BENNETT, and J.R. PETERSON, Molecular Physics, SRI.--A drift tube mass spectrometer and an argon ion laser have been used to investigate the photodestruction of O^-, OH^-, CO_3^-, $CO_3^-\cdot H_2O$, HCO_3^- and $HCO_3^-\cdot H_2O$ at photon energies between 2.35 and 2.72 eV. Results on CO_3^- have been recently published.[1] $CO_3^-\cdot H_2O$ photodissociates into CO_3^- + H_2O with a cross section near 3×10^{-18} cm^2. The photodestruction cross section for HCO_3^- and $HCO_3^-\cdot H_2O$ is very small, less than 5×10^{-20} cm^2. The ion-molecule reactions forming CO_3^-, HCO_3^- and their hydrates are also being investigated.

*Research supported by U.S. Army Ballistics Research Laboratory through the U.S. Army Research Office.

[1] J.T. Moseley, R.A. Bennett, and J.R. Peterson, Chem. Phys. Letters 26, 288 (1974).

IA-7 Dissociation Yields as a Function of Energy, G.M. Lawrence, LASP, Univ. of Colo. - Photodissociation yields to given excited fragments have been measured as a function of $h\nu$ in CO_2, O_2, and NO_2. The fractional yields are smooth functions of energy even though the total absorption cross-section has pronounced structure. The known counter-examples to this smooth variation occur above the ionization limit. We postulate surface crossings outside the Franck-Condon region to explain the amnesia of the molecules regarding the absorption process.

SESSION IB

9:00 AM - 10:10 AM, Thursday, October 24

Brazos Room

AFTERGLOWS

Chairman: J. W. Keto, Rice University

IB-1 Quenching Rates for Rare-Gas Excimer Molecules and Excited Atomic Oxygen.* FELTON W. BINGHAM, A. WAYNE JOHNSON, AND JAMES K. RICE, SANDIA LABS.-- A very-short-pulse ($\sim$ 2 nsec, 440 keV) electron-beam system has been used to measure the quenching rates of the $2p^4\ ^1S$ level of atomic oxygen and the quenching rates of rare-gas excimer molecules at temperatures of $\sim$ 300°K. These rates, which control lifetimes ranging from a few nsec to hundreds of μsec, were studied in mixtures of oxygen-bearing compounds and high-pressure rare gases; such mixtures are important in the possible construction of an $O(^1S)$ laser. The $O(^1S)$ level is strongly quenched by water vapor ($1.27 \times 10^{-10} cm^3 sec^{-1}$). The Ar_2^* molecule (1270 Å continuum radiator) was found to be quenched by O_2 with a rate larger than 4×10^{-10} $cm^3 sec^{-1}$.

*Work supported by the U. S. Atomic Energy Commission.

IB-2 Formation and Destruction of $XeO(^1S)$ in High Pressure Xe and N_2O and CO_2 Mixtures.* G. C. TISONE and J. M. HOFFMAN, Sandia Laboratories.--A 3 nsec, 0.6 MeV electron beam has been used to excite high pressure mixtures of Xe (to 3000 Torr) with small amounts of CO_2 and N_2O (to 10 Torr). The time dependence of the $XeO(^1S)$ green bands and UV band at 3080 Å was studied. A simple model has been developed to explain the late time decay. Within the framework of this simple model a three body formation rate of 10^{-32} cm^6 sec^{-1}, a two body destruction rate of 7×10^{-13} cm^3 sec^{-1} and a lifetime of 1 μsec for the $XeO(^1S)$ has been determined. Effective quenching coefficients for CO_2 and N_2O have been found to be the same as the quenching coefficients for $O(^1S)$.

*Work supported by the U. S. Atomic Energy Commission.

IB-3 Kinetic and Spectral Behavior Of High Pressure, High Power Hg Vapor Discharges[+] L.A. Schlie, B.D. Guenther[+] and D.L. Drummond, Air Force Weapons Lab, Kirtland AFB, N.M. 87117---A Febetron 701 electron gun (600KeV, 1.5 K amp, 30 ns) was used to excite high pressure Hg (100-7600 Torr) vapor discharge to high power levels (~800MW) Both the spectral and kinetic behavior of these discharge were examined. It was found spectrally that these high power Hg vapor discharges produced three bands centered at 3350, 4400 and 5300 Å. This is in contrast to that seen with conventional optical resonant lamp or low power (<20 KW) electrical excitation experiments where only one band centered at 5100 Å is seen. By examing the transient behavior of these two bands, it is shown that this anomalous spectra is due to the vibrational nonequilibrium in the $A^3O_u^-$ state of Hg_2. The time resolved spectra show that the 4400 and 5300 Å band evolve into one band centered at 5100 Å at late times in the afterglow. Also from the analysis of the kinetics of the 3350 Å ($A^3\Pi_u \rightarrow X^1\Sigma_g^+$) and the 5100 Å ($A^3O_u^- \rightarrow X^1\Sigma_g^+$) bands, it is shown that the $A^3O_u^-$ and $A^3\Pi_u$ electronic states of Hg_2 are in thermodynamic equilibrium.

[+] Permanent Address: Physical Sciences Directorate, Army Missile Command, Redstone Arsenal, Alabama 35809

IB-4 Excimer Formation Rate in NaAr.* J. G. EDEN, J. T. VERDEYEN, AND B. E. CHERRINGTON, Gaseous Electronics Laboratory, University of Illinois at Urbana-Champaign--
The three-body formation rate of the NaAr excimer (i.e., $Na^* + 2\ Ar \xrightarrow{k_f} (NaAr)^* + Ar$) has been determined by measuring the spectrally-resolved fluorescence of the excited molecule as a function of the Argon perturber pressure. The combined fluorescence of the $(NaAr)^*$ $A^2\Pi_{1/2}$ and $A^2\Pi_{3/2}$ states was monitored for Argon pressures up to 800 Torr. The excimer formation rate determined from the data is consistent with a value previously published for another alkali-rare gas excimer[1]. The rate for this recombination process was determined on the basis of a simple four-level model for the NaAr molecule.

1. C. G. Carrington and A. Gallagher, J. Chem. Phys., 60, 3436 (1974).

*Work supported by NASA, Lewis Research Center.

IB-5 Vacuum-Ultraviolet Emissions from Neon. P. K. Leichner and J. D. Cook, U. of Kentucky. -- A pulsed beam of 250-keV electrons was used to determine two- and three-body collision coefficients for Ne($^1P_1$), Ne($^3P_1$) and Ne($^3P_2$) atoms and to measure the radiative lifetime of the $Ne_2[1_u(^3P_2)]$ molecular state. The two-body de-excitation rate of the $^1P_1$ level is 5.5×10^4 $(Torr \cdot s)^{-1}$. Atoms in the $^3P_1$ state are destroyed by two- and three-body collisions with coefficients 1.8×10^3 $(Torr \cdot s)^{-1}$ and 5.2 $Torr^{-2}s^{-1}$, respectively. The two-body de-excitation rate of the $^3P_1$ level is in agreement with the measurements of Phelps.[1] The three-body collision coefficient for the $^3P_2$ state is 0.4 $Torr^{-2}s^{-1}$. The radiative lifetime of the $Ne_2[1_u(^3P_2)]$ molecule is about 5 μs, in agreement with the measurements of Oka et al.[2] A model for the formation of neon molecules will be presented.

[1]A. V. Phelps, Phys. Rev. 114, 1011 (1959).

[2]T. Oka, K. V. S. Rama Rao, J. L. Redpath, and R. F. Firestone (to be published).

IB-6 Time Dependence in the Early Afterglow of Argon Spectral Line Intensity in High Pressure Neon/Argon Penning Mixtures, W. E. AHEARN and O. SAHNI, IBM Watson Research Center, Yorktown Heights, N.Y. 10598. - Experimental data have been obtained on the early afterglow ($\lesssim 20\mu$sec) decay of argon spectral line intensities in high pressure (100-800 Torr) neon-argon Penning mixtures for a variety of argon concentrations and discharge conditions. The active discharge is struck between closely spaced electrode configurations. The argon intensity showed a pronounced peak in the afterglow followed by an exponential time decay. The position of the intensity peak and the decay time constant were both found to be dependent on the total pressure and argon concentration. Specific mention will be made of the strong dependence of the decay parameters on gas impurities. A theoretical analysis based on the collisional transfer of excitation energy from the neon metastable states will be discussed.

IB-7 Electron Temperature Dependence of Recombination of NO^+ Ions with Electrons.* CHOU-MOU HUANG, MANFRED A. BIONDI and RAINER JOHNSEN, University of Pittsburgh. --- The electron temperature dependence of the recombination of mass-identified NO^+ ions with electrons is studied by means of a microwave-afterglow/mass-spectrometer apparatus employing microwave heating of the electrons. Under conditions where the ion wall current "tracks" the volume electron-density decay, the electron-decay data indicate that the recombination coefficient, $\alpha(NO^+)$, decreases as $T_e^{-0.36 \pm 0.03}$ over the range 380 K $\leq T_e \leq$ 5470 K. The values of $\alpha(NO^+)$ obtained at 300 K and 380 K are $(4.37 \pm 0.3) \times 10^{-7}$ and $(3.50 \pm 0.3) \times 10^{-7}$ cm^3/sec, respectively. These values are in good agreement with previous afterglow measurements[1]. Our $T_e^{-0.36}$ variation agrees well with Bardsley's theoretical prediction[2] of an approximate $T_e^{-0.4}$ variation, but is in deep disagreement with the approximate $T_e^{-0.85}$ variation obtained using ion storage techniques[3].

*Supported in part by the Army Research Office.

[1]C. S. Weller and M. A. Biondi, Phys. Rev. 172, 198 (1968).

[2]J. N. Bardsley, Phys. Rev. A2, 1359 (1970).

[3]F. Walls and G. Dunn, J. Geophys. Res. 79, 1911 (1974).

SESSION KA

1:30 PM - 3:00 PM, Thursday, October 24

Crystal Ballroom

EQUILIBRIUM PHENOMENA IN ARCS II AND NON-EQUILIBRIUM AND VACUUM ARC PHENOMENA

Chairman: P. W. Schreiber, Wright-Patterson AFB

KA-1 An Improved Method for VUV Radiometric Calibrations Using Hydrogen Arcs. W. R. OTT and G. GIERES, National Bureau of Standards, Washington, D.C.--A wall-stabilized hydrogen arc can be utilized as a standard source of spectral radiance since the continuum emission coefficient for a nearly completely ionized hydrogen plasma which is in or close to LTE is calculable to within a few percent. Previous efforts to apply this concept have been impeded by relatively large uncertainties associated with the plasma diagnostics. In contrast, the present approach delivers absolute continuum intensities independent of other radiometric standards or the accuracy of any plasma diagnostics. A 2 mm diameter hydrogen arc is operated such that the axis temperature reaches about 20,000 K. At this so-called Fowler-Milne point, the continuum emission coefficient reaches a broad maximum, an optimum condition brought about by the compensating effects of an increase in ionization and a decrease in total number density as the arc current is increased. This unique maximum is exactly calculable and has been used to calibrate the sensitivity of our spectrometer-detector system between 124-360 nm and the spectral radiance of several types of transfer sources. Results of comparisons with other primary standards are consistent with an estimated 5% uncertainty in the arc intensities.

KA-2 "METHANE/CARBON DIOXIDE DECOMPOSITION IN AN ARGON PLASMA"

C.H. LEIGH, E.A. DANCY, IREQ RESEARCH INSTITUTE, CANADA.

An investigation of the thermal decomposition, at atmospheric pressure, of an equimolar mixture of methane and carbon dioxide in an argon arc plasma has been completed.

The products of the reaction occuring in the high temperature argon plasma have been found to be those products predicted from thermodynamics, namely, hydrogen and carbon monoxide.

The reaction can be represented accurately by $CH_4 + CO_2 \rightarrow 2CO + 2H_2$. The reaction products, an equimolar mixture of high temperature hydrogen and carbon monoxide, can be used directly as a reducing gas for reduction of metallic oxides, and thus this process can be considered as a possible replacement for catalytically reformed natural gas in those industrial processes requiring a reducing atmosphere.

Complete conversion of methane - carbon dioxide mixtures can be obtained, and other hydrocarbons can be substituted for methane.

KA-3 Wall-Stabilized Arc in Air* R. S. DEVOTO, U. H. BAUDER, J. CAILLETEAU and E. SHIRES.--- A wall-stabilized air arc has been operated at 12-160 A in a cascade chamber of 5mm diameter. The air was introduced into the channel between cascade plates just downstream of the argon-shielded axial cathode. Purity of the gas was verified spectroscopically. The characteristic was determined by using plates as probes and is very similar to that for N_2. Total emitted radiation, as measured with a Hilger thermopile, is also similar to that for N_2. Temperature profiles were deduced from the total emission from the NI 4935 and OI 4368 lines as well as from the band head of the N_2^+ (0-0) first negative system at 3914. Temperatures from the OI line were consistently higher that those from the NI line, indicating possible inaccuracies in the transition probabilities.

*Supported by AEDC contract F 40600-74-C-0007

KA-4 On the Range of Validity of MTE Plasma Diagnostics. T. L. Eddy, West Virginia Institute of Technology. The Multithermal Equilibrium (MTE) multifluids model was discussed at the 26th Gaseous Electronics Conference. Specific consideration is now given to deviations of actual or partial MTE "partition function" values from complete MTE values. This deviation increases with the lowering of the ionization potential but the effect is usually reduced because conditions in which the amount of lowering increases usually have populations closer to CMTE populations. In arc plasmas of hydrogen-like species at subatmospheric pressures the actual "partition function" should not deviate more than about 1% from the CMTE value. Non-hydrogen like ionic structures are shown to increase the diviation significantly. Also considered are the regions in which complete, partial, or non-MTE might exist. Using the source function for typical transitions after Thomas' New Spectroscopy, it is shown that resonance transitions are not collisionally dominated even down to pressures of a millibar. As pressure decreases, a multibranched excitation temperature results. The general result is that all plasmas which do not have some strong peculiarity (such as lasing action) and have a hydrogen like structure can be described by either the CMTE or PMTE model.

KA-5 The Continuum Emission Coefficient Relation for the Multithermal Equilibrium Model for Non-LTE plasmas. T. L. Eddy, West Virginia Institute of Technology. The MTE continuum emission coefficient for free-bound recombination is derived using the Partial MTE ionization equation and non-hydrogenic Gaunt factors of Schlüter. The resulting form including free-bound and free-free contributions is similar to that suggested by Biberman and others (Watt-Sec/cm^3 sr):

$$\epsilon_\nu = 5.44\times10^{-46} z^2 n_e n_i T_e^{-1/2} \xi[\nu, T_e, T_{ex\beta}, T_c]$$

Where $T_{ex\beta}$ and T_c are the upper level excitation temperature and the continuum temperature defined by the Planck function for recombinations into a bound level, respectively. Then

$$\xi = \frac{g_{1,i}}{Z_{exi}}\left(\frac{z^2 E_H}{kT_e}\right)\xi'_{fb}[\nu, T_{ex\beta}]\, e^{\frac{-h\nu}{kT_c}} + \xi_{ff}[\nu, T_e] e^{\frac{\Delta E_s - h\nu}{kT_e}}$$

where

$$\xi'_{fb}[\nu,T] = \left(\frac{z^2 E_H}{kT}\right)\left(\exp\left[\frac{h\nu}{kT}\right] - 1\right)\xi_{fb,\ Schlüter}[\nu,T]$$

A more detailed analysis is possible with different T_c for recombination into different levels using relations given by Schluter [Z. Phys. 210, 80-91 (1968)]. Calculated electron densities are compared with those from H_β broadening in a constricted argon arc.

KA-6 Non-LTE Excitation of Molecules in Tin-Iodide Arcs. E. FISCHER, L. REHDER, Philips Research Labs Aachen.-- Simultaneous emission and absorption measurements of pure tin-iodide arc plasmas have shown, that the electronically excited states of radiating SnI-molecules are underpopulated by a factor of about 8 (E.Fischer, L.Rehder, 26th G.E.C. Madison). Increase of the collision rate by adding increasing amounts of mercury has only minor influence, whereas the increase of the axis temperature strongly affects the molecular emission. Spatially resolved spectroscopic measurements in the afterglow of decaying tin iodide arcs yield the time constants for a number of atomic and molecular emission and absorption processes.

From these experiments it can be concluded, that the formation of electronically excited SnI-molecules should mainly be due to the recombination of diffusing metastable tin atoms with ground state iodine, rather than to thermal excitation of the SnI ground state.

KA-7 Observation of Stimulated Raman Emission at UHF from Laboratory Plasmas - C. C. LEIBY, JR. and B. PRASAD, AFCRL, Hanscom AFB, Bedford, MA 01730 --- Four bands of e-m radiation have been observed to emanate from flow-stabilized DC discharges in argon gas at very low pressures (~2.5μ). Far-field signals were detected by four different (λ = 136,70, 50, and 40 cm) dipole antennas, and near-field signals by a 6.8 cm monopole probe, a 3.5 cm dia. loop and a 2-turn coil around the discharges (80 cm long, 5.8 cm i.d.). The signals, displayed on a broad-band (100-1100 MHz) spectrum analyzer, were qualitatively the same for all detectors and were identified as the $\omega_p/\sqrt{2}$ (dipole), ω_p (plasma freq), $\sqrt{2}\omega_p$ (weak, sometimes missing), and $\sim 2\omega_p$ (Raman) bands. As in types 2 and 3 solar radio bursts, the Raman-band was actually $\sim 1.7\omega_p$ and ~20% as strong as the ω_p-band, indicating that it must be generated by a stimulated emission process.[1] The near-field probes revealed that the Raman radiation was generated in the discharge's cathode-fall region (~10 cm long) where a double humped electron velocity distribution exists. The high energy (~12 eV) hump of this distribution constitutes an electron beam which (according to theory[1]) generates the stimulated Raman emission band.

1. B. Prasad, Bull. Am. Phys. Soc. 18, 1297 (1973).

KA-8 Copper Vapor Plasma Produced from a Vacuum Arc Source.* D.P. MALONE, SUNY/Buffalo-- A copper vapor plasma has been produced by creating a vacuum arc between a copper cathode and anode, and allowing the metal vapor plasma to pass through a 1 cm hole in the anode into the evacuated region beyond the anode. Diagnostic measurements were then made on the copper vapor plasma utilizing swept probe techniques and spectroscopic techniques.

The data obtained using a 600 volt, 45 amp 2 msec plasma pulse indicate a kinetic temperature of $25 \times 10^{3}{}^{\circ}K$ and an ion density of $8 \times 10^{20} m^{-3}$. Neutral density measurements have also been made.

The data indicate that this device provides a source of an easily generated laboratory plasma which falls between the density and (kT) regions obtainable from high pressure or low pressure arcs.

*Work supported by U.S.A.F.-RADC.

KA-9 Neutral Vapor Temperatures Derived from Pulsed Vacuum Arcs. C.L. CHEN and P.J. CHANTRY, Westinghouse Research Laboratories, and T. UTSUMI, Bell Telephone Laboratories.--Previously published data,[1] together with more recent data obtained by the time of flight technique[1] has been interpreted using a revised[2] model which properly relates the distributions measured in the collisionless region to the temperature in the collision dominated region. The electrode materials include: Au, Ag, Cu, Co, Re and Ti. The derived neutral temperature, within experimental error, is equal to the melting point of the cathode material, and is apparently too low to account for the established rate of evaporation of material from the cathode spot of a dc arc. This result is not fully understood at present, but some speculation can be offered.

1. T. UTSUMI, Applied Phys. Lett. 18, 218 (1971).
2. The need for such revision has been independently pointed out to one of us (T.U.) by J.C. Sherman. (Private Communication).

KA-10 Projection Tube Studies of Vacuum Arcs From Tungsten and Niobium Wires.* G.H. MILEY, Univ. of Ill. C-U Campus--Both pre- and post-voltage-breakdown vacuum arcs (0-150 kV),[1] from 2 to 10-mil wires in a cylindrical projection tube were studied using a high-speed camera to record phosphorescent patterns. Observations are correlated with protrusions on the wire surface photographed with an electron microscope. Cathode arc "roots" are frequently marked by spherical condensation of micron size droplets of aluminum and silicate transported from the tube (anode) by pre-breakdown currents. The local density of microarcs increases with voltage prior to breakdown and is proliferated over long distances by debris and shock effects occuring during precursor breakdown arcs. However, the breakdown voltage is insensitive to the arc density. A model for growth of the arc density is proposed involving dynamic formation of protrusions and work function variations. Further aspects were studied using helium ion bombardment to blister the wire surface.

*Work supported by the A.E.C. - Lawrence Livermore Lab.

[1] I. Brodie and L. Weissman, Vacuum, 14, 299 (1964).

SESSION KB

1:30 PM - 2:40 PM, Thursday, October 24

Brazos Room

HOLLOW CATHODES AND ELECTRON TRANSPORT

Chairman: L. Frommhold, University of Texas

KB-1 Reactions of Ions in $N_2 + H_2O$ in a Hollow Cathode Discharge. F. HOWORKA, W. LINDINGER*, U. of Innsbruck, and R.N. VARNEY†, Lockheed Palo Alto.--The experimental arrangement consists of a cylindrical hollow cathode with a hole-probe that can be used to scan radially across the cylinder and read the space potential and also the ion composition, by a mass spectrometer beyond the hole, at every radial position. The results show primary ions, N^+ and N_2^+ at the outer edge of the glow giving way to N_2H^+, H_2O^+, H_3O^+, and a trace of NO^+ near the cylinder axis. Ion-molecule reactions are proceeding with decreasing radius to cause the results. There is not more than 0.1 V potential difference between the axis and the glow edge so that diffusion is the chief agent causing ionic transport within the glow. It has been possible to set up the diffusion equation with production and loss of species and to evaluate reaction rate constants for the chief processes. The values in general agree with earlier ones except for that for $N_2H^+ + H_2O \rightarrow H_3O^+ + N_2$ for which we obtain $(5.5\pm2.0) \times 10^{-9}$ $cm^3 s^{-1}$ as compared with $(2.5\text{-}2.9) \times 10^{-9}$ by others.

*Max Kade Found. Fellow at NOAA-ERL-Boulder.
†Work done in part as Fulbright Lctrer,U.of Innsbruck.

KB-2 Mass Spectrometric Analysis of N_2, SF_6, and NH_3 Gases in Cylindrical Hollow Cathode Discharge. M. SAPOROSCHENKO, Southern Illinois U.--The ion components from the negative glow of a cylindrical hollow cathode discharge were analyzed with help of a quadrupole mass spectrometer. The ion intensities were studied as functions of the gas pressure, the discharge current, and the potential difference between the exit aperture and the anode is ultrapure N_2, SF_6, and NH_3 gases. The energy distribution and the reaction processes of the ions in the negative glow of the discharge will be discussed.

KB-3 Experimental Electron-Energy Distributions in Transverse Hollow-Cathode Discharges.* R. A. OLSON, D. R. NORDLUND,† and B. SARKA, JR., Systems Research Laboratories, Inc.--Spherical probes were used to measure the plasma properties within a slotted-hollow-cathode discharge for various gases as a function of pressure, current, radial position, and tube diameter. Discharges in He, He-Ne (10:1), Ne, Ar, and He-Cd were investigated. A harmonic second-derivative system was used to obtain probe data. Electron-energy-distribution functions f(V) were calculated, using the Druyvesteyn relation, from calibrated second-derivative curves. These functions were characterized by an approximately Maxwellian group at low energy (0 to 2-4 V), followed by a higher-energy group which was curtailed in the vicinity of the first excitation potential. For He, slight peaks in f(V) at 14-15 and 19-20 V can be attributed to Penning ionization in collisions between 2^3S_1 metastables and to collisions of the second kind between 2^3S_1 metastables and slow electrons, respectively. A peak in f(V) for He-Cd at 11 V may be the result of Penning ionization of Cd atoms by 2^3S_1 He metastables.

*Supported by USAF Contract F33615-71-C-1168.
†Present address: Princeton University.

KB-4 Electrical Probe Diagnostics of Anisotropic Plasmas in Lasers. I.P. SHKAROFSKY and A. BONNIER, RCA Ltd. R&D Labs. Quebec -- A theoretical study of the response of an electrostatic probe in a lasing medium with an anisotropic electron distribution function is presented. We consider different geometries, namely the plane, spherical and cylindrical probes, all in the situation of a collisionless sheath. The deduction of the first three Cartesian tensor components of the distribution function from the current collected by a plane probe, whose orientation is varied, is also provided.

KB-5 Relaxation Phenomena of Electrons Emitted from a Wall, G. ECKER and A. SCHOLZ, Ruhr-Universität, Bochum -- The relaxation problem of wall electrons in an one dimensional stationary plasma is investigated accounting as well for elastic and inelastic collisions with neutrals as for electron-electron interactions. The Debye length is assumed to be small compared with the mean free path of the electrons. Starting from the eigensolutions and Green's function of a separable part of the kinetic equation we construct an integral equation for the electron distribution function. From this equation the distribution function may in general be calculated by iteration. Under favourable conditions analytical solution free of iteration is possible. In all cases we find a simultaneous description of the energy and momentum relaxation.

KB-6 Electron Density Measurements in Collision Dominated Plasmas*. T. V. GEORGE and L. J. DENES. Westinghouse Research Labs.--A simple technique, based on the absorption of far infrared radiation, is shown to provide direct electron number density data in atmospheric, large-volume plasmas. Spatially and temporally resolved measurements of electron density were obtained from a 10 cm plasma over the range 10^{11} to 3×10^{13} cm^{-3} using a 337 μm laser source. The measurement configuration allowed a 0.5 cm spatial resolution and a 200 nsec temporal resolution. The results are compared against the average electron density obtained from the V-I characteristics of the discharge.

*Work supported in part by the U. S. Air Force Weapons Laboratory under Contract No. F29601-73-C-0121.

KB-7 Negative Differential Conductivity in Molecular Gas-Rare Gas Mixtures: Nitrogen - Argon. W. H. LONG, Jr., W. F. BAILEY, and A. GARSCADDEN, Aerospace Research Laboratories, Wright-Patterson AFB.--The energy distribution, average energy and drift velocity of electrons in mixtures containing a small amount of molecular gas in a rare gas diluent were calculated using a numerical solution of the Boltzmann transport equation including inelastic collisions. The results in N_2-A agree well with available experimental measurements where gas purity was strictly controlled. The theoretical drift velocity exhibits a local maximum versus E/N and an absolute maximum as a function of N_2 concentration, thus resolving a disparity between previous theory and experiment. A model using an analytical form of the electron energy distribution in a gas with piecewise constant cross section yields similar conclusions. The significance of the negative differential conductivity on discharge stability is discussed.

SESSION LA

3:30 PM - 4:45 PM, Thursday, October 24

Crystal Ballroom

ION MOBILITY AND HELIUM AFTERGLOWS

Chairman: C. Collins, U. of Texas at Dallas

LA-1 Mobility of Intermediate Sized Aqueous Ions in an Argon Gas. Donald E. Hagen, Paul C. Yue, and James L. Kassner, Jr., Univ. of Missouri-Rolla -- The mobility of an aqueous ion is calculated for the low electric field regime in a gas composed of argon atoms. These aqueous ions are in the size range of several hundred molecules, and their mobility falls into the intermediate range where the Langevin theory does not work well. A theory is developed which is specifically applicable to the intermediate size range. It is based on the Chapman-Enskog approach to transport phenomena, and involves details of the cluster ion-argon interaction potential. Our potential includes a Lennard-Jones valence and dispersion term and a dipole induced dipole term to account for the interaction between the individual water molecules of the aqueous ion and the argon gas atoms, and a polarization term to account for the interaction between the ion's charge and the argon atoms. This theory is applied to mobility measurements made in a Wilson cloud chamber operating near saturation at room temperature.

LA-2 Semi-Empirical Construction of Joint Ion-Neutral Speed Distributions.* S.B. Woo, J.H. Whealton and S.P. Hong, Univ. of Del.--Knowledge of the joint ion-neutral speed distribution, $g(v_r)$, is required for the inference of ion-molecule reaction cross section, σ. Monte-Carlo simulation techniques or theoretical calculations are capable of yielding precise solutions corresponding to given ion-neutral potentials. But they can not be relied on for the purpose of finding speed distributions to infer σ because these methods require the assumption of interaction potentials, elastic and inelastic, while the latter at least is still to be found. Hence semi-empirical construction of speed distributions is attempted. The idea is to find a way to construct fairly accurate $g(v_r)$'s from just such measured quantities of the drift experiment as v_d, D_T, m_i, m_g, T_g, N and E/N. A modified two-temperature displaced Maxwellian is found which promises to approximate well ion speed distributions, $f(v_i)$, in a large parametric space of m_i/m_g, E/N, T_g and interaction potentials, except when $m_i/m_g \ll 1$ or $KT_g \ll (1/40)$eV. The accuracy of the approximation, when measured against the known $f(v_i)$'s obtained by Skullerud with the Monte-Carlo simulation techniques, is better than 10% at F>0.1, where $F = \int_0^{v_i} f(v_i')dv_i' / \int_0^{\infty} f(v_i')dv_i'$. The accuracy of the corresponding $g(v_r)$ is expected to be better still. *Work supported in part by ARO-D.

LA-3 Convergent Ion Transport Theory for Large Ion Density Gradients. J. H. WHEALTON, Joint Institute for Laboratory Astrophysics.--A moment solution to the Boltzmann equation is considered for a weakly ionized gas in a uniform electric field of arbitrary strength. The first nontrivial approximation yields an equation of motion of the ion density at the Navier-Stokes level

$$\frac{\partial^2 n}{\partial t^2} + \frac{\partial n}{\partial t} + \frac{\partial n}{\partial z} - \alpha \frac{\partial^2 n}{\partial z^2} = 0$$

where times are scaled by the mean free time and distances by the mean drift distance in one collision time. The diffusion-like transport coefficient α is greater than 1. The Greens function in unbounded space is found analytically. It reduces to the analogous diffusion equation solution in the limit of large time, meanwhile exhibiting shock waves which travel at a velocity $\pm \sqrt{\alpha}$ and persist longest for small $(\alpha - 1)$. The procedure is conjectured to be convergent for large density gradients.

LA-4 Asymptotic Ion Transport Theory for Small Ion Density Gradients. J. H. WHEALTON, Joint Institute for Laboratory Astrophysics.--Ion transport theories for a weakly ionized gas in a strong electric field of the form

$$\frac{\partial n}{\partial t} + \frac{\partial n}{\partial z} - D_z \frac{\partial^2 n}{\partial z^2} + Q_z \frac{\partial^3 n}{\partial z^3} - R_z \frac{\partial^4 n}{\partial z^4} + \cdots = 0$$

are scrutinized. In steady state, for high fields it is not enough to throw away the time derivative term because the transport coefficients in the field direction are different from those in the transient case. This difference is enhanced by large mass ratios and is thus virtually negligible for elastically colliding electrons. This could be relevant in the interpretation of Townsend-Huxley experiments for ions. Other difficulties arise if the density gradients are large whereby including one correction term to the diffusion equation (4 terms) in the above theory may result in negative densities and inclusion of further correction terms results in instabilities.

LA-5 Monte-Carlo Simulation of the Drift of H^- Ions in He.* -- S. L. LIN and J. N. BARDSLEY, University of Pittsburgh. The dependence of the velocity distribution and mobility of ions in a drift tube upon the ion-atom interaction potential is investigated through Monte-Carlo simulation of the ion motion. The individual ion-atom collisions are treated by the JWKB approximation. For high values of the ratio E/N, a development of Skullerud's technique[1] is used in which a single ion is followed through about 20,000 collisions, and the time-average of the motion is studied. At low values of E/N, for which the drift velocity is comparable to the rate of diffusion, a swarm of ions is followed through a smaller number of collisions; two runs are made, one with a field and one without, and the mobility is deduced from a comparison of the two cases. An interaction potential is derived from the observed variation[2] of mobility with E/N and the corresponding velocity distribution is shown.

*Research supported, in part, by ARPA.

[1]H. R. Skullerud, J. Phys. B 6, 918 (1973).
[2]M. McFarland et al., J. Chem. Phys. 59, 6610 (1973).

LA-6 An Experimental Study of Electron Temperature and Metastable Atoms in a Recombining Helium Plasma.* C. C. POON and F. ROBBEN, University of California at Berkeley.--Number densities of excited states in an RF induction-heated flowing helium plasma afterglow supersonic jet have been measured. Number densities of states with $n>3$ are determined spectroscopically from plasma absolute emission, and those with $n=2$ are determined by the absorption of the lines 3889Å, 5016Å, 5876Å, and 6678Å from an external source. Typical electron density n_e and temperature T_e are between 10^{11}-10^{13} cm^{-3} and .03-.1 eV respectively. The inferred recombination rate coefficient at low values of n_e and T_e is much greater than that based on the Bates, Kingston and McWhirter[1] model. A calculation of the rate balance of the n=2 states using known processes require the introduction of the reactions $He(2^1P)+e^- \rightarrow He(2^3P)+e^- \rightarrow He(2^1S)+e^-$, resulting in an estimation of their rate coefficients.

[1]D.R.Bates, A.E.Kingston, and R.W.P.McWhirter, Proc. Roy. Soc. A267, 297 and A270, 155 (1962).

*Work supported by National Science Foundation

LA-7 Ionization and Electron Heating by Metastable Atoms in Helium Afterglows.* F. R. CASTELL and MANFRED A. BIONDI, University of Pittsburgh. -- Microwave and optical emission and absorption techniques have been used to study low pressure ($\sim$ 3-10 Torr), weakly ionized ($n_e \lesssim 10^{10}$ cm^{-3}) pure helium afterglows. The principal afterglow processes evidently are strong electron production by metastable-metastable and metastable-fast electron ionizing collisions balanced by enhanced ambipolar diffusion loss. These conditions result from the large metastable He(2^3S) concentrations ($> 10^{11}$ cm^{-3}) which greatly elevate the electron mean energy in the first msecs of the afterglow. The He(2^3S) metastable-metastable ionizing coefficient at 300K is found to be $\beta = (1.7 \pm 0.3) \times 10^{-9}$ cm^3/sec. An electron production term sensitive to the electron mean energy - possibly electron impact ionization of metastable atoms - is deduced from pulsed microwave heating experiments. Comparisons with previous work[1,2] are given.

*Supported, in part, by the Army Research Office.
[1]M. A. Biondi, Phys. Rev. 88, 660 (1952).
[2]A. V. Phelps and J. P. Molnar, Phys. Rev. 89, 1202 (1953).

LA-8 The Helium Afterglow.* J. B. GERARDO, J. R. FREEMAN, F. O. LANE, A. WAYNE JOHNSON, Sandia Labs.-- We report the results of a numerical study of the helium afterglow. These results are compared to much of the experimental helium-afterglow data that has been published during the last 25 years. Main emphasis is placed on pressures between 15 and 100 Torr where the dominant ion is He_2^+. The model includes the effect of ionizing collisions between metastable species (both atomic and molecular metastables). We compare the numerical results with published data on the decay of electrons, of atomic metastables and of molecular metastables. The results of this study indicate that within the framework of present-day knowledge there is not a set of coefficients that can satisfactorily predict all published helium-afterglow data. This failure necessitates a reevaluation of the physics. In addition, the hazards involved in deriving a unique set of coefficients from a limited amount of data will be demonstrated.

*Work supported by the U. S. Atomic Energy Commission.

SESSION LB

3:30 PM - 4:35 PM, Thursday, October 24

Brazos Room

RESONANT SCATTERING

Chairman: F. Read, JILA

LB-1 H^- Shape Resonance Studies with an Arc Plasma. J. SLATER*, G. GIERES*, and W. R. OTT, National Bureau of Standards, Washington, D.C.--Calculations by Macek have shown that the H^- photoabsorption cross section should be affected by a shape resonance at 1129.5 Å. This experiment is an attempt to observe the resonance in emission according to the reaction $e + H \rightarrow [H^-]^* \rightarrow H^- + h\nu$. The plasma is in a condition of LTE and is generated by a stationary wall-stabilized hydrogen arc. With an axis temperature of 15,000 K and 1 atm pressure, the H^- free-bound continuum contributes only about 1% of the total radiation which is dominated in the 1130 Å region by the Ly α wing. However, the peak of the shape resonance, according to Macek, should have a cross section about 25 times greater than the continuous free-bound cross section; it should, therefore, appear as a very noticeable 25% structure superimposed on the Ly α wing. Except for some small features which are attributed to weak molecular emission, there is no obvious indication of the shape resonance in either deuterium or hydrogen spectra between 1105 Å and 1135 Å. It is estimated that the minimum feature which could have been detected at 1129 Å was about 2% of the total signal.

*Permanent addresses: University of Colorado and Universität Düsseldorf, respectively.

LB-2 Resonances and Their Effects Above and Below The Electron Impact Ionization Threshold. A. WEINGARTSHOFER, M. EYB, E.M. CLARKE, and J.Wm. MCGOWAN, St. Francis Xavier University, Antigonish, Nova Scotia. -- We present two types of electron impact spectra obtained with low energy bombarding electrons and a resolution of 40 meV. The spectrum excited with fixed incident electron energy of 25 eV agrees with known Rydberg states and most important with photoionization data. The threshold excitation spectrum agrees with five series of triplet states which are produced via series of resonance bands which lie with 30 meV of these triplets. The $d^3\Pi_u$ and $k^3\Pi_u$ triplets play an important role in the electron impact ionization process at threshold. We present evidence that these triplets autoionize decaying to the nearest H_2^+ vibrational level.

LB-3 Electron Scattering on Na and K. M. Eyb*, Fachbereich Physik, Univ. Kaiserslautern, West Germany

In a crossed beam experiment the differential elastic and inelastic cross sections for e^- - Na (1) and e^- - K scattering have been measured for angles between 20° and 140° in the energy range of the lowest excited states of the atoms. Near the thresholds, the cross sections are strongly influenced by resonances and for the first inelastic threshold also by threshold effects. The orbital angular momenta of the negative ion states have been determined and the mean lifetime of one resonance has been estimated. The spike at the first threshold of K is helpful for energy calibration.

*) Present address: Dept. of Physics, St. F. X. Univ. Antigonish, N.S., Canada

(1) Andrick D., Eyb M., and Hofmann H.; J. Phys. B: Atom. Mol. Phys. 5, L15 (1972).

LB-4 Resonances in Mercury Vapor.* P.D. BURROW and J. A. MICHEJDA, Yale U--The high-resolution electron transmission method using the modulation technique introduced by Sanche and Schulz[1] is used to locate resonances in the total scattering cross section in Hg. Three resonances are found in the energy range 4.5-5.5 eV, whose energies (4.545, 4.913, 5.495 eV) are in disagreement with previous studies[2] but are consistent with many other aspects of electron-mercury scattering such as excitation functions. Pronounced structure at energy below 1 eV is observed and attributed to a $(6s^2 6p)^2P$ shape resonance near 0.63 eV. This yields an electron affinity for Hg of -0.63 ± 0.05 eV. The shape of the elastic cross section in the energy range 0.3-1.0 eV is in agreement with the momentum transfer cross section derived by Rockwood[3] from the transport coefficients.

*Work supported by the National Science Foundation.

[1]L. Sanche and G.J. Schulz, Phys. Rev. A 5, 1672 (1972).

[2]C.E. Kuyatt, J.A. Simpson and S.R. Mielczarek, Phys. Rev. 138, A 385 (1965); M. Düweke, N. Kirchner, E. Reichert and E. Staudt, J. Phys. B 6, L208 (1973).

[3]S.D. Rockwood, Phys. Rev. A 8 2349 (1973).

LB-5 Resonant Electron - Molecule Scattering: The Impulse Approximation in N_2O.* L. DUBE and A. HERZENBERG, Yale U --

N_2O is a linear triatomic molecule. Electron scattering shows a $^2\Sigma^+$ shape resonance at $\sim$ 2.3 eV. The electronic width Γ turns out to be so large - 0.7 eV - that one has an impulse picture, in which the nuclei acquire velocity but suffer little displacement during the residence of the projectile electron. The nuclear wave equation at the resonance is solved in the impulse approximation and shown to give a good account of the excitation of more than 20 vibrational states observed by Azria, Wong and Schulz.

*Work supported in part by ONR.

SESSION MA

9:00 AM - 10:25 AM, Friday, October 25

Crystal Ballroom

PENNING IONIZATION

Chairman: G. K. Walters, Rice University

MA-1 Temperature Dependence of De-excitation Rate Constants of He(2^3S) by Various Neutrals. W. LINDINGER*, A. L. SCHMELTEKOPF and F. C. FEHSENFELD, NOAA/ERL, Boulder, CO 80302.--Reaction rate constants for the quenching of the 2^3S state of helium by Ne, Ar, Xe, H_2, N_2, O_2, CO_2 and NH_3 have been measured as a function of temperature between 300°K and 900°K in a flowing afterglow. All these rate constants $k_x(T)$ increased with temperature following the expression

$$k_x(T) = 1.9 \times 10^{-9} \exp(-\Delta E_x/0.057 - \Delta E_x/RT)\ cm^3 sec^{-1},$$

with a specific ΔE_x for each reactant gas, ranging from ΔE_{NH_3} = 12 meV to ΔE_{Ne} = 112 meV. The increase of the rate constants between 300°K and 900°K is about 20 for Ne, 7 for H_2 and 4.5 for He and N_2. The results offer an explanation for the discrepancies among recently published values for the reaction rate constants of He(2^3S) with these gases obtained in beam and afterglow experiments.

* Max Kade Foundation Fellow. Permanent address: U. of Innsbruck, Inst. f. Atomphys. 6020 Innsbruck, Austria

MA-2 Chemi-ionization in Collisions of Metastable Ne with Ar.* R. H. NEYNABER and G. D. MAGNUSON, Intelcom Rad Tech. --Merging beams were used to measure cross sections Q for the Penning ionization (PI) reaction $Ne^* + Ar \rightarrow Ne + Ar^+ + e$ and the associative ionization (AI) reaction $Ne^* + Ar \rightarrow NeAr^+ + e$. The Ne^* represents Ne($^3P_2$) and Ne($^3P_0$). Cross sections for PI (defined as Q_{PI}) were measured in the range 0.01 eV $\leq W \leq$ 600 eV, where W is the relative KE of the reactants. Cross sections for AI (defined as Q_{AI}) were obtained over the range 0.01 eV $\leq W \leq$ 0.5 eV. The general shape of each cross-section curve shows a rise in Q with decreasing W, although Q_{AI} is much more strongly dependent on W than is Q_{PI}. The sum of Q_{AI} and Q_{PI} is compared with the sum obtained from theory and from other experiments conducted at thermal energy and near W = 100 eV.

*Research sponsored by the Air Force Office of Scientific Research (AFSC) United States Air Force, under Contract F44620-74-C-0002 and by the Office of Naval Research, Contract No. N00014-74-C-0011.

MA-3 Associative Ionization and Excitation Transfer in Helium.* J.S. COHEN, Los Alamos Scientific Laboratory.--*Ab initio* calculations have been performed on the Rydberg states of the He_2 molecule, obtaining adiabatic and diabatic potential curves of $^3\Sigma_g^+$, $^3\Pi_g$, $^3\Sigma_u^+$, and $^3\Pi_u$ symmetry. Matrix elements for potential coupling of the orthogonalized diabatic states and angular coupling of Σ and Π states have been evaluated. Polarization effects are important in some of the diabatic states. A semiclassical scattering model has been derived to treat the multistate curve crossing problem, including threshold and closed channel effects. Associative ionization (Hornbeck-Molnar process) and excitation-transfer cross sections have been calculated for collisions of He* in the n^3S, n^3P, and n^3D states, $n \leq 4$, with the ground-state helium atom at energies from thermal up to 100 eV. Ionization is found to have a significant effect on excitation transfer. The results are in good agreement with experiment including explanation of why association ionization does not occur for some states where it is energetically allowed. These calculations provide a quantitative verification of a qualitative model for associative ionization proposed by Mulliken.

*Work performed under the auspicies of the U. S. Atomic Energy Commission.

MA-4 Associative Ionization Involving Rare Gas Metastable Atoms* W. P. WEST, T. B. COOK, F. B. DUNNING, R. D. RUNDEL, and R. F. STEBBINGS, Rice Univ., Houston, Texas--A crossed beams apparatus has been used to measure the fractional occurrence of associative ionization in chemiionizing thermal energy collisions of He, Ne, Ar, and Kr metastable atoms with Ar, Kr, NO, N_2, CO, O_2, and H_2. The present data, obtained by mass analysis of product ions, are in good agreement with previous results obtained from Penning electron spectroscopy for Ne*-Ar, Kr collisions. For He*-Ar, however, the two methods produce different results, and possible reasons for this discrepancy will be discussed.

*Work supported by NSF grant No. GA27169 and by the Robert A. Welch Foundation.

MA-5 Collisional Transfer of Excitation and Non-Metastable Penning Ionization of Nitrogen by Neon $2p_1$ P. E. THIESS, G. H. MILEY, J. L. GORECKI, and L. ZINKIEWICZ, Univ. of Illinois--Measurements of Ne $2p_1$ and N_2^+ $B^2\Sigma_u^+$ excited state densities as functions of pressure, field, and concentration in Ne-N_2 and He-Ne-N_2 dc Townsend discharges has shown that enhanced fluorescence produced in the first negative system of N_2^+ (e.g. 3914-Å) is a result of non-metastable Penning ionization from the Ne $2p_1$ (18.96eV) state which is in close resonance with the $B^2\Sigma_u^+$ state (19.75eV); i.e. $Ne(2p_1) + N_2 \rightarrow Ne + N_2^+(B^2\Sigma_u^+)$. Non-metastable Penning ionization has been postulated before to explain ionization found in high pressure noble gas mixtures[†], but this measurement appears to be the first to clearly show that the transfer does take place from a short lived state. Similarly enhanced fluorescence in Ne-N_2 discharges, previously explained in terms of charge exchange, must occur by this reaction. Studies covered the pressure range from 10 to 760 Torr and 0.01 to 10% N_2. Helium was used to alter the pressure behavior of the 2p states and further establish the transfer mechanism and rate constant. Ne-H_2 and Ne-O_2 were also studied but showed transfer from Ne_2^+ and Ne^m and Ne_2^m respectively. [†]Hurst, J.Chem.Phys., 42, 713(1965); Kubota, J.Phys.Soc.Japan, 29, 101(1970).

MA-6 Absolute Rates of Collisional Deactivation of Hg($6p\ ^3P_2$) by Nitrogen and Carbon Monoxide. R. BURNHAM, Science Applications Inc., and N. DJEU, Naval Research Laboratory - The total rates of collisional deactivation of the $6p\ ^3P_2$ state of mercury by nitrogen and carbon monoxide have been measured. The experimental technique involved the use of a narrow-band cw dye laser to probe the absorption at the center of the 5461 Å line of mercury in an optically pumped cell as a function of the pressure of the deactivating gases. The measured rates at 325°K were $3.0 \times 10^6 sec^{-1} torr^{-1}$ and $6.2 \times 10^6 sec^{-1} torr^{-1}$ for deactivation by N_2 and CO respectively. Also measured were the rates of collisional deactivation from the $7s\ ^3S_1$ level into the $6p\ ^3P_2$ level. These partial quenching rates were found to be less than $7 \times 10^5\ sec^{-1} torr^{-1}$ for N_2, and equal to $4.4 \times 10^6\ sec^{-1} torr^{-1}$ for CO.

MA-7 Measurements Involving Rare Gas Atoms in High Rydberg States* T. B. COOK, W. P. WEST, F. B. DUNNING, and R. F. STEBBINGS, Rice Univ., Houston, Texas--High Rydberg states of the type $He(n^1P)$, Kr $p^5(^2P_{3/2})np$, nf and Xe $p^5(^2P_{3/2})np$, nf have been populated by photoexcitation from the $He(2^1S)$, $Kr(^3P_0)$ and $Xe(^3P_0)$ metastable levels using a tunable dye laser. $He(n^1P)$ atoms have been observed through the vacuum uv radiation emitted as they decay to the $He(1^1S)$ ground state. High Rydberg atoms of the heavier rare gases have been detected through photoionization and through field ionization resulting from the application of an electric field of several kV cm^{-1}. For $n \geq 25$ this field is sufficient to ionize essentially all high Rydberg atoms before their spontaneous decay, and the resulting ion current thus provides an absolute measure of the high Rydberg state production.

*Work supported by NSF grant No. GP39024 and by the Welch Foundation.

SESSION MB

9:00 AM - 10:10 AM, Friday, October 25

Brazos Room

POSITIVE COLUMN AND IONIZATION

Chairman: A. V. Phelps, JILA

MB-1 Positive column of A.C. operated Na-Ne-Ar low-pressure discharges. H.v.Tongeren and J. de Ruyter, Philips Research Labs., Eindhoven, The Netherlands.--Time-resolved measurements have been made on the axial electric field of the positive column of 50 Hz a.c. operated Na-Ne-Ar discharges, R=1cm, P_{Ne-Ar}=5.5 Torr (1% Ar, 99% Ne). The plots of E against the discharge current I show pronounced hysteresis effects which increase with increasing current amplitudes $\hat{I}$, $I=\hat{I}\sin\varphi(t)$, $\varphi(t)=100\pi t$. It follows from time-dependent calculations on a three-level model[1] of the Na-atom that this hysteresis is caused by depletion of the diffusion controlled Na-atom distribution which cannot follow the time variations in I. At $\hat{I}$=1060mA, I=750mA and a Na density of $4.6\times10^{19}m^{-3}$ we find E_{exp}=62 V/m at $\varphi=\frac{1}{4}\pi$ and E_{exp}=91 V/m at $\varphi=\frac{3}{4}\pi$ while calculations result in E_{calc}=88 V/m and E_{calc}=100 V/m, respectively.

1) H. v. Tongeren, J. Appl. Phys. 45, 89 (1974)

MB-2 Calculations on low pressure sodium-mercury-neon discharges. T.G. Verbeek, Light Division, N.V. Philips Gloeilampenfabrieken, Eindhoven, Netherlands.

The characteristics of the positive column of a low pressure D.C. sodium-mercury-neon discharge are calculated with the aid of a mathematrical model in which the sodium atom is represented by a three level model and the mercury atom by a five level model. Special attention is paid to the description of the ambipolar diffusion in a plasma with several ion species. In such a plasma the diffusion to the wall cannot be described by a single and constant ambipolar diffusion coefficient. This leads to a more complex set of continuity equations.
Calculations have been carried out for a cylindrically symmetrical discharge. As the discharge current increases that part of the discharge in which excitation and ionisation of sodium occurs gradually moves towards the wall. At the same time the mercury discharge becomes more dominant near the axis of the tube.

MB-3 Radiation measurements of low pressure cadmium-neon discharges. H.J.F.G. Smets and T.G. Verbeek, Light Division, N.V. Philips, Gloeilampenfabrieken, Eindhoven, Netherlands.

The U.V. power radiated at 326.1 nm and 228.8 nm by a low pressure Cd-Ne discharge (tube radius 12 mm) is measured as function of D.C and A.C discharge current (0.3-1.2 A), neon pressure (2, 5, 10 torr) and tube wall temperature (220-280°C). The electric field strength of the discharge is measured by means of external or internal probes for D.C or A.C currents respectively. The radiation measurements are carried out making use of an integrating sphere coated with $BaSO_4$. This integrating sphere has been calibrated using a standard U.V. arc. The measurements are compared with those of Springer and Barnes 1). The maximum of the radiation at 326.1 nm is found at a tube wall temperature 30°C below that found by Springer and Barnes. Apart from this the results are comparable.

1) Springer R.H., Barnes B.T., J.A.P. 39, 3100 (1968)

MB-4 Maintenance Electric Fields in a H_2-He d.c. Glow Discharge. C.H. Muller and A.V. Phelps, Joint Institute for Laboratory Astrophysics -- Measurements have been made of E/N versus total pressure in a cylindrically confined glow discharge consisting of approximately 2% H_2 in He. The Boltzmann equation was solved using published cross sections[1] to obtain ionization rate coefficients in the H_2-He mixtures. The ionization rate was then balanced against ambipolar diffusion to predict E/N versus total pressure. Good agreement between experiment and theory has been obtained over a total pressure range of 5 to 500 torr for a tube diameter of 4 mm. The corresponding range of E/N was from 3×10^{-16} to 6×10^{-17} V-cm^2 and the discharge currents varied from 70 to 40 μA.

1. A.G. Engelhardt and A.V. Phelps, Phys. Rev. 131, 2115 (1963).
L.S. Frost and A.V. Phelps, Phys. Rev. 136, A1538 (1964).

MB-5 Investigation of the Two Forms of the Oxygen Discharge. J. W. DETTMER and A. GARSCADDEN, Aerospace Research Laboratories, WPAFB, O.--The positive column of the oxygen glow discharge can exist in two distinct forms: high field and low field where the ratio of the fields is typically 5. The transition between the forms is sudden and it is a sensitive function of current density and pressure. Using high impedance current regulation, the points of transition were experimentally determined for the parameter ranges .1 to 100 Torr and .03 to 30ma/cm^2. Also, the existence and parameters of ionization instabilities in the two regions were determined. The effects on the transition point and on the two forms due to mixing He or Ar with the oxygen were measured. Using calculated electron energy distributions, the forward rates for ionization, metastable excitation, and atom production were determined for conditions of the two forms adjacent to the transitions.

MB-6 Determination of Townsend's First Ionization Coefficient for O_2 Using H_2 to Suppress the Reactions of O^-.* R.J. CORBIN† and LOTHAR FROMMHOLD, Univ. of Texas at Austin--Current transients of electron avalanches in uniform fields in mixtures of oxygen and hydrogen have been studied to determine Townsend's first ionization coefficient α. A simple extrapolation to zero hydrogen pressure is used to determine α for pure oxygen. Following the reasoning of Price, Lucas, and Moruzzi[1], these mixtures were chosen to remove the primary negative ion O^- by a rapid associative detachment reaction with H_2. The negative ion currents were significantly reduced. However, small concentrations of negative ions, probably O_2^- and/or OH^- were discovered, with lifetimes against detachment of 10^{-6} sec under the conditions of this experiment.

*Supported by NSF Grant GP-28489 and by the Joint Services Electronics Program.
†Now at the Univ. of Missouri-Rolla, Rolla, MO 65401
[1]D.A. Price, J. Lucas, and J.L. Moruzzi, J. Phys. D, 5, 1249 (1972).

MB-7 Spectroscopic Measurements of the Electron Density Evolution within a Corona Discharge in Oxygen., F. BASTIEN, B. FERTIL, E. MARODE, Labo. Phys. Décharges, 10, av. P. Larousse 92240 MALAKOFF FRANCE-- A temporal study of the electron density in a point to plane discharge in oxygen by spectroscopic technic is presented. The method consists of adding hydrogen traces and measuring the profiles of H_α and H_β lines emitted by hydrogen atoms. At a pressure of 270 torrs and for Gaussian radial electron density the mean measured densities decrease from $5.\ 10^{15}$ to $1.\ 10^{15}$ e/cm^3 between t = 100 ns and t = 230 ns after the beginning of the discharge. These results seem to indicate that for atmospheric pressure the electron density at the beginning of discharge can probably reach 10^{17} $e/\ cm^3$ near the axis.

SESSION NA

10:45 AM - 11:55 AM, Friday, October 25

Crystal Ballroom

LASER BREAKDOWN AND DISCHARGE MODELING

Chairman: B. E. Cherrington, U. of Illinois

NA-1 Two-Dimensional Model for Subsonic Laser Sparks. J. H. BATTEH and D. R. KEEFER, Univ. of Florida.--The two-dimensional energy equation describing the steady state, subsonic propagation of laser-maintained discharges was solved in closed form for a simple model. The propagation mechanism was assumed to be thermal conduction and thermal radiation was included as an optically thin emission term. The solution yields two-dimensional temperature profiles as well as the relationship between the propagation velocity and the laser parameters. Threshold calculations for air sparks maintained by CO_2 laser radiation agree with available experimental data. However, the theory fails at predicting the observed propagation velocities of several meters per second. It is postulated that, at these velocities, re-absorption of thermal radiation creates a nonequilibrium layer ahead of the spark front which enhances the absorption of laser radiation and increases the propagation velocity.

NA-2 Spectroscopic Study of a Stationary Laser Produced Air Plasma. DENNIS R. KEEFER, University of Florida, BRUCE B. HENRIKSEN and WILLIAM F. BRAERMAN, U.S. Army Ballistic Research Laboratories.--A stationary, arc like plasma was produced in air at a pressure of one atmoshpere using a cw carbon dioxide laser with a nominal power of 6 KW. Spectroscopic measurements revealed that a peak temperature of 17,000°K occurs 1.1 cm ahead of the focal point. Two-dimensional temperature profiles were obtained from photographs of the continuum radiation using a narrow bandpass filter. The radiation surrounding the hot plasma core was found to consist primarily, of the first negative system of nitrogen.

NA-3 Loss Mechanisms in Argon Gas Breakdown Using 10.6μ Radiation.* CARLTON D. MOODY, US Army Missile Command, Redstone Arsenal, Alabama.- An experimental study of the breakdown in argon by radiation of 10.6μ from a low power CW laser was made, and a theoretical model for the maintenance of a continuous (long-duration) optical discharge at threshold is presented. This continuous discharge was formed in the gas by using the radiation from a pulsed CO_2 laser to ionize (short-duration discharge) the gas and then to maintain this ionization level using the radiation from the CW laser. It is found that the CW power required to maintain ionization is several orders of magnitude smaller than the pulse power threshold because of the shift in emphasis to the ambipolar diffusion loss mechanisms. A discussion is presented on the part thermal equilibrium has in influencing this low threshold. The classical microwave cascade theory is found to adequately describe CW gas breakdown and predicts a p^{-2} dependence on the gas pressure as was confirmed by the experimental results.

*Submitted by C. H. Chan

NA-4 Experimental Evidence for Two-Step Excitation/Ionization in High Pressure Rare Gas DC Townsend Discharges P. E. THIESS, G. H. MILEY, Univ. of Illinois--Studies of excited state densities in low current (<10μa) coaxial rare gas dc Townsend discharges made over the pressure range of 10 to 760 Torr are explained in terms of 2-step excitation and ionization from metastables as well as single-step excitation and radiative and collisional losses. While analytic studies to explain glow discharge phenomena and laser produced plasmas(1-4) including the 2-step process have been conducted, no clear experimental proof of its importance appears in the literature and it has never been considered in analysis of a pulsed Townsend discharge or breakdown phenomena. Line intensities for the 2p-1s transitions in Ne and Ar and the n=3 states in He were recorded at various field strengths and for constant current conditions. Analysis shows that the pressure variation found follows that of the metastables. Studies in binary and ternary mixtures containing a small Penning additive (i.e., He-Ne, He-N_2, Ne-Ar, Ar-Kr & He-Ne-Ar) shows this too but with an altered pressure variation and decreased density. 1. Mewe, Physica, 47, 373 (1970), 2. Cherrington, Bul. Am. Phys. Soc., 19, 146 (1974), 3. Maceda and Miley, submitted 27th GEC, 4. Drawin, pp. 705 in Physics of Ionized Gases 1972.

NA-5 Non-Maxwellian Electron Excitation in Helium. EDWARD L. MACEDA, G. H. MILEY, Univ. of Illinois--Electron beams and other energetic electron sources cause non-Maxwellian fluxes within a gas. The excitations created from such a flux should be different from other types of gaseous excitations. It is to this end this paper is addressed. One and two step electron excitations of helium due to a non-Maxwellian flux[1] in an infinite medium, steady state gas at a temperature of 1000°K and pressure of 10 torr with an electron density of 10^{12} electrons/cc are considered in this paper. Singlet and triplet states with principle quantum number of seven or less and S, P, and D degeneracies are computed. Optical decay[2], recombination and collisional excitation[3,4] are the terms included in the rate equations. Population inversions are found in both the one and two step excitation cases. Collisional mixing due to excitation from the metastable states causes a shifting of relative populations and reduces the number of population inversions. 1. R. Lo, Ph.D. Thesis, U. of Illinois (1972). 2. F. E. Niles, Ballistic Research Lab Report No. 1354 (1967). 3. R. St. John, F. Miller and C. Liu, Phys. Rev., 134 (1964). 4. B. C. Moisewitsch and S. J. Smith, N.B.S. 25 (1968).

NA-6 NUMERICAL SIMULATION OF AC GAS DISPLAY DISCHARGES. C. Lanza, W. E. Howard and O. Sahni, IBM Research, N.Y.

The present work reports on a one-dimensional dynamic simulation, incorporating space charge effects, of the build-up and decay of discharge activity in isolated high (> 100 Torr) pressure discharges in conventional (Ne + 0.1% Ar) Penning mixtures confined within a narrow gap ($\sim 10^{-2}$ cm) formed at the intersection of orthogonal metal line conductors covered by insulator surfaces. Extensive modelling has been done of the dynamics of successive avalanches triggered by the secondary cathode emission due to ionic species, photons and metastables. The basic continuity equations of the problem deal with the following collisional phenomena in the gas volume--(i) electron impact excitation and ionization of neon, (ii) collisional ionization involving excited states, (iii) 2-body and 3-body collisional energy transfer processes, and (iv) resonant radiation effects. The computed results were matched to discharge current data by adjusting the cathode secondary emission coefficients. Sample results are presented for the spatial and temporal profiles of the electric field, charged particles concentrations, and the metastable volume density.

NA-7 Electron Beam Controlled Low Impedance Discharges, R. O. HUNTER, Maxwell Laboratories -- High electron drift velocities at low E/N values for an applied electric field are found in gases which have a low total collision cross section and a high fractional energy loss per collision[1]. This effect has been combined with electron beam ionization[2] to create a controlled low impedance discharge in CH_4, which has high fractional losses due to vibration and rotation as well as a Ramsauer minimum between .1 and .5 volts. A discharge at atmospheric pressure was sustained in a 10 x 10 x 100 cm volume with a 250 kV, 1-5 kiloampere cold cathode electron beam. In this configuration the discharge acted as a 25,000 ampere switch with an impedance less than .1 ohm. The temporal behavior of this discharge indicates that it is controlled by volumetric ionization and recombination.

[1]T. L. Cottrell and J. C. Walker, Trans. Farad. Soc. 61, 1585 (1965).

[2]C. A. Fenstermacher, M. J. Nutter, J. P. Rink, and K. Boyer Bull. Amer. Phys. Soc. 16, 42, (1972).

J. D. Daugherty, E. R. Pugh, and P. H. Douglas-Hamilton, Bull. Amer. Phys. Soc. 17, 399, (1972).

SESSION NB

10:45 AM - 11:45 AM, Friday, October 25

Brazos Room

HEAVY PARTICLES

Chairman: C. Latimer, Rice University

NB-1 Radiative Lifetimes of the (0,0) Band of the $B^2\Sigma^-$ State of CH*. D.M. WILCOX and R.A. ANDERSON, Univ. of MO-Rolla--The lifetimes of approximately 12 lines of the (0,0) band of CH were measured. Data was taken at five pressures for each line with a pulsed rf discharge and delayed coincidence apparatus. Variation of lifetimes of the rotational lines over the band will be reported.

*Supported by ONR Contract N00014-69-A-0141-0004

NB-2 Measurement of the Dissociative Lifetimes of Doubly-Ionized Metastable Diatomic Molecules-CO^{++}. R.G. Hirsch, R.J. VanBrunt, and W.D. Whitehead, Univ. of Va. New techniques employing a variable length time-of-flight mass spectrometer were used to measure metastable ion lifetimes in the 1-100 μsec range. Results for metastable CO^{++} produced by 150 eV electrons indicate that more than 70% of the ions have a mean lifetime between 9 and 18 μsec; the remaining live longer than 10^{-4} sec. This indicates that CO^{++} is predominantly produced in the ground $X^3\Pi$ state. Results for CO^{++} produced by Auger transitions following photoionization by 1.5 keV x rays show a single long-lived component. These measurements are compared with earlier work by Newton and Sciamanna[1] and Auger electron spectra of Siegbahn et al[2], and are explained using CO^{++} potential curves derived from Hurley's semi-emperical method.[3]

[1]A.S. Newton and A.F. Sciamanna, J. Chem. Phys. 53, 132 (1970).
[2]K. Siegbahn et al, ESCA: Applied to Free Molecules (North Holland, Amsterdam, 1969).
[3]A.C. Hurley, J. Mol. Spectr. 9, 18 (1962).

NB-3 Rate Processes Related to the Jesse Effect in He.* M. G. PAYNE, G. S. HURST, and C. E. KLOTS, Oak Ridge Nat'l. Lab. --When He is excited by fast charged particles, about 50% of the excited state population eventually cascades to the relatively long-lived (due to resonance trapping) 2^1P state. Even though the 2^1P state is long lived at low pressure ($P<1$ torr) and has a large cross section ($\sigma \approx 10^{-15} cm^2$) for ionizing collisions with impurities, the pressure dependence of the Jesse effect suggests that most of the effect for 100 torr $< P_{He} <$ 300 torr comes from He(2^1S). Bartell and Hurst have observed an exponential decay constant for He(2^1P) given by $\beta = 3 \times 10^6 + 6 \times 10^4 P + 70P^2$ (P in torr and β in sec^{-1}). We show that the 6×10^4 P term probably comes from He(2^1P) + He(1^1S) $\rightarrow$ He(2^1S) + He(1^1S), with the mechanism being rotational coupling between the $^1\Pi_g$ ($2^1P + 1^1S$) and the $^1\Sigma_g^+$ ($2^1S + 1^1S$) states, whose potential curves cross at a separation of 2.0 Å. Thus, with 100 torr $< P_{He} <$ 300 torr and with relatively low impurity concentrations, He(2^1P) is rapidly converted to He(2^1S) and Penning ionization from the latter state gives most of the Jesse effect.

*Research sponsored by the U. S. Atomic Energy Commission under contract with the Union Carbide Corporation.

NB-4 The Emission of Ultraviolet Radiation Resulting from Low Energy Argon Atom-Atom Collisions. HAROLD L. ROTHWELL, ROBERT C. AMME, and BERT VAN ZYL, U. of Denver. -- Earlier observations of vacuum-ultraviolet radiation resulting from collisions between ground-state neutral argon atoms have been extended to lower energies. Emission has now been observed down to about 0.5 eV excess c.m. energy (24 eV beam energy). At a beam energy of 25 eV, the total cross section for V-UV production is about 1×10^{-19} cm^2. A vacuum monochromator employing near-normal incidence and channel electron multiplier detection is utilized to study the spectral character of the radiation over the interval 50 nm to 120 nm. Preliminary data identify the Ar resonance lines ($4s^1[1/2]^o \rightarrow 3p^6\ ^1S$) and ($4s[3/2]^o \rightarrow 3p^6\ ^1S$) at 104.8 nm and 106.7 nm, respectively, as major contributors to the observed emission. Work is in progress to extend the spectroscopic measurements to these lower energies, as well as to search for other emission from Ar and Ar^+.

[1] P.O. Haugsjaa and R. C. Amme, Phys. Rev. Letters 23, 633 (1969).

NB-5 Rotational Excitation of HF by He Collisions*--L.A. Collins and N.F. Lane, Physics Dept., Rice U. Rotational excitation cross sections for HF in collision with He atoms were obtained in a converged close-coupling calculation employing numerical quadrature of the integral equations[1]. A model potential surface was generated by averaging an e-He pseudopotential over the charge density of HF. Representative j to j' cross sections (j,j') at 0.1 eV were found to be (in units of a_o^2): 3.2(0,1), 1.7(0,2), 1.6(0,3), and 0.2(0,4). Uncertainties in the potential surface and resulting cross sections will be discussed as well as applications to other atom-molecule systems.

*Work supported in part by the U.S. Atomic Energy Commission and the Robert A. Welch Foundation.

[1] W.N. Sams and D.J. Kouri, J. Chem. Phys. 51, 5814 (1969); E.F. Hayes, C.A. Wells, and D.J. Kouri, Phys. Rev. A 4, 1017 (1971).

NB-6 Ion Conversion Rates in the Afterglow of High Power Argon Plasmas* P. J. MURPHY and M. C. SEXTON, University College, Cork, Ireland- The dependence of the reaction rate constant k for the process $Ar^+ + 2Ar \rightarrow Ar_2^+ + Ar$ was examined with a 35 GHz microwave interferometer over the electron density range $10^{13} - 10^{11}$ cm^{-3} in argon afterglows. The value of k varied from 2.9 to 1.5 x 10^{-31} cm^6 sec^{-1} as the input power increased from 15 to 350 mJ cm^{-3}. Moreover, the gas pressure at which the onset of the conversion process occurred increased during the same range of input power.

*Work supported in part by AFOSR (London)

INDEX TO ABSTRACTS

Johnson, B. W. IA-1

Johnson, P. D. FA-6

Johnson, R. DB-4, DB-5

Jones, J. D. IA-2

Jones, W. W. DA-12

Karras, T. W. DA-11

Kassner, Jr., J. L. LA-1

Keefer, D. R. NA-1, NA-2

Keto, J. W. IA-4, IA-5

Kieffer, L. J. AB-6

Kinsinger, R. E. FA-7, WC-1

Kircher, M. J. AA-7

Kline, L. E. AA-9

Klots, C. E. NB-3

Kogelschatz, U. H-1, H-2, WC-2

Lane, F. O. LA-8

Lane, N. F. E-2, GB-4, NB-5

Lanza, C. NA-6

Lawrence, G. M. IA-7

Lee, E.T.P. FB-5

Lees, A. B. DB-3

Leffert, C. B. AB-5

Legner, H. H. AA-1

Leiby, Jr., C. C. KA-7

Leickner, P. K. IB-5

Leigh, C. H. KA-2

Leland, W. T. AA-7

Liebermann, R. W. AA-3, FA-3

Lin, C. C. FB-1

Lin, S. L. LA-5

Lindinger, W. L. DB-6, KB-1, MA-1

Long, Jr., W. H. B-4, KB-7

Lowder, R. S. AA-4

Lowke, J. J. FA-3, H-4, WC-3

Ludwig, H. C. H-4

Lundstrom, E. A. CA-5

Maceda, E. L. NA-5

Magnuson, G. D. CB-5, MA-2

Maier II, W. B. CB-1

Malarkey, E. CA-6

Malone, D. P. KA-8

Mani, S. A. B-1

Marode, E. MB-7

McAllister, G. L. CA-4

McCann, K. J. GB-1

McFarland, M. DB-6

McGowan, J. W. LB-2

McMillan, C. S. GA-4

McPherson, D. A. GB-6

Meyer, T. N. GA-3

Michejda, J. A. LB-4

Miley, G. H. DA-13, KA-10, MA-5, NA-4,NA-5

Mirza, M. Y. IA-1

Moody, C. D. NA-3

Morrison, M. E-2

Moseley, J. T. IA-6

Mullen, J. M. CB-2

Muller, C. H. MB-4

Murphree, D. L. GA-4

Murphy, P. J. NB-6

Myers, G. D. DA-3

Nathrath, N. GA-1

Nenner, I. E-4

Nesbet, R. K. WB-3

Neumann, H. CB-7

Stockton, M. DA-1, DA-3
Storm, D. DB-2
Sullivan, G. W. CA-2
Tang, S. Y. AB-4, AB-5
Taylor, L. H. AA-3
Thiess, P. E. MA-5, NA-4
Thweatt, W. L. CA-2
Tisone, G. C. IB-2
Topham, D. R. H-7
Trajmar, S. FB-6
Trenchard, H. CA-6
Truhlar, D. C. WB-5
Utsumi, T. KA-9
Van Brunt, R. J. AB-6, NB-2
van Tongeren, H. V. MB-1
Van Zyl, B. CB-6, NB-4
Varney, R. N. KB-1
Verbeek, T. G. MB-2, MB-3
Verdeyen, J. T. IB-4
Vriens, L. FA-5
Vroom, D. A. CB-3, CB-4
Vrtilek, J. M. CA-7
Waller, R. A. DA-3
Walters, G. K. IA-4, IA-5
Waszink, J. H. FA-2
Watson, Jr., J. FA-4
Waymouth, J. F. FA-4
Weaver, L. A. AA-3
Weber, R. F. CA-2
Weingartshofer, A. LB-2
Weissler, G. L. J
Wells, W. E. DA-13
West, W. P. MA-4, MA-7
Whealton, J. H. LA-2, LA-3, LA-4
Whitehead, W. D. NB-2
Wiegand, W. J. B-2, WA-6
Wilcox, D. M. NB-1
Winter, T. G. GB-4
Witting, H. L. H-9
Wong, S. F. E-1
Woo, S. B. LA-2
Wu, F. T. CA-5
Wu, J-L GA-5
Yoder, M. J. AA-2
Yue, P. C. LA-1
Zarowin, C. B. DA-10
Ziesel, J. P. E-4
Zinkiewicz, L. MA-5
Zollweg, R. J. FA-3